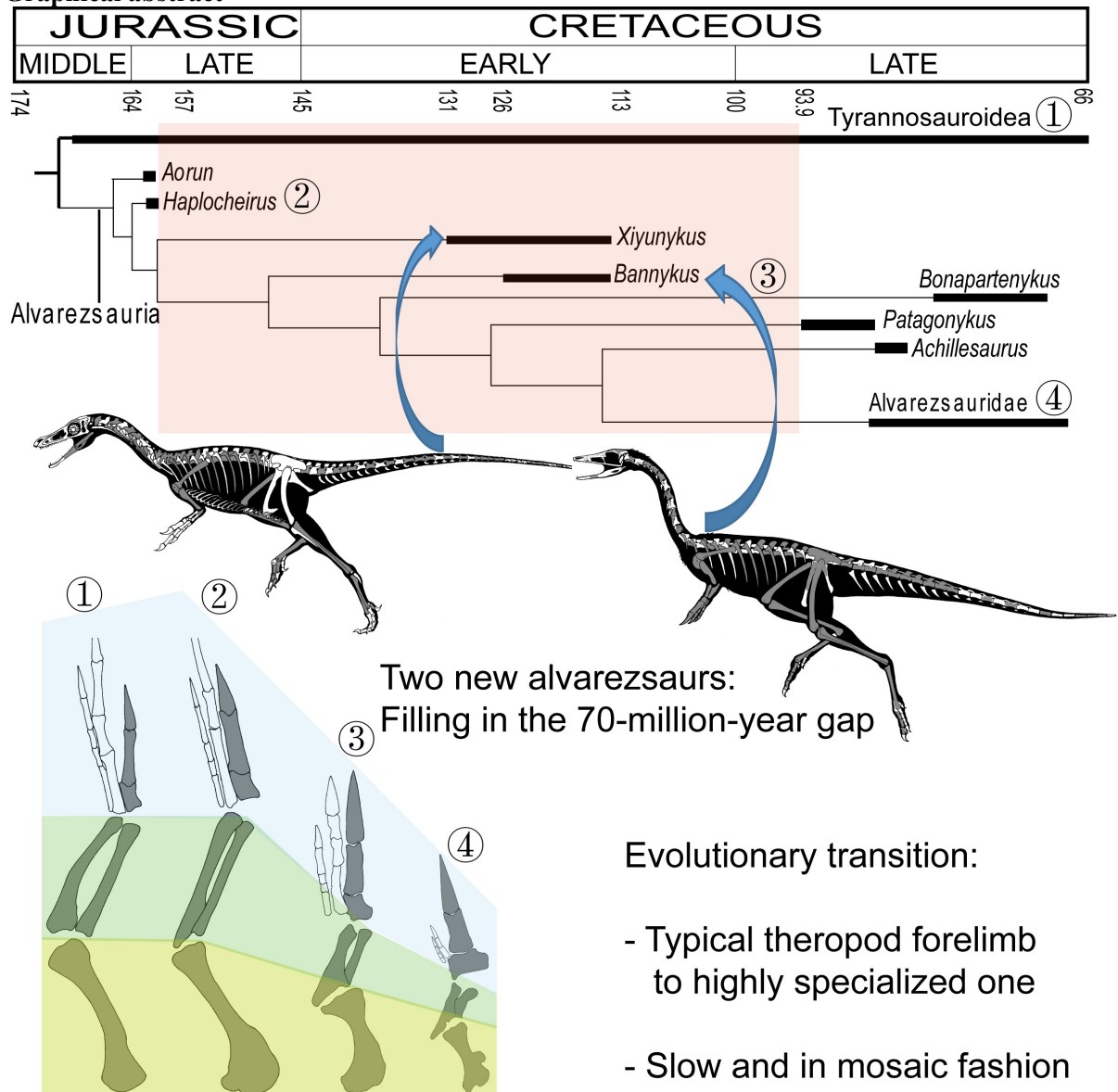


Graphical abstract



Two Early Cretaceous Fossils Document Transitional Stages in Alvarezsaurian Dinosaur Evolution

Xing Xu^{1,2,3,15,*‡}, Jonah Choiniere^{4,5‡}, Qingwei Tan⁶, Roger B. J. Benson^{7‡}, James Clark^{8,9}, Corwin Sullivan^{10,11}, Qi Zhao¹, Fenglu Han¹², Qingyu Ma¹, Yiming He¹³, Shuo Wang¹⁴, Hai Xing¹⁵, Lin Tan⁶

¹Key Laboratory of Vertebrate Evolution and Human Origins, Institute of Vertebrate Paleontology & Paleoanthropology, Chinese Academy of Sciences, 142 Xiwai Street, Beijing 100044, China

²CAS Center for Excellence in Life and Paleoenvironment, 142 Xiwai Street, Beijing, 100044, China

³Centre for Research and Education on Biological Evolution and Environment, 163 Xianlin Road, Nanjing University, Nanjing, 210045, China

⁴Evolutionary Studies Institute, University of the Witwatersrand, Private Bag 3, Johannesburg WITS 2050, South Africa

⁵Department of Vertebrate Paleontology and Richard Gilder Graduate School, American Museum of Natural History, Central Park West at 79th Street, New York, 10024, USA

⁶Long Hao Institute of Geology and Paleontology, Jia 29, Fengzhou Road, Hohhot, Nei Mongol 010010, China

⁷Department of Earth Sciences, University of Oxford, South Parks Road, Oxford OX1 3AN, UK

⁸Department of Biological Sciences, George Washington University, 2023 G Street NW, Washington, DC 20052, USA

⁹Centre for Vertebrate Evolutionary Biology, Yunnan University, 2 Green Lake North Road, Kunming, 650091, China

¹⁰Department of Biological Sciences, University of Alberta, 11455 Saskatchewan Drive, Edmonton, Alberta, T6G 2E9, Canada

¹¹Philip J. Currie Dinosaur Museum, 9301-112 Ave Wembley, Alberta, T0H 3S0, Canada

¹²School of Earth Sciences, China University of Geosciences, 388 Lumo Road, Wuhan 430074, China

¹³School of Earth Sciences and Engineering, Nanjing University, 163 Xianlin Road, Nanjing 210045, China

¹⁴College of Life Science, Capital Normal University, 105 West 3rd Ring Road North, Beijing 100048, China

¹⁵Beijing Museum of Natural History, Beijing Academy of Science and Technology, 126 South Tianqiao Street, Beijing 100050, China

¹⁶Lead Contact

*Correspondence: xingxu@vip.sina.com

‡These authors contributed equally.

SUMMARY

Highly specialized animals are often difficult to place phylogenetically. The Late Cretaceous members of Alvarezsauria represent such an example, having been posited as members of various theropod lineages, including birds [1-11]. A 70-million year ghost lineage exists between them and the Late Jurassic putative alvarezsaurian *Haplocheirus* [12], which preserves so few derived features that its membership in Alvarezsauria has recently been questioned [13]. If *Haplocheirus* is indeed an alvarezsaurian, then the 70 million year gap between *Haplocheirus* and other alvarezsaurians represents the longest temporal hiatus within the fossil record of any theropod subgroup [14]. Here we report two new alvarezsaurians from the Early Cretaceous of western China, which document successive, transitional stages in alvarezsaurian evolution. They provide further support for *Haplocheirus* as an alvarezsaurian and for alvarezsaurians as basal maniraptorans. Furthermore, they suggest that the early biogeographic history of the Alvarezsauria involved dispersals from Asia to other continents. The new specimens are temporally, morphologically and functionally intermediate between *Haplocheirus* and other known alvarezsaurians and provide a striking example of the evolutionary transition from a typical theropod forelimb configuration (i.e., the relatively long arm and three-digit grasping hand of typical tetanuran form in early-branching alvarezsaurians) to a highly specialized one (i.e., the highly modified and shortened arm and one-digit digging hand of Late Cretaceous parvicursorines such as *Linhenykus* [1, 15]). Comprehensive analyses incorporating data from these new finds show that the specialized alvarezsaurian forelimb morphology evolved slowly and in a mosaic fashion during the Cretaceous.

Key words: Early Cretaceous, Transitional Morphology, Alvarezsaur, Maniraptoran, Theropod, Biogeography, Forelimb Reduction, Mosaic Evolution

RESULTS AND DISCUSSION

Systematic Paleontology

Dinosauria Owen, 1842 [16]

Theropoda Marsh, 1881 [17]

Alvarezsauria Bonaparte, 1991 [2]

Xiyunykus pengi gen. et sp. nov. (Figure 1)

Etymology

“*Xiyu*” (Mandarin), Western Regions, referring to Central Asia including Xinjiang, and “*onyx*” (Greek), claw; specific name is in honor of Prof. Peng Xiling, who has contributed greatly to the study

of geology in Xinjiang.

Holotype

The holotype is a partial, disarticulated skeleton (Figure 1A), catalogued as IVPP (Institute of Vertebrate Paleontology & Paleoanthropology) V22783.

Locality and horizon

Wucaiwan area, Junggar Basin, Xinjiang, China; Upper Cretaceous (Barremian-Aptian?) upper part of the Tugulu Group [18].

Diagnosis

Distinguishable from other alvarezsaurians, to the extent that they are known, in possessing the following autapomorphies: large basal tubera formed exclusively by basioccipital; basisphenoid recess with basioccipital contribution and containing multiple deep fossae; cultriform process with poorly ossified dorsal margin which parallels ventral margin in lateral view; two horizontally-arranged pneumatic fossae on lateral central surface of each anterior or middle cervical vertebra; distinct tubercle along ventrolateral edge of each anterior cervical centrum; groove present medial to each posterior cervical epipophysis; posterior surface of cervical and dorsal neural arches each bearing multiple deep fossae above neural canal; deep, curved groove on scapular lateral surface immediately anterior to glenoid fossa; long, deep groove along posterior edge of proximal half of scapular blade; sharp and short groove on lateral surface of femoral distal end; and proximal end of tibia with deep groove on posterior condyle.

Description and comparisons

The holotype of *Xiyunykus pengi* is estimated to have had a body mass of 15 kg based on femoral shaft circumference [19]. Based on histological analysis, this individual was in its 9th year of life and was probably a sub-adult (Data S1; Figure 1B).

Xiyunykus possesses a cranial morphology (Figures 1C-I) transitional between the early-branching alvarezsaurian *Haplocheirus* and parvicursorine alvarezsaurians [1, 20]. Most preserved elements, including the frontal, opisthotic-exoccipital complex, dentary, angular, and surangular, are nearly identical in general morphology to those of *Haplocheirus*. However, a few cranial features, including a prominent ventral ridge on the cultriform process and a large dorsomedially projecting tab on the retroarticular process of the articular, are reminiscent of specialized parvicursorine alvarezsaurians such as *Shuvuuia* [5]. *Xiyunykus* also homoplastically shares several derived cranial features (Figures 1C-I) with the early-branching coelurosaurian group Ornithomimosauria [21], including: 1) anterior

border of supratemporal fossa strongly convex and located on posterolateral corner of frontal; 2) basioccipital excluded from foramen magnum by exoccipitals; 3) “lateral depression” present on lateral wall of braincase (also known in troodontids) [21, 22]; 4) infracondylar fossa present ventral to occipital condyle; 5) well-developed subcondylar and subotic recesses; 6) inflated, hollow cultriform process; 7) dentary sub-triangular in lateral view; and 8) surangular with dorsolateral flange lateral to glenoid region. Features 2, 3, 4, and 6 are absent in *Haplocheirus*, and whether feature 5 is also absent cannot be ascertained.

Similar to alvarezsaurids, all cervical centra are strongly opisthocoelous, the anterior dorsal centra are weakly opisthocoelous, and the last sacral centrum possesses a large ventral keel (Figure 1J). In contrast, each preserved caudal centrum is plesiomorphically amphicoelous (Figure 1J) and lacks a deep ventral sulcus. The scapula is proportionally long, rather than short as in parvicursorines [1], and the coracoid has a pyramidal but very small coracoid tubercle (Figure 1K). The humerus is plesiomorphic in being relatively slender, having a relatively small and distally located internal tuberosity, and bearing distally projecting radial and ulnar condyles (Figure 1L), but the ulna shows incipiently developed derived features including a proximally projecting, laterally compressed olecranon process (Figure 1M). The hind limbs largely show a plesiomorphic coelurosaurian morphology, but also display several features seen in parvicursorines. For example, the distal portion of the shaft of metatarsal III is sub-triangular in cross section (Figure 1N).

Dinosauria Owen, 1842 [16]

Theropoda Marsh, 1881 [17]

Alvarezsauria Bonaparte, 1991 [2]

Bannykus wulatensis gen. et sp. nov. (Figure 2)

Etymology

“*Ban*” (Mandarin), half, referring to the transitional features seen in this animal, and “*onyx*” (Greek), claw; specific name is derived from Wulatehouqi (Wulate Rear Banner), the county-level administrative division in which the type locality is situated.

Holotype

The holotype specimen is a partial, semi-articulated skeleton (Figure 2A), catalogued as IVPP V25026.

Locality and horizon

Chaoge, Wulatehouqi, Inner Mongolia, China; Lower Cretaceous (Aptian) Bayingobi Formation [23].

Diagnosis

Differs from other alvarezsaurians in possessing the following autapomorphies: notch between basal tubera nearly absent, surangular foramen large, posterior dorsal vertebrae with distal ends of transverse processes strongly expanded in posterior direction, humeral internal tuberosity deflected posteriorly, well-developed facet on lateral surface of metacarpal II for articulation with metacarpal III, metacarpal III curved medially, prominent ventral heel at proximal end of manual phalanx III-1, manual phalanx III-2 with proximovertrally located tubercles on medial and lateral surfaces and two sulci bounded by three parallel condyles on distal end, manual phalanx III-3 without median vertical ridge on proximal articular surface (note that we identify the three manual digits of tetanurans as II-III-IV following some recent paleontological [24]), posterolateral margin of fibular condyle of tibia bears pyramidal lateral projection, and deep groove along posterior margin of proximal half of fibular crest.

Description and comparisons

The holotype individual of *Bannykus wulatensis* is estimated to have had a body mass of 24 kg, based on femoral circumference [19]. Based on histological analysis, it was in its 8th year of life and was probably a sub-adult (Data S1; Figure 2B).

Bannykus is more similar in its preserved cranial morphology to parvicursorines such as *Shuvuuia* than to *Xiyunykus* and *Haplocheirus*. For example, the supratemporal fossa is poorly defined anteriorly, the infracondylar fossa is absent, and the surangular crest is relatively indistinct (Figures 2C-E).

Bannykus possesses many of the vertebral features described above for *Xiyunykus*, but also shares some additional derived features with early-branching alvarezsaurids and even parvicursorines (Figures 2F-H): the cervical centra each have a ventral groove, the dorsal vertebrae have laterally protruding parapophyses, the anteriormost caudal centra are ventrally keeled, and most of the caudal vertebrae are procoelous and bear deep sulci on their ventral surfaces. *Bannykus* is also transitional between *Xiyunykus* and Late Cretaceous alvarezsaurians in the morphology of the scapula and coracoid [1]: the scapular blade is nearly straight and the coracoid bears a weak, ridge-like coracoid tubercle (Figure 2I).

The forelimbs of *Bannykus* are highly modified, but not to the degree seen in Late Cretaceous alvarezsaurians [1, 25]. The humerus is 38% as long as the femur, and has a similar mid-shaft diameter. The humerus bears a large, proximally projecting, trapezoidal internal tuberosity as well as

a large and distally located ectepicondyle and entepicondyle [12], but is plesiomorphic in that the internal tuberosity, ectepicondyle and entepicondyle are not hypertrophied, sub-spherical structures (Figure 2J). The ulna has a mediolaterally compressed olecranon process (Figure 2K), intermediate in size between those of *Xiyunykus* and Late Cretaceous alvarezsaurians [1, 12]. Manual digit II is significantly enlarged and digit IV is shortened (Figure 2L), but neither is modified to the degree seen in alvarezsaurids [15, 25, 26]. Metacarpal II bears a deep notch on its lateral surface for articulation with metacarpal III (Figure 2L), whereas these two metacarpals are tightly syndesmosed or co-ossified in alvarezsaurids [1].

The ilium is plesiomorphic in lacking all modifications (Figure 2M) seen in Late Cretaceous alvarezsaurians [1]. The hind limbs are generally similar to those of *X. pengi*, but display a few apomorphic features. The medial distal condyle of the femur is transversely flattened and the popliteal fossa is bounded laterally and medially by two ridges (Figure 2N). The distal end of the tibia has only two facets for articulation with the proximal tarsals, and the proximal end of metatarsal III is strongly compressed (Figure 2O).

Phylogenetic Analysis

Until now there have been no transitional alvarezsaurians linking the plesiomorphic morphology of the Late Jurassic *Haplocheirus* [12] to the more derived anatomical features of Upper Cretaceous alvarezsaurians [2, 15, 27-29]. This lack of evidence was manifest in a recent maximum-likelihood analysis that suggested that *Haplocheirus* was instead an early-branching ornithomimosaur whereas the Late Cretaceous alvarezsaurians constituted a clade within Avialae [13]. The relatively large Early Cretaceous alvarezsaurians (Table S1) *Xiyunykus* and *Bannykus* interrupt the long branch leading to Late Cretaceous members of the clade and provide clear morphological evidence linking these advanced taxa to *Haplocheirus*. Our phylogenetic analysis places *Xiyunykus* and *Bannykus* successively closer to the short-armed, Late Cretaceous alvarezsaurians, confirms a relatively basal position for Alvarezsauria within Maniraptora, and places *Haplocheirus* firmly within Alvarezsauria (Data S1). Somewhat surprisingly, it also groups the Late Jurassic Shishugou form *Aorun* [20] and the enigmatic Early Cretaceous Tugulu Formation theropod *Tugulusaurus* [30] within Alvarezsauria, suggesting that early-branching alvarezsaurians were more common than previously thought (Figures 3 and S1).

Alvarezsaurian Biogeography

The phylogenetic positions of the Late Jurassic *Aorun* and *Haplocheirus*, and the Early Cretaceous *Xiyunykus*, *Tugulusaurus* and *Bannykus* along the stem of Alvarezsauria suggest that dispersal [15, 27, 31, 32] rather than vicariance [e.g., 28, 33] characterizes the early biogeographic history of the

group, given that all these taxa are Asian. More specifically, our analysis indicates that alvarezsaurians originated in Asia and remained there throughout the Cretaceous, with dispersal to other continents occurring after the appearance of *Bannykus* and *Xiyunykus*. The alternative vicariance hypothesis would involve alvarezsaurians spreading throughout Pangaea before the Aptian, with different species ending up on different continents as Pangaea broke apart. The dispersal hypothesis is also supported by our statistical biogeographical analysis (Data S1; Figure S2). Previous studies have suggested a vicariant distribution of several theropod lineages including alvarezsaurids based on either the relatively basal positions or the endemic nature of Gondwanan taxa within their respective clades [34]. Our results illustrate the potential of increased taxon sampling to change biogeographic inferences.

Mosaic Evolution

As phylogenetically, temporally, and morphologically transitional forms, the two new alvarezsaurians illuminate the pattern, pace, and timing of evolution of the bizarre, highly-specialized alvarezsaurian skeleton [35], and particularly the forelimb (Figure 3). Our analysis shows that alvarezsaurian skeletal evolution occurred in a somewhat modular manner, with different skeletal parts being modified at different evolutionary rates. The presacral and sacral vertebrae were evidently modified earlier than the caudal vertebrae, and the pectoral girdle and forelimb earlier than the pelvic girdle and hindlimb, implying a general pattern in which anterior parts of the skeleton were modified earlier than posterior parts. To some degree the tail, pelvis and hindlimbs acted as an integrated locomotor unit in non-avian dinosaurs because of the role of the caudofemoralis muscle in femoral retraction [36], and patterns of alvarezsaurian skeletal evolution suggest that this locomotor unit might have been relatively conservative in evolutionary terms.

Forelimb Reduction and Modification

Phylogenetic regression provides strong evidence for weak negative allometry of forelimb length in non-paravian theropods (Data S1; Table S2). *Bannykus* shows slight proportional reduction of the forelimb compared to *Haplocheirus*, and the same was true of *Xiyunykus* based on the similar sizes of the preserved elements. Nevertheless, the forelimbs of these Early Cretaceous alvarezsaurians were relatively unreduced compared to those of other theropods (Figures 4 and S3), and therefore unlike those of Late Cretaceous alvarezsaurians (parvicursorines, represented by *Mononykus*).

Parvicursorines display a level of proportional arm reduction that is among the greatest seen in any dinosaur group, being exceeded only in some tyrannosaurids and abelisaurids (Figure 4A). Our results show that this extreme arm reduction occurred late in alvarezsaurian evolution, and at small body mass (estimated around 24 kg; Figure 4A).

The new finds demonstrate that some key functional features of the parvicursorine forelimb were also present in Early Cretaceous alvarezsaurians. These include increased olecranon length and digit robustness, which respectively increased the extensor moment arm of the elbow joint and the mechanical strength of the hand. These features may suggest that the forelimb had a fossorial function in the Early Cretaceous taxa, as well as in parvicursorines [27, 37]. Nevertheless, other characteristic parvicursorine features, including substantial forelimb length reduction, are absent in our Early Cretaceous specimens, showing that the extreme forelimb modifications seen in Late Cretaceous alvarezsaurians evolved incrementally (Figure 3). This is best exemplified by the manus, which in parvicursorines is the most obviously specialized body part. The Late Jurassic *Haplocheirus* has a grasping hand as in typical theropods, though it shows several alvarezsaurid features in an incipient form [12]. The Early Cretaceous *Bannykus*, by contrast, possesses a dorsoventrally compressed hand with a hypertrophied thumb and shortened lateral digits (though some unusual manual features in *Bannykus* suggest a specialized function, see Data S1), indicating a shift away from grasping function. Finally, the Late Cretaceous alvarezsaurians have a highly specialized hand with only one functional digit, namely a thumb that is even more enlarged than in *Bannykus* (best exemplified by the monodactyl *Linhenykus* [15]). The highly reduced length of the parvicursorine forelimb has been a source of functional controversy [3, 27, 28, 37, 38], with some research suggesting that it would not have been long enough to function effectively in fossorial activities [27, 28, 39]. *Bannykus* and *Xiyunykus* share many of the fossorial features of the forelimb of parvicursorines but retain a plesiomorphically longer forelimb. Thus, early modification of the alvarezsaurian forelimb would have no conflict with fossorial function, and perhaps only the most derived parvicursorine forelimbs were used in a different fashion. This provides a striking example of digit reduction and specialization among theropods, comparable to the classic example in horse evolution [40]. Alvarezsaurian digit reduction occurred over 50 million years, about half the total duration of alvarezsaurian evolution (~95 million years).

SUPPLEMENTAL INFORMATION

Document 1 Figures S1-S3, Tables S1-S2, and Supplemental references

Document 2 Data S1 for supplementary text and data for phylogenetic analysis (Related to Results and Discussion, and STAR methods)

ACKNOWLEDGMENTS

We thank Gao Hong, Bayaer, Zhiqiang Bao, Jianmin Wang, Jinsheng Liu and Dong Xiao for coordinating the fieldwork in Inner Mongolia, and Hongjun Chu and Dengjie Ma for doing the same in Xinjiang. We also thank Tao Yu for discovering IVPP V22783 and Jianqiang Hao for IVPP V25026, Haijun Wang and Jianqiang Hao for collecting the specimens, Rongshan Li for the line drawings, Yun Feng for CT images, and Lishi Xiang, Tao Yu, and Xiaoqing Ding for preparing the

specimens. This work is supported by the National Natural Science Foundation of China (grant numbers: 41688103, 91514302, 41120124002, 41602013, and 41602006), the Strategic Priority Research Program of the Chinese Academy of Sciences (Grant No. XDB18030504), and NSF of USA (EAR 0922187). JNC was supported by the DST and NRF of South Africa (via AOP #98800 and IRG #95449), by the Palaeontological Scientific Trust (PAST), by the Kalbfleisch and Gerstner Scholarship of the Richard Gilder Graduate School, American Museum of Natural History, and by the Friedel Sellschop Award, and HX by Innovative Team Program (IG201705N) of the Beijing Academy of Science and Technology. Parts of this work were funded by the European Union's Horizon 2020 research and innovation programme 2014–2018 under grant agreement 677774 (ERC Starting Grant: TEMPO) to RBJB.

AUTHOR CONTRIBUTIONS

X.X., J.C., Jo.C., and R.B. designed the research project. Jo.C. conducted the phylogenetic analysis, R.B. the forelimb reduction analysis, Q.Z. the histological analysis, H. X. the biogeographical analysis, X.X. Jo.C, Q.T., J.C., C.S., Q.Z., F.H., Q.M., Y.H., S.W., H.X., and L.T collected and analyzed the specimens, X.X., Jo.C., R.B., J.C., Q.Z., H.X. and C.S. wrote the manuscript.

DECLARATION OF INTERESTS

The authors declare no competing interests.

REFERENCES

1. Chiappe, L.M., Norell, M.A., and Clark, J.M. (2002). The Cretaceous, short-armed Alvarezsauridae: *Mononykus* and its kin. In Mesozoic birds: above the heads of dinosaurs, L.M. Chiappe and L.M. Witmer, eds. (Berkeley: University of California Press), pp. 87-120.
2. Bonaparte, J.F. (1991). Los vertebrados fósiles de la Formación Río Colorado, de la ciudad de Neuquén y cercanías, Cretácico superior, Argentina. Rev. del Museo argent. de Ciencias Naturales "Bernardino Rivadavia" Paleontología 4, 17-123.
3. Perle, A., Norell, M.A., Chiappe, L., and Clark, J.M. (1993). Flightless bird from the Cretaceous of Mongolia. Nature 362, 623-626.
4. Naish, D., and Dyke, G.J. (2004). *Heptasteornis* was no ornithomimid, troodontid, dromaeosaurid or owl: the first alvarezsaurid (Dinosauria: Theropoda) from Europe. Neues Jahrbuch für Geologie und Paläontologie Monatshefte 7, 385-401.
5. Chiappe, L.M., Norell, M.A., and Clark, J.M. (1998). The skull of a relative of the stem-group bird *Mononykus*. Nature 392, 275-278.
6. Sereno, P.C. (1999). Dinosaurian biogeography; vicariance, dispersal and regional extinction. National Science Museum Monographs 15, 249-257.
7. Rauhut, O.W.M. (2003). The interrelationships and evolution of basal theropod dinosaurs. Palaeontology 69, 1-215.
8. Norell, M.A., Clark, J.M., and Makovicky, P.J. (2001). Phylogenetic relationships among coelurosaurian dinosaurs. In New perspectives on the origin and evolution of birds, J. Gauthier and L.F. Gall, eds. (New Haven: Yale University Press), pp. 49-67.
9. Turner, A.H., Pol, D., Clarke, J.A., Erickson, G.M., and Norell, M.A. (2007). A basal dromaeosaurid and size evolution preceding avian flight. Science 317, 1378-1381.
10. Senter, P. (2007). A new look at the phylogeny of coelurosauria (Dinosauria: Theropoda). Journal of Systematic Palaeontology 5, 429-463.
11. Holtz, T., R., Jr. (1998). A new phylogeny of the carnivorous dinosaurs. Gaia 15, 5-61.

12. Choiniere, J.N., Xu, X., Clark, J.M., Forster, C.A., Guo, Y., and Han, F. (2010). A basal alvarezsauroid theropod from the early Late Jurassic of Xinjiang, China. *Science* 327, 571-574.
13. Lee, M.S.Y., and Worthy, T.H. (2012). Likelihood reinstates *Archaeopteryx* as a primitive bird. *Biology letters* 8, 299-303.
14. Weishampel, D.B., Barrett, P.M., Coria, R.A., Loeuff, J.L., Xu, X., Zhao, X.J., Sahni, A., Gomani, E., and Noto, C.R. (2004). Dinosaur distribution. In *The Dinosauria* (second edition), D.B. Weishampel, P. Dodson and H. Osmolska, eds. (Berkeley: University of California Press), pp. 517-606.
15. Xu, X., Sullivan, C., Pittman, M., Choiniere, J.N., Hone, D., Upchurch, P., Tan, Q., Xiao, D., Tan, L., and Han, F. (2011). A monodactyl nonavian dinosaur and the complex evolution of the alvarezsauroid hand. *Proceedings of the National Academy of Sciences of the United States of America* 108, 2338-2342.
16. Owen, R. (1842). Report on british fossil reptiles. part II. Report of the British Association for the Advancement of Science 11, 60-204.
17. Marsh, O.C. (1881). Classification of the Dinosauria. *American Journal of Science* (series 3) 18, 81-86.
18. Eberth, D.A., Brinkman, D.B., Chen, P.-J., Yuan, F.-T., Wu, S.-Z., Li, G., and Cheng, X.-S. (2001). Sequence stratigraphy, paleoclimate patterns, and vertebrate fossil preservation in Jurassic Cretaceous strata of the Junggar Basin, Xinjiang Autonomous Region, People's Republic of China. *Canadian Journal of Earth Sciences* 38, 1627-1644.
19. Campione, N.E., Evans, D.C., Brown, C.M., and Carrano, M.T. (2014). Body mass estimation in non-avian bipeds using a theoretical conversion to quadrupedal stylopodial proportions. *Methods in Ecology and Evolution* 5, 913-923.
20. Choiniere, J.N., Clark, J.M., Forster, C.A., Norell, M.A., Eberth, D.A., Erickson, G.M., Chu, H., and Xu, X. (2014). A juvenile specimen of a new coelurosaur (Dinosauria: Theropoda) from the Middle–Late Jurassic Shishugou Formation of Xinjiang, People's Republic of China. *Journal of Systematic Palaeontology* 12, 177-215.
21. Makovicky, P.J., Kobayashi, Y., and Currie, P.J. (2004). Ornithomimosauria. In *The Dinosauria* (second edition), D.B. Weishampel, P. Dodson and H. Osmolska, eds. (Berkeley: University of California Press), pp. 137-150.
22. Makovicky, P.J., Norell, M.A., Clark, J.M., and Rowe, T. (2003). Osteology and relationships of *Byronosaurus jaffei* (Theropoda: Troodontidae). *American Museum Novitates* 3402, 1-32.
23. Fu, G.B., Li, G.L., Ren, Y.G., Ren, Z.Y., and Ding, L.T. (2007). Early Cretaceous conchostracans from the Bayingebi Formation of Inner Mongolia, China. *Acta Palaeontologica Sinica* 46, 244-248.
24. Xu, X., Clark, J.M., Mo, J., Choiniere, J., Forster, C.A., Erickson, G.M., Hone, D.W., Sullivan, C., Eberth, D.A., and Nesbitt, S. (2009). A Jurassic ceratosaur from China helps clarify avian digital homologies. *Nature* 459, 940-944.
25. Novas, F.E. (1997). Anatomy of *Patagonykus puertai* (Theropoda, Avialae, Alvarezsauridae), from the Late Cretaceous of Patagonia. *Journal of Vertebrate Paleontology* 17, 137-166.
26. Suzuki, S., Chiappe, L.M., Dyke, G.J., Watabe, M., Barsbold, R., and Tsogtbaatar, K. (2002). A new specimen of *Shuvuuia deserti* Chiappe et al., 1998, from the Mongolian Late Cretaceous with a discussion of the relationships of alvarezsaurids to other theropod dinosaurs. *Contributions in Science* (Los Angeles) 494, 1-18.
27. Longrich, N.R., and Currie, P.J. (2009). *Albertonykus borealis*, a new alvarezsaur (Dinosauria: Theropoda) from the Early Maastrichtian of Alberta, Canada: implications for the systematics and ecology of the Alvarezsauridae. *Cretaceous Research* 30, 239-252.
28. Novas, F.E. (1996). Alvarezsauridae, Cretaceous maniraptorans from Patagonia and Mongolia. *Memoirs of the Queensland Museum* 39, 675-702.

29. Sues, H.-D., and Averianov, A. (2016). Ornithomimidae (Dinosauria: Theropoda) from the Bissekty Formation (Upper Cretaceous: Turonian) of Uzbekistan. *Cretaceous Research* 57, 90-110.
30. Rauhut, O.W.M., and Xu, X. (2005). The small theropod dinosaurs *Tugulusaurus* and *Phaedrolosaurus* from the Early Cretaceous of Xinjiang, China. *Journal of Vertebrate Paleontology* 25, 107-118.
31. Averianov, A., and Sues, H.-D. (2017). The oldest record of Alvarezsauridae (Dinosauria: Theropoda) in the Northern Hemisphere. *PLoS ONE* 12, e0186254.
32. Martinelli, A.G., and Vera, E. (2007). *Achillesaurus manazzonei*, a new alvarezsaurid theropod (Dinosauria) from the Late Cretaceous Bajo de la Carpa Formation, Río Negro Province, Argentina. *Zootaxa* 1582, 1-17.
33. Choiniere, J.N., Forster, C.A., and de Klerk, W.J. (2012). New information on *Nqwebasaurus thwazi*, a coelurosaurian theropod from the Early Cretaceous Kirkwood Formation in South Africa. *Journal of African Earth Sciences* 71-72, 1-17.
34. Makovicky, P.J., Apesteguiá, S., and Agnolín, F.L. (2005). The earliest dromaeosaurid theropod from South America. *Nature* 437, 1007-1011.
35. Prieto-Márquez, A., Stubbs, T.L., Benton, M.J., and Brusatte, S. (2016). Regional morphological disparity and rates of evolution in coelurosaurian theropod dinosaurs. *Journal of Vertebrate Paleontology* 36 (Supplement to 5), 208.
36. Gatesy, S.M. (1990). Caudofemoral musculature and the evolution of theropod locomotion. *Paleobiology* 16, 170-186.
37. Senter, P. (2005). Function in the stunted forelimbs of *Mononykus olecranus* (Theropoda), a dinosaurian anteater. *Paleobiology* 31, 373-381.
38. Zhou, Z.H. (1995). Is *Mononykus* a bird? *Auk* 112, 958-963.
39. Altangarel, P., Chiappe, L.M., Rinchen, B., Clark, J.M., and Norell, M.A. (1994). Skeletal morphology of *Mononykus olecranus* (Theropoda: Avialae) from the Late Cretaceous of Mongolia. *American Museum Novitates* 3105, 1-29.
40. MacFadden, B.J. (2005). Fossil horses-evidence for evolution. *Science* 307, 1728-1730.
41. Maddison, W.P., and Maddison, D.R. (2011). Mesquite: a modular system for evolutionary analysis. Version 2.75 Edition., p. <http://mesquiteproject.org>.
42. Norell, M.A., Clark, J.M., Turner, A., Makovicky, P.J., Barsbold, R., and Rowe, T. (2006). A new dromaeosaurid theropod from Ukhaa Tolgod (Omnogov, Mongolia). *American Museum Novitates* 3545, 1-51.
43. Turner, A., H., Makovicky, P.J., and Norell, M.A. (2012). A review of dromaeosaurid systematics and paravian phylogeny. *Bulletin of the American Museum of Natural History* 371, 1-206.
44. Zanno, L.E. (2010). A taxonomic and phylogenetic re-evaluation of Therizinosauria (Dinosauria: Maniraptora). *Journal of Systematic Palaeontology* 8, 503-543.
45. Zanno, L.E., and Makovicky, P.J. (2011). Herbivorous ecomorphology and specialization patterns in theropod dinosaur evolution. *Proceedings of the National Academy of Sciences of the United States of America* 108, 232-237.
46. Agnolín, F.L., Powell, J.E., Novas, F.E., and Kundrat, M. (2012). New alvarezsaurid (Dinosauria, Theropoda) from uppermost Cretaceous of north-western Patagonia with associated eggs. *Cretaceous Research* 35, 33-56.
47. Nesbitt, S.J., Clarke, J.A., Turner, A.H., and Norell, M.A. (2011). A small alvarezsaurid from the eastern Gobi Desert offers insight into evolutionary patterns in the Alvarezsauroidea. *Journal of Vertebrate Paleontology* 31, 144-153.
48. Goloboff, P.A., Farris, J.S., and Nixon, K.C. (2008). TNT, a free program for phylogenetic analysis. *Cladistics* 24, 774-786.
49. Goloboff, P.A. (1999). Analyzing large datasets in reasonable times: solutions for composite optima. *Cladistics* 15, 415-428.

50. Goloboff, P.A., Farris, J.S., Källersjö, M., Oxelman, B., Ramírez, M., and Szumik, C.A. (2003). Improvements to resampling measures of group support. *Cladistics* 19, 324-332.
51. Bremer, K. (1994). Branch support and tree stability. *Cladistics* 10, 295-304.
52. Bremer, K. (1988). The limits of amino acid sequence data in angiospermic phylogenetic reconstruction. *Evolution* 42, 795-803.
53. Turner, A.H., Nesbitt, S.J., and Norell, M.A. (2009). A large alvarezsaurid from the Late Cretaceous of Mongolia. *American Museum Novitates* 3648, 1-14.
54. Albert, M., *et, and al* (2014). Inkscape. (<http://www.inkscape.org/>).
55. Benson, R.B.J., and Choiniere, J.N. (2013). Rates of dinosaur limb evolution provide evidence for exceptional radiation in Mesozoic birds. *Proceedings of the Royal Society B: Biological Sciences* 280, 20131780.
56. Benson, R.B.J., Hunt, G., Carrano, M.T., and Campione, N. (2018). Cope's rule and the adaptive landscape of dinosaur body size evolution. *Palaeontology* 61, 13-48.
57. Campione, N.E., and Evans, D.C. (2012). A universal scaling relationship between body mass and proximal limb bone dimensions in quadrupedal terrestrial tetrapods. *BMC biology* 10, 1-21.
58. Carrano, M.T. (2006). Body-size evolution in the Dinosauria. In *Amniote paleobiology: perspectives on the evolution of mammals, birds, and reptiles.*, M.T. Carrano, T.J. Gaudin, R.W. Blob and J.R. Wible, eds. (Chicago: The University of Chicago Press), pp. 225-269.
59. Puttick, M.N., Thomas, G.H., and Benton, M.J. (2014). High rates of evolution preceded the origin of birds. *Evolution* 68, 1497-1510.
60. Lee, M.S.Y., Cau, A., Naish, D., and Dyke, G.J. (2014). Sustained miniaturization and anatomical innovation in the dinosaurian ancestors of birds. *Science* 345, 562-566.
61. Dececchi, A., and Larrson, H.C.E. (2013). Body and limb size dissociation at the origin of birds: Uncoupling allometric constraints across a macroevolutionary transition. *Evolution* 67, 2741-2752
62. Galton, P.M., and Jensen, J.A. (1979). A new large theropod dinosaur from the Upper Jurassic of Colorado. *Brigham Young University Geological Study* 26, 1-12.
63. Siegwarth, J.D., Lindbeck, R.A., Redman, P.D., Southwell, E.H., and Bakker, R.T. (1997). Giant carnivorous dinosaurs of the family Megalosauridae from the Late Jurassic Morrison Formation of eastern Wyoming. *Contributions from the Tate Museum Collections, Casper, Wyoming* 2, 1-33
64. Carrano, M.T., Benson, R.B.J., and Sampson, S.D. (2012). The phylogeny of Tetanurae (Dinosauria: Theropoda). *Journal of Systematic Palaeontology* 10, 211-300.
65. Birch, S.H., and Carrano, M.T. (2012). An articulated pectoral girdle and forelimb of the abelisaurid theropod *Majungasaurus crenatissimus* from the Late Cretaceous of Madagascar. *Journal of Vertebrate Paleontology* 32, 1-16.
66. Carrano, M.T. (2007). The appendicular skeleton of *Majungasaurus crenatissimus* (Theropoda, Abelisauridae) from the late Cretaceous of Madagascar. *Society of Vertebrate Paleontology Memoir* 8, 163-170.
67. Novas, F.E. (1993). New information on the systematics and postcranial skeleton of *Herrerasaurus ischigualastensis* (Theropoda: Herrerasauridae) from the Ischigualasto Formation (Upper Triassic) of Argentina. *Journal of Vertebrate Paleontology* 13, 400-423.
68. Colbert, E.H. (1989). The Triassic dinosaur *Coelophysis*. *Mus. N. Ariz. Bull.* 57, 1-160.
69. Raath, M.A. (1969). A new coelurosaurian dinosaur from the Forest Sandstone of Rhodesia. *Arnoldia (Rhodesia)* 4, 1-25.
70. Osmólska, H., and Roniewicz, E. (1970). Deinoceridae, a few family of theropod dinosaurs. *Acta Palaeontologica Polonica* 21, 5-19.
71. Osmólska, H., Roniewica, H., and Barsbold, R. (1972). A new dinosaur, *Gallimimus bullatus* n. gen., n. sp. (Ornithomimidae) from the Upper Cretaceous of Mongolia. *Palaeontologia Polonica* 27, 103-143.

72. Russell, D.A. (1972). Ostrich dinosaurs from the Late Cretaceous of western Canada. *Canadian Journal of Earth Sciences* 9, 375-402.
73. Kobayashi, Y., and Barsbold, R. (2005). Reexamination of a primitive ornithomimosaur, *Garudimimus brevipes* Barsbold, 1981 (Dinosauria: Theropoda), from the Late Cretaceous of Mongolia. *Canadian Journal of Earth Sciences* 42, 1501-1521.
74. Barsbold, R. (1988). A new Late Cretaceous ornithomimid from the Mongolian People's Republic. *Paleontological Journal* 22, 124-127.
75. Jin, L., Chen, J., and Godefroit, P. (2012). A new basal ornithomimosaur (Dinosauria: Theropoda) from the Early Cretaceous Yixian Formation, Northeast China. In *Bernissart Dinosaurs and Early Cretaceous Terrestrial Ecosystems*, P. Godefroit, ed. (Bloomington: Indiana University Press), pp. 467-487.
76. Middleton, K.M., and Gatesy, S.M. (2000). Theropod forelimb design and evolution. *Zoological Journal of the Linnean Society* 128, 149-187.
77. Grafen, A. (1989). The phylogenetic regression. *Philosophical Transactions of the Royal Society of London B* 326, 119-157.
78. Pinheiro, J., Bates, D., DebRoy, S., Sarkar, D., and Team, R.C. (2014). nlme: Linear and Nonlinear Mixed Effects Models_. R package version 3.1-117.
79. Paradis, E., Claude, J., and Strimmer, K. (2004). APE: analyses of phylogenetics and evolution in R language. *Bioinformatics* 20, 289–290.
80. Team, R.C. (2017). R: A language and environment for statistical computing. . (Vienna, Austria: R Foundation for Statistical Computing).
81. Felsenstein, J. (1985). Phylogenies and the comparative method. *Am Nat* 125, 1-15.
82. Garland, T.J., and Ives, A.R. (2001). Using the past to predict the present: confidence intervals for regression equations in phylogenetic comparative methods. *American Naturalist* 155, 346–364.
83. Pagel, M. (1999). Inferring the historical patterns of biological evolution. *Nature* 401, 877-884.
84. O'Leary, M.A., and Kaufman, S.G. (2012). MorphoBank 3.0: Web application for morphological phylogenetics and taxonomy. (<http://www.morphobank.org>).

Figure legend

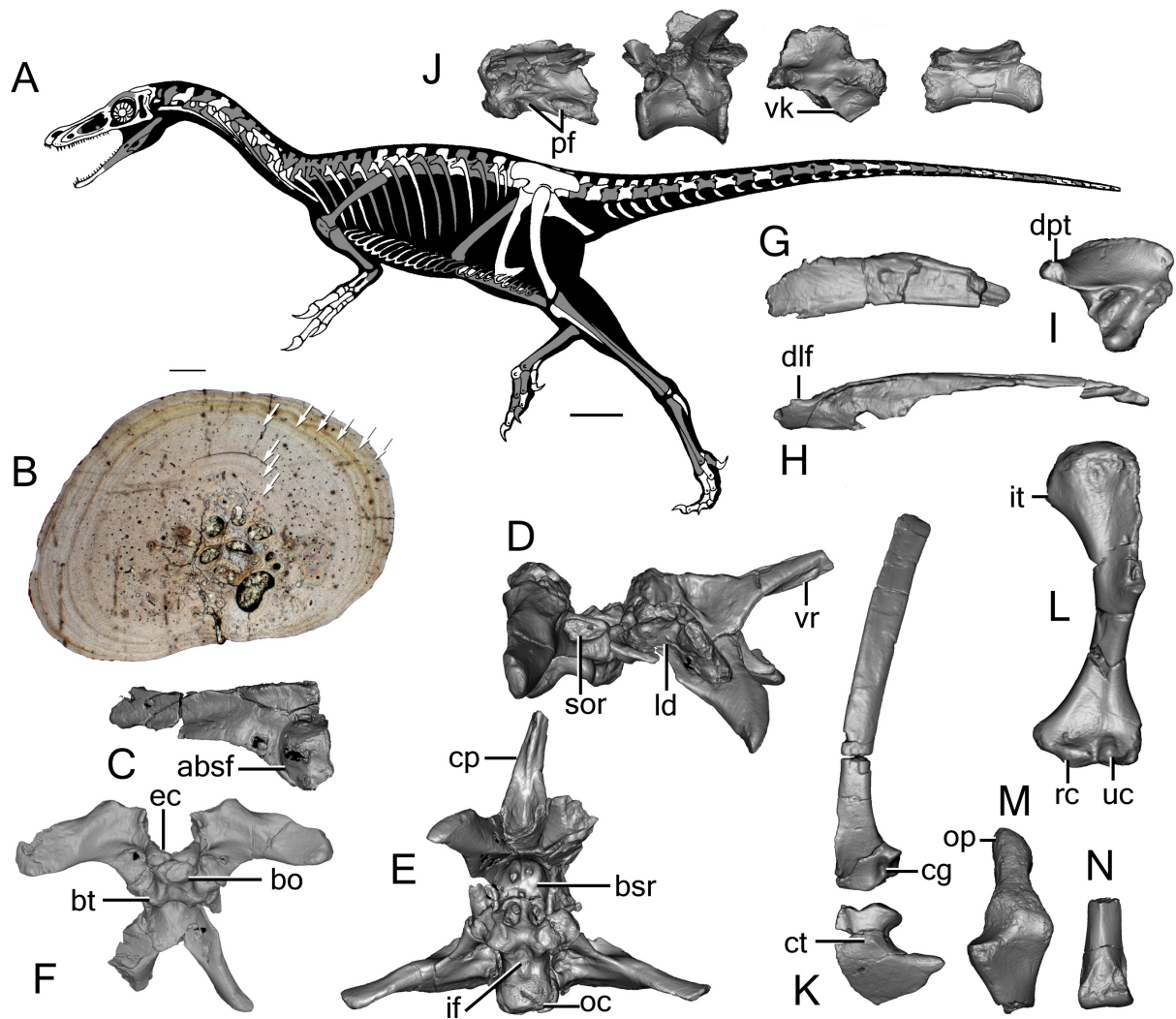


Figure 1. Skeletal anatomy of *Xiyunykus pengi* IVPP V22783.

(A) Skeletal silhouette showing preserved bones (in gray).

(B) Histological thin-section of the fibula. Arrows denote growth lines used to age the specimen (see SI for a detailed explanation).

(C) Left frontal in dorsal view.

(D-G) Partial braincase in left lateral (D), ventral (E) and posterior (F) views.

(G, H) Right dentary (G) and right surangular (H) in lateral view.

(I) Left articular in dorsal view.

(J) A middle cervical (left), a middle dorsal (middle left), the last sacral (middle right) vertebra, and a posterior caudal (right) in left lateral view.

(K) Left scapula and coracoid in lateral view.

(L) Left humerus in anterior view.

(M) Right ulna in anterior view.

(N) Partial left metatarsal III in ventral view.

Scale bar equals 100 mm for (A) and 500 μ m for (B). Abbreviations: absf, anterior border of

supratemporal fossa; bo, basioccipital; bt, basal tuber; bsr, basisphenoid recess; cg, curved groove; cp, cultriform process; ct, coracoid tubercle; dlf, dorsolateral flange; dpt, dorsomedially projecting tab; ec, exoccipital; if, infracondylar fossa; it, internal tuberosity; ld, lateral depression; oc, occipital condyle; op, olecranon process; pf, pneumatic fossa; rc, radial condyle; sor, subotic recess; uc, ulnar condyle; vk ventral keel; vr, ventral ridge. No scale for (C)-(N).

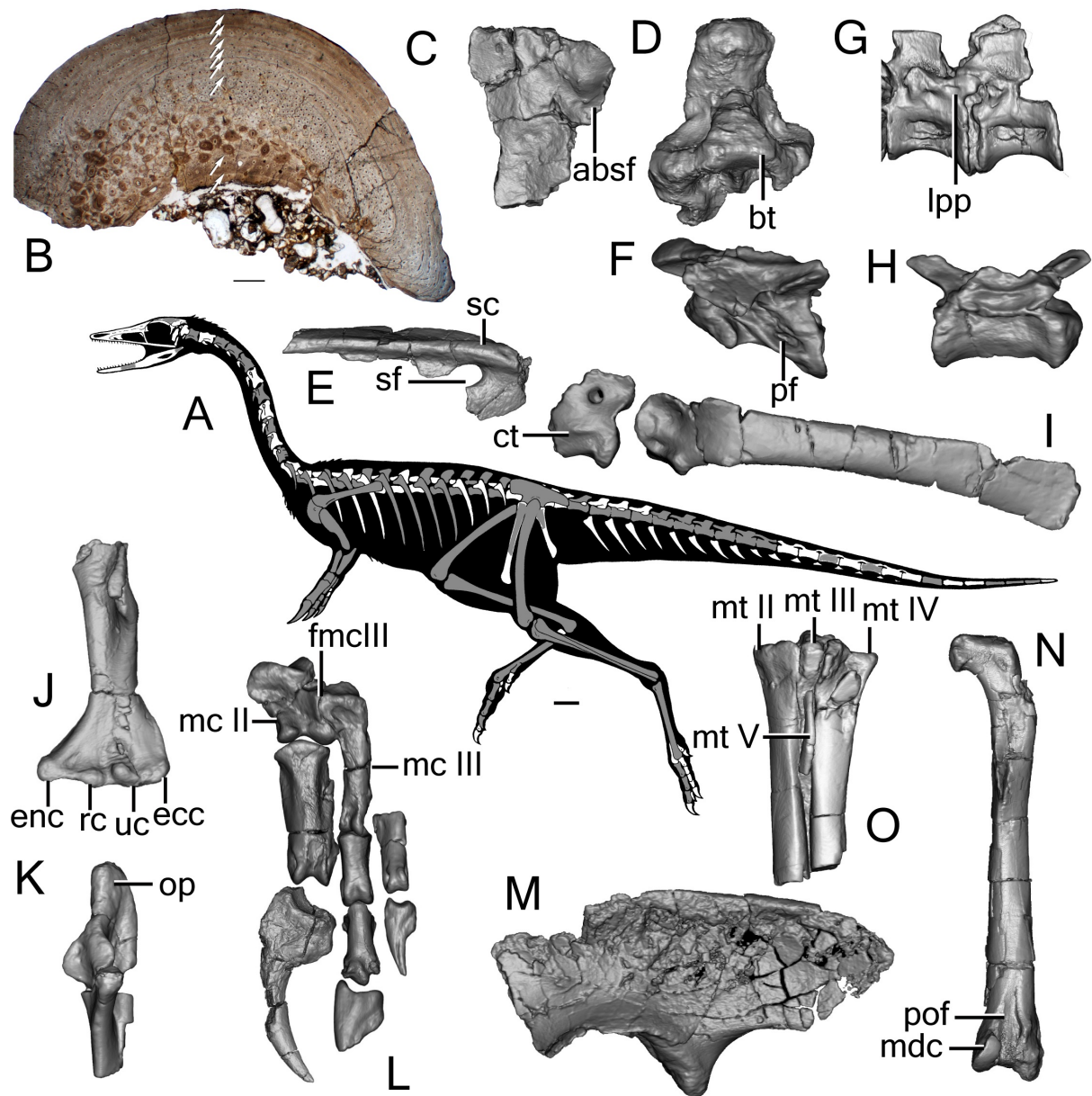


Figure 2. Skeletal anatomy of *Bannykus wulatensis* IVPP V25026.

- (A) Skeletal silhouette showing preserved bones (in gray).
 (B) Histological thin-section of the fibula.
 (C) Left frontal in dorsal view.
 (D) Basioccipital in ventral view.

(E) Left surangular in lateral view.

(F-H) A middle cervical (F), a middle dorsal (G), and a middle caudal (H) vertebra in left lateral view.

(I) Left scapula and coracoid in lateral view.

(J, K) Left humerus (J), left ulna (K) in anterior view.

(L) Left manus in anterior view.

(M) Left ilium in lateral view.

(N) Right femur in posterior view.

(O) Right metatarsals in posterior view.

Scale bar equals 100 mm for (A) and 500 μ m for (B). Abbreviations: absf, anterior border of supratemporal fossa; bt, basal tuber; ct, coracoid tubercle; ecc, ectepicondyle; enc, entepicondyle; fmcIII, facet for metacarpal III; lpp, laterally protruding parapophysis; mc II-III, metacarpals II-III; mdc, medial distal condyle; mt II-V, metatarsals II-V; pof, popliteal fossa; oc, occipital condyle; op, olecranon process; pf, pneumatic fossa; rc, radial condyle; uc, ulnar condyle; sc, surangular crest; sf, surangular foramen.

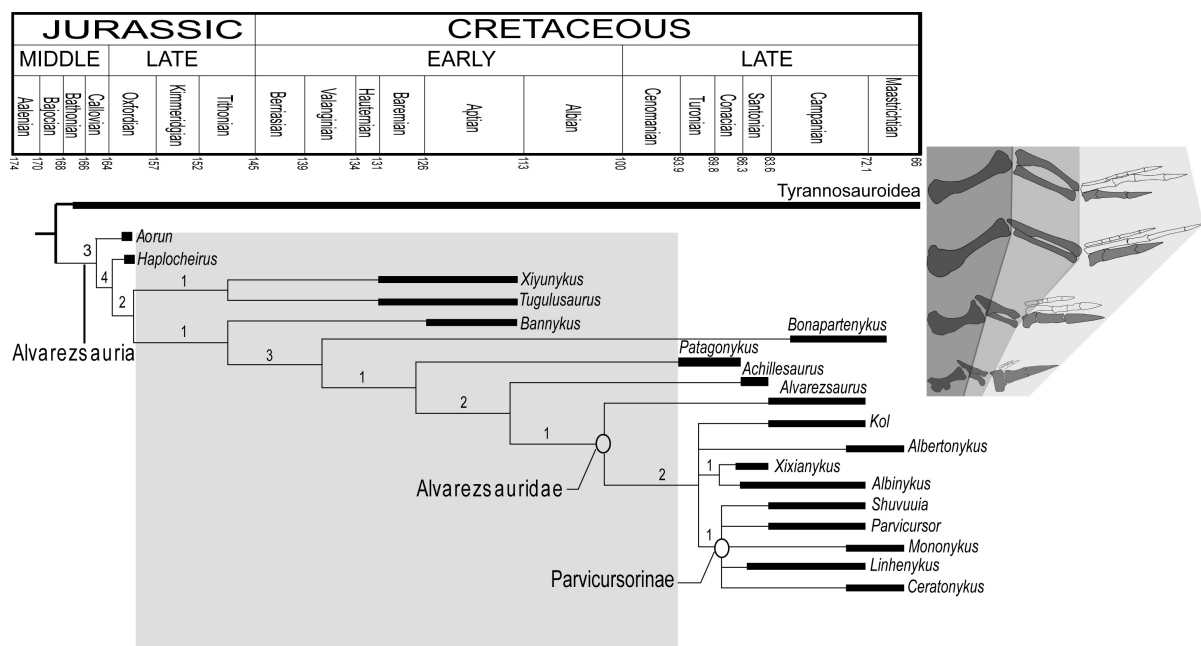


Figure 3. Time-calibrated simplified theropod phylogeny showing evolution of alvarezsaurian forelimb.

Forelimbs scaled to the femoral length of the generalized basal coelurosaur *Guanlong* (top) and selected alvarezsaurians. Note the medial finger (in gray) enlargement and lateral finger reduction in *Haplocheirus* (upper middle), significant forelimb shortening and further forelimb modification in *Bannykus* (lower middle), and extremely shortened and specialized forelimb in *Shuvuuia* (bottom).

Numbers above nodes indicate Bremer Support values when *Kol ghuva* is excluded from support calculation. Grey rectangle indicates the temporal area where the previous gap in alvarezsaurian fossil records. See also Figures S1 and S2.

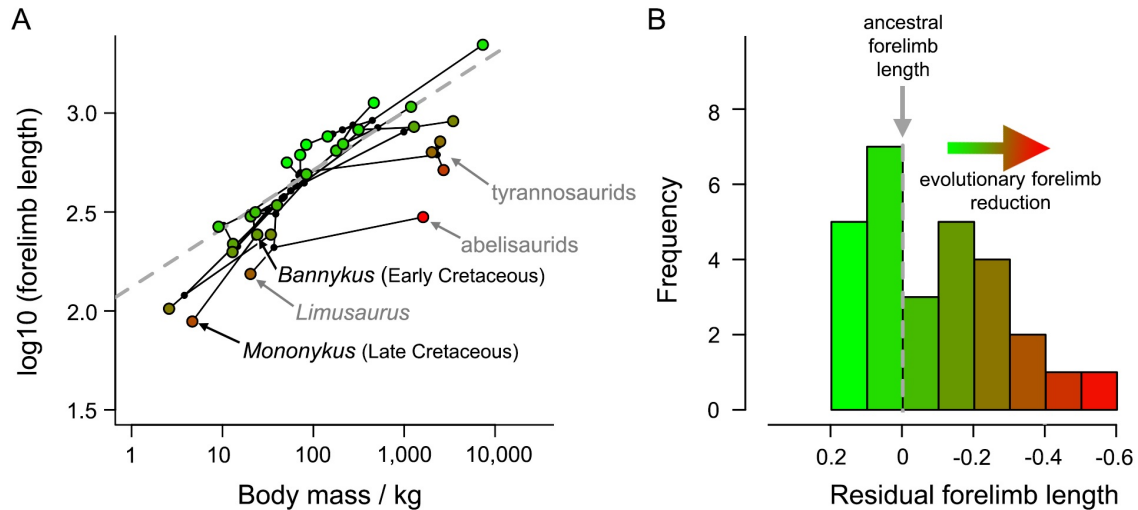


Figure 4. Relationship of forelimb length with body mass in non-paravian theropods and reduction of the alvarezsaurian forelimb.

(A) Phylomorphospace showing relationship of partial forelimb length with body mass, with points colored according to residuals from the phylogenetic generalized least squares regression (dashed, gray line; $\log_{10}(\text{arm length}) = 0.30 * \log_{10}(\text{body mass} + 2.12)$, $p < 0.001$, $N = 28$; Table S2).

(B) Histogram of residuals from the regression in (A) showing the extent of forelimb reduction in alvarezsaurians, and that theropods in general underwent greater proportional forelimb reduction than enlargement compared to their ancestor (ancestor residual = 0.0). See also Figure S3.

STAR METHODS

CONTACT FOR REAGENT AND RESOURCE SHARING

Further information and requests for resources and reagents should be directed to and will be fulfilled by the Lead Contact, Xing Xu (xu.xing@ivpp.ac.cn)

EXPERIMENTAL MODEL AND SUBJECT DETAILS

The experimental subject is the fossilized holotypes of the alvarezsaurian dinosaurs *Xiyunykus pengi* (IVPP V22783) and *Bannykus wulatensis* (IVPP V25026), which are housed at the Institute of Vertebrate Paleontology and Paleanthropology, Beijing, China. The sex states of both specimens are unknown, and both specimens are inferred to be at the sub-adult ontogenetic stage.

METHOD DETAILS

CT images.

IVPP V22783 and IVPP V25026 were scanned using both 225kv (for small skeletal elements) and 450 kV (for large skeletal elements) micro-computerized-tomography apparatus (developed by the Institute of High Energy Physics, Chinese Academy of Sciences (CAS)) at the Key Laboratory of Vertebrate Evolution and Human Origins, CAS. A total of 720 transmission images were reconstituted into a stack of 1563 slices each measuring 2048*2048 pixels for each small-sized skeletal element, and a total of 1,440 transmission images were reconstituted into a stack of 2,048 slices each measuring 2048*2048 for each large-sized skeletal element, using two-dimensional reconstruction software developed by the Institute of High Energy Physics, CAS. 3D segmentation of the CT data was performed using Mimics (Version 10.01).

Histology.

Histological thin sections of long bones were made using standard techniques. To minimize damage to the specimens, the fibulae of IVPP V22783 and IVPP V25026 were each dismantled at a natural break and then sectioned 5 mm from the preserved distal end of the proximal segment to ensure a nearly complete cross section. The proximal end of the distal segment was then re-attached to the proximal segment. Subsequently, both samples were embedded in resin, and diaphyseal transverse thin-sections were cut using a diamond circular saw fitted with a diamond-tipped wafering blade. One surface of each section was smoothed with a wheel grinder/polisher, and then ground manually using grinding powder (600 grit) to produce a smooth texture ideal for gluing to a glass slide. The section was then cut to a thickness of about 250 μm with a diamond circular saw before being ground further to the desired final thickness of 50–80 μm , leaving the exposed surface of the section smooth. Each slide was then cleaned in a water-filled ultrasonic cleaner to remove microscopic grit, and finally capped with a glass cover slip. The completed thin sections were studied in normal and polarized light.

Phylogenetic analysis.

The data matrix was assembled in Mesquite v 3.03 [41], and comprises 113 species-level theropod taxa and 594 morphological characters (see below). Taxa were selected to broadly sample species from higher taxa within Maniraptora as well as from non-maniraptoran theropod outgroups, and were scored based on both primary observations of specimens and the literature. Character definitions were

primarily based on previous work, largely by the authors, members of the Theropod Working Group [8, 9, 12, 20, 22, 33, 42-45], and alvarezsaur workers [1, 5, 12, 27, 32, 46, 47]. Twenty-three new characters were added to the dataset based on observations generated from this research (Data S1).

The matrix was subjected to phylogenetic analysis under the parsimony optimality criterion in TNT [48]. The search strategy employed alternating rounds of Sectorial Searches and Tree Drift [49] with default settings. The search for optimal topologies was terminated after stabilizing the consensus of most parsimonious topologies five times with a factor of 75. This strategy resulted in 144 most parsimonious trees (MPTs) of length 3202 steps, consistency index 0.218 and retention index 0.602. Further TBR swapping and Tree Drifting of the MPTs revealed additional, non-identical most-parsimonious topologies, but did not improve the length nor result in decreased resolution of the strict consensus relative to the initial 144 MPTs.

Strict consensus topologies (Figure S1) were calculated in TNT [48, 50] using this pool of 144 MPTs. Absolute Bremer support [51, 52] for nodes in the strict consensus was calculated in TNT and used a pool of trees created by TBR swapping on the 144 MPTs recovered from the initial analysis, saving suboptimal trees by up to 10 steps, and saving 10,000 trees. An additional Bremer support analysis was conducted using an identical pool of trees, but excluding the alvarezsaurid taxon *Kol ghuva* [53] from support calculations (Figure S1). Synapomorphies common to all trees (see below) were explored using TNT [48, 50]. Tree diagrams were edited for clarity and produced for publication using InkScape [54].

Biogeographic inference.

To reconstruct the biogeographic history of global alvarezsaurians, a statistical dispersal-vicariance analysis (SDVA) of Alvarezsauria was performed in the program RASP, where maximum parsimony was used as the standard criterion. This analysis was conducted with the maximum areas set to 3 and maximum reconstructions set to 100, under the “Allow Reconstruction” and “Allow Extinction” options. The phylogenetic framework used in the SDVA comes from the strict consensus tree produced by the traditional search with the TBR branch-swapping algorithm in the program TNT. Prior to the SDVA, the codes of the strict consensus with a file format of TREES were divided into data of 12 most parsimonious trees that denote no polytomies in topologies (Figure S2). Here, ranges of the potential ancestral area(s) for each internal node of Alvarezsauria are restricted to Asia (A), South America (B), North America (C), Asia–North America (AC) and South America–North America (BC). The direct land link between Asia and South America is considered unavailable during the Jurassic and Cretaceous, although a land link between the two continents would have occurred through North America during that period (see Dr Ronald C. Blakey’s online database at <https://deeptimemaps.com/>).

Analysis of forelimb allometry and reduction.

Dataset. We analysed patterns of forelimb evolution using an extended version of the dataset of ref. [55], combined with mass estimates from ref. [56]. These mass estimates were based on the scaling relationship of femoral robustness presented by Campione et al. [19], an approach that has been shown to be relatively independent of phylogeny and limb orientation in extant tetrapods [57]. As such, it should provide a reasonable index of body size that is independent of body proportions. Many previous studies instead used length measurements, predominantly femoral length, as proxies for dinosaur body size (e.g. refs. [58-60]; and trunk length: [61]). The use of femoral length is particularly problematic for studies of limb evolution, in which it would be difficult to distinguish changes in

relative hindlimb length, or hindlimb proportions from proportional changes in just forelimb length (also discussed in ref. [61]).

Most of our sets of measurements came from single individuals, with two exceptions. First, measurements from two similarly-sized individuals of *Torvosaurus tanneri* were compiled to form a composite of the two specimens, using forelimb measurements from ref. [62] and body mass based on the femur of a specimen reported by Siegwarth et al. 1997 [63]; see Carrano et al 2012 [64] for referral of these specimens to a single species). Second, forelimb measurements from one specimen of *Majungasaurus* [65] were combined with a body mass estimate for a similar-sized individual (FMNH PR 2278; ref. [66]). These steps were considered to be important because otherwise we would not have complete data from any member of Megalosauridae or Abelisauridae, clades with large body size and proportionally reduced forelimbs.

Total forelimb length was based on the summed lengths of the humerus, radius (sometimes an estimate based on measurement of the equivalent portion of the ulna), and longest digit. The longest digit is typically digit II in non-tetanuran theropods, and is digit III in most tetanurans (following the digital homologies used here, presented by ref. [24]; note that our digit III of tetanurans has been considered as homologous to digit II of non-tetanurans by many earlier studies). This is subject to some variation, as described below. Digit lengths were calculated excluding the ungual phalanx for two reasons. First, the ungual phalanx was frequently disarticulated and not preserved. Second, methods of reporting ungual lengths vary among publications. Some descriptions report proximodistal lengths along curved surfaces of the phalanx, whereas others report straight-line distances.

In total, N = 26 non-paravian theropod species in our dataset preserve sufficiently complete hand skeletons that the lengths of digits II and III (in non-tetanurans) or III and IV (in tetanurans) can be compared (including metacarpals and excluding ungual phalanges). Digit II (non-tetanurans) or III (tetanurans) is the longest digit in most of these species (N = 19), a condition that seems to be widespread across theropod phylogeny. Nevertheless, digit IV is longest in early theropods, and this condition is likely primitive for Theropoda (*Herrerasaurus* [67]; and coelophysoids: *Coelophysis bauri* and *Coelophysis rhodesiensis* [68, 69]). Digit IV is longest in some ornithomimosaur [70-75]. Based on this information, we used metacarpal II and digit II for computing total arm length in most non-tetanuran theropods, and metacarpal III and digit III in most tetanurans (following the digit homologies of ref. [24]). We used digit II and metacarpal II for *Mononykus*, the only parvicursorine that was sufficiently complete to be included in our analyses. And we used digit III and metacarpal III for *Herrerasaurus* and coelophysoids, and digit IV and metacarpal IV for ornithomimosaur.

In total, N = 28 non-paravian theropod species included in our phylogeny provided estimates of both body mass and complete forelimb length (summed humerus, radius, metacarpal and digit lengths). This is fewer than the N = 46 species that provide information on both body mass and partial forelimb length (summed humerus, radius and metacarpal lengths, omitting digit lengths). Partial forelimb length was also analysed here, for comparison with previous studies of theropod forelimb evolution (e.g. [55, 61, 76]; but see [59] for an example using complete forelimb length).

Phylogenetic regression of forelimb length on body mass. We used phylogenetic generalized least squares regression (pGLS [77]) to quantify the allometric relationship of forelimb length on body mass in non-paravian theropods (Figure S3 and Table S2). Data were log₁₀-transformed prior to analysis, and non-paravians were analysed because previous studies identified a change in this relationship among paravian theropods, associated with an evolutionary increase in forelimb length

[59]. This approach was implemented using the packages nlme 3.1-131 [78] and ape 4.1 [79] in the R version 3.3.3 [80]. We used a version of the phylogenies presented by Benson et al. 2018 [56], resolving polytomies at random, then calibrating the tree to time by (1) randomly assigning numerical ages to taxa from a uniform distribution between their maximum and minimum possible ages of occurrence, and (2) extending zero-length branches by setting a minimum branch duration of 1 Ma. The phylogeny was further modified by the addition of the alvarezsauroids *Bannykus*, *Xiyunykus* and *Tugulusaurus* following the phylogenetic results obtained in the present work. Results are reported across a sample of 100 time-calibrated phylogenies.

The pGLS method uses the covariances expected among taxa given a phylogenetic tree to modify the assumptions of ordinary least-squares regression. Principally, and unlike in ordinary least-squares, observations of species in a phylogeny have varying levels of non-independence from each other due to phylogenetic relationships. When Brownian motion [81] is assumed, pGLS is mathematically analogous to ordinary least-squares regression of phylogenetic independent contrasts [82]. This represents a model in which strong phylogenetic signal is present in a relationship of interest due to evolution along lineages, causing the intercept of the relationship between variables to drift at a constant, non-directional and stochastic rate on the phylogeny.

Estimation of the phylogenetic signal in the relationship between forelimb length and body mass was done using Pagel's λ [83]. This is a parameter that scales the strength of phylogenetic signal between the inferred phylogeny with its branch lengths ($\lambda = 1$; i.e. Brownian motion), and a star phylogeny in which all taxa effectively represent independent observations ($k = 0$; for ultrametric trees; equivalent to ordinary least squares regression).

DATA AND SOFTWARE AVAILABILITY

The holotypes of the alvarezsaurian dinosaurs *Xiyunykus pengi* (IVPP V22783) and *Bannykus wulatensis* (IVPP V25026) are accessible to both professionals and the general public. The matrix for phylogenetic analysis is given in Data S1, and is also available on Morphobank [84] at the following link: <http://morphobank.org/permalink/?P2127>. Mesquite V 3.03 is available at <http://www.mesquiteproject.org/>; TNT software is available at <https://cladistics.org/tnt/>; R software is available at <https://www.r-project.org/>; RASP is available at <http://mnh.scu.edu.cn/soft/blog/RASP/>.

NOMENCLATURE.

This published work and the nomenclatural acts it contains have been registered in ZooBank, the proposed online registration system for the International Code of Zoological Nomenclature. The ZooBank life science identifiers can be resolved and the associated information viewed by appending the life science identifiers to the prefix <http://zoobank.org/>. The life science identifiers (LSID) for this publication are urn:lsid:zoobank.org:pub:E60C9E1C-AEFF-4589-8C5A-A32C664DFD5E.

Data S1. Supplementary text and data for phylogenetic analysis (Related to Results and Discussion, and STAR methods).

Supplementary information

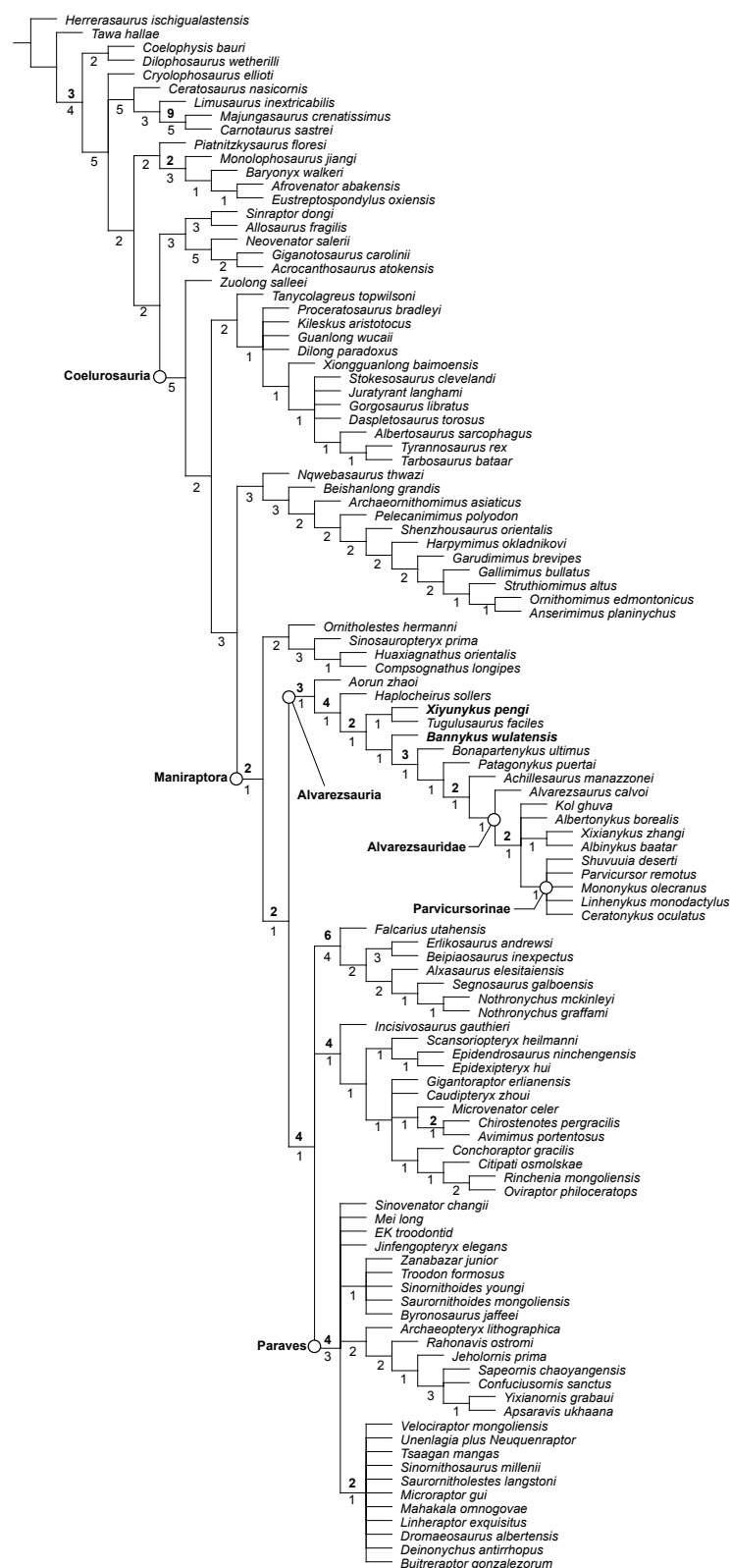


Figure S1. Strict consensus of 144 MPTs (Related to STAR Methods). Numbers below nodes indicate Bremer Support values. Bolded numbers above nodes indicate reduced Bremer Support values when *Kol ghuvu* is excluded from support calculation. Open circles with bolded names indicate

selected clades of interest. Synapomorphies of these clades discussed in text. Bolded italicized species names indicate phylogenetic positions of new taxa in this study.

Optimal reconstruction:

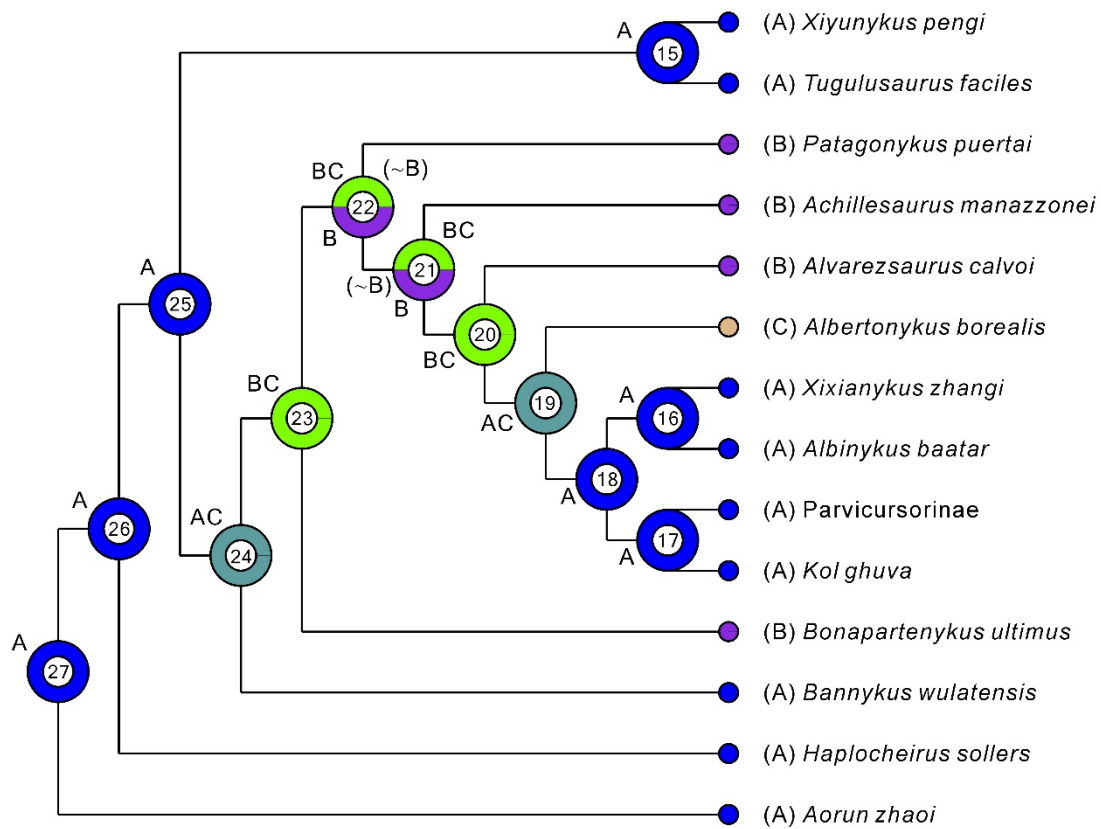


Figure S2. Optimal most parsimonious tree of Alvarezsauria showing the possible ancestral area(s) of each node, based on the result of the SDVA using RASP (Related to STAR Methods).

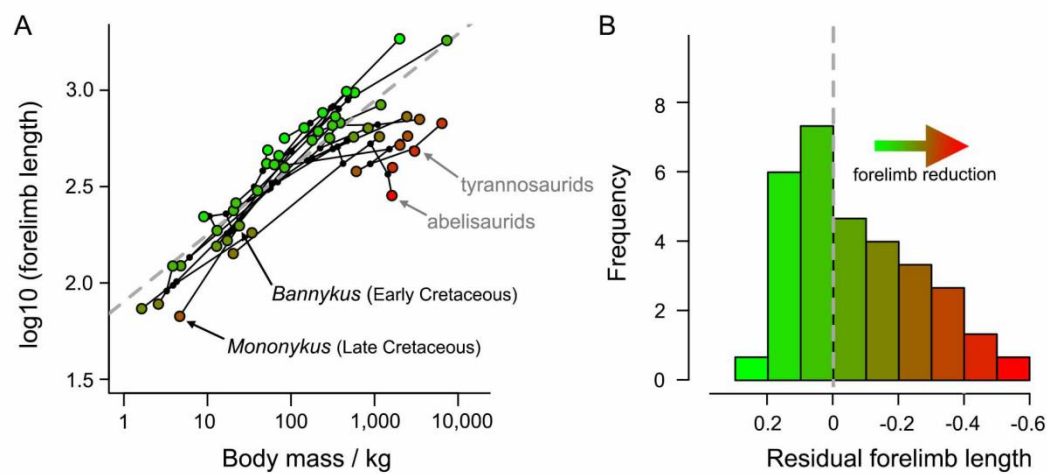


Figure S3. Theropod forelimb reduction (Related to STAR Methods). (A) Phylomorphospace showing relationship of partial forelimb length with body mass with points colored according to residuals from the pGLS regressions (dashed, grey line; coefficients in Table S3). (B) Histogram of residuals from the regression in (A) showing that theropods underwent greater proportional forelimb reduction than enlargement compared to their ancestor (residuals = 0.0).

	IVPP V22783	IVPP V25026	*esti
Surangular length/width	126/9	?/8	mate
Frontal width	13.5	11.5	d
Occipital condyle transverse diameter	10.3	8.7	leng
Anterior cervical centrum length	28	36	th;
Mid-posterior cervical centrum length	33	42	all
Posteriormost cervical centrum length	22		cent
Anteriormost dorsal centrum length	23	28*	rum
Anterior-middle dorsal centrum length	24		heig
Middle dorsal centrum length	28	34	hts
Posterior dorsal centrum length	27	41	and
Anterior caudal centrum length	29	30	widt
Anterior-middle caudal centrum length	30	36	hs
Middle caudal centrum length	31		were
Posterior caudal centrum length	25	22	mea
Scapular length	145*	141	sure
Coracoidal anteroposterior length	56*		d at
Humeral length	87	95	the
Humeral distal end maximum width	29	43	post
Radius length	59*	58.7	erior
Ulna length		85*	end
Metacarpal II length		24	and
Metacarpal II width		24	cent
Metacarpal III length		46	rum
Metacarpal III width		14	leng
Manual phalanx II-1 length		48	th
Manual phalanx II-2 length		64	mea
Manual phalanx III-1 length		26	sure
Manual phalanx III-2 length		27	d
Femoral length	208*	255	excl
Femoral distal end mediolateral width	40	45	udin
Tibial length	241	270	g
Tibial distal end maximum width	38	47	the
Metatarsal III length	134*	164	ante
			rior
condyle.			

Table S1. Selected measurements of *X. pengi* and *B. wulatensis* (Related to Figures 1 and 2, and Results and Discussion)

Model	N _{taxa}	R ²	λ	Variable	Coefficient	p-value
Complete arm length ~ body mass	28	0.64 (0.57–0.71)	0.98 (0.97–1.00)	(intercept)	2.12 (2.07–2.14)	<0.001*
				arm length	0.30 (0.29–0.32)	<0.001*
Partial arm length ~ body mass	47	0.79 (0.76–0.82)	0.97 (0.95–0.99)	(intercept)	1.92 (1.8–1.92)	<0.001*
				arm length	0.35 (0.33–0.37)	<0.001*

Table S2. Results of pGLS regression of arm length on body mass (both log₁₀-transformed) (Related to STAR Methods). Median values for analyses using 100 different time-scaled phylogenies are shown, with the full range of returned values in brackets. R² is the generalised R² of Nagelkerke (1991) obtained by comparison to an intercept-only null model.

Supplemental References

- S1. Huene, F.v. (1914). Das natürliche system der Saurischia. Zentralblatt Mineralogie, Geologie, und Palaeontologie B 1914, 154-158.
- S2. Gauthier, J. (1986). Saurischian monophyly and the origin of birds. Memoirs of the California Academy of Sciences 8, 1-55.
- S3. Bonaparte, J.F. (1991). The vertebrate fossils of the Rio Colorado Formation, from the city of Neuquén and surrounding areas, Upper Cretaceous, Argentina (Translated from Spanish). Paleontología 4, 17-123.
- S4. Agnolin, F.L., Powell, J.E., Novas, F.E., and Kundrat, M. (2012). New alvarezsaurid (Dinosauria, Theropoda) from uppermost Cretaceous of north-western Patagonia with associated eggs. Cretaceous Research 35, 33-56.
- S5. Karkhu, A.A., and Rautian, A.S. (1996). A new family of Maniraptora (Dinosauria: Saurischia) from the Late Cretaceous of Mongolia. Paleontological Journal 30, 583–592.
- S6. Sereno, P.C. (1997). The origin and evolution of dinosaurs. Annual Review of Earth and Planetary Sciences 25, 435-489.
- S7. Norell, M.A., Clark, J.M., and Makovicky, P.J. (2001). Phylogenetic relationships among coelurosaurian dinosaurs. In New perspectives on the origin and evolution of birds, J. Gauthier and L.F. Gall, eds. (New Haven: Yale University Press), pp. 49-67.
- S8. Kirkland, J.I., Zanno, L.E., Sampson, S.D., Clark, J.M., and DeBlieux, D.D. (2005). A primitive therizinosauroid dinosaur from the Early Cretaceous of Utah. Nature 435, 84-87.
- S9. O'Leary, M.A., and Kaufman, S.G. (2012). MorphoBank 3.0: Web application for morphological phylogenetics and taxonomy. (<http://www.morphobank.org>).
- S10. Xu, X., Clark, J.M., Mo, J., Choiniere, J., Forster, C.A., Erickson, G.M., Hone, D.W., Sullivan, C., Eberth, D.A., and Nesbitt, S. (2009). A Jurassic ceratosaur from China helps clarify avian digital homologies. Nature 459, 940-944.
- S11. Carrano, M.T., Benson, R.B.J., and Sampson, S.D. (2012). The phylogeny of Tetanurae (Dinosauria: Theropoda). Journal of Systematic Palaeontology 10, 211-300.
- S12. Brusatte, S.L., Lloyd, G.T., Wang, S.C., and Norell, M.A. (2014). Gradual assembly of avian body plan culminated in rapid rates of evolution across the dinosaur-bird transition. Current Biology 24, 2386-2392.
- S13. Choiniere, J.N., Clark, J.M., Forster, C.A., Norell, M.A., Eberth, D.A., Erickson, G.M., Chu, H., and Xu, X. (2014). A juvenile specimen of a new coelurosaur (Dinosauria: Theropoda) from the Middle–Late Jurassic Shishugou Formation of Xinjiang, People's Republic of China. Journal of Systematic Palaeontology 12, 177-215.
- S14. O'Connor, J., and Sullivan, C. (2014). Reinterpretation of the Early Cretaceous maniraptoran (Dinosauria: Theropoda) *Zhongornis haonae* as a scansoriopterygid-like non-avian, and morphological resemblances between scansoriopterygidfs and basal oviraptorosaurs. Vertebrata Pal Asiatica 52, 3-30.
- S15. Choiniere, J.N., Xu, X., Clark, J.M., Forster, C.A., Guo, Y., and Han, F. (2010). A basal alvarezsaurid theropod from the early Late Jurassic of Xinjiang, China. Science 327, 571-574.
- S16. Choiniere, J.N., Forster, C.A., and de Klerk, W.J. (2012). New information on *Nqwebasaurus thwazi*, a coelurosaurian theropod from the Early Cretaceous Kirkwood Formation in South

- Africa. *Journal of African Earth Sciences* 71-72, 1-17.
- S17. Zanno, L.E. (2010). A taxonomic and phylogenetic re-evaluation of Therizinosauria (Dinosauria: Maniraptora). *Journal of Systematic Palaeontology* 8, 503-543.
- S18. Choiniere, J., Clark, J., Forster, C., and Xu, X. (2010). A basal coelurosaur (Dinosauria: Theropoda) from the Late Jurassic (Oxfordian) of the Shishugou Formation in Wucuiwan, People's Republic of China. *Journal of Vertebrate Paleontology* 30, 1773-1796.
- S19. Rauhut, O.W.M., and Xu, X. (2005). The small theropod dinosaurs *Tugulusaurus* and *Phaedrolosaurus* from the Early Cretaceous of Xinjiang, China. *Journal of Vertebrate Paleontology* 25, 107-118.
- S20. Lee, M.S.Y., and Worthy, T.H. (2012). Likelihood reinstates *Archaeopteryx* as a primitive bird. *Biology letters* 8, 299-303.
- S21. Longrich, N.R., and Currie, P.J. (2009). *Albertonykus borealis*, a new alvarezsaur (Dinosauria: Theropoda) from the Early Maastrichtian of Alberta, Canada: implications for the systematics and ecology of the Alvarezsauridae. *Cretaceous Research* 30, 239-252.
- S22. Nesbitt, S.J., Clarke, J.A., Turner, A.H., and Norell, M.A. (2011). A small alvarezsaurid from the eastern Gobi Desert offers insight into evolutionary patterns in the Alvarezsauroidea. *Journal of Vertebrate Paleontology* 31, 144-153.
- S23. Martinelli, A.G., and Vera, E. (2007). *Achillesaurus manazzonei*, a new alvarezsaurid theropod (Dinosauria) from the Late Cretaceous Bajo de la Carpa Formation, Río Negro Province, Argentina. *Zootaxa* 1582, 1-17.
- S24. Turner, A.H., Nesbitt, S.J., and Norell, M.A. (2009). A large alvarezsaurid from the Late Cretaceous of Mongolia. *American Museum Novitates* 3648, 1-14.
- S25. Naish, D., and Dyke, G.J. (2004). *Heptasteornis* was no ornithomimid, troodontid, dromaeosaurid or owl: the first alvarezsaurid (Dinosauria: Theropoda) from Europe. *Neues Jahrbuch für Geologie und Paläontologie Monatshefte* 7, 385-401.
- S26. Holtz, T.R. (1995). The arctometatarsalian pes, an unusual structure of the metatarsus of Cretaceous Theropoda (Dinosauria: Saurischia). *Journal of Vertebrate Paleontology* 14, 480-519.
- S27. Makovicky, P.J., Apesteguía, S., and Gianechinia, F. (2012). A new coelurosaurian theropod from the La Buitrera Fossil Locality of Río Negro, Argentina. *Fieldiana Life and Earth Sciences* 5, 90-98.
- S28. Xu, X., Upchurch, P., Ma, Q., Pittman, M., Choiniere, J., Sullivan, C., Hone, D.W.E., Tan, Q., Tan, L., Xiao, D., et al. (2013). Osteology of the alvarezsaurid *Linhonykus monodactylus* from the Upper Cretaceous Wulansuhai Formation of Inner Mongolia, China, and comments on alvarezsaurid biogeography. *Acta Palaeontologica Polonica* 58, 25-46.
- S29. Novas, F.E. (1996). Alvarezsauridae, Cretaceous maniraptorans from Patagonia and Mongolia. *Memoirs of the Queensland Museum* 39, 675-702.
- S30. Felsenstein, J. (1985). Phylogenies and the comparative method. *Am Nat* 125, 1-15.
- S31. Garland, T.J., and Ives, A.R. (2001). Using the past to predict the present: confidence intervals for regression equations in phylogenetic comparative methods. *American Naturalist* 155, 346-364.
- S32. Novas, F.E. (1997). Anatomy of *Patagonykus puertai* (Theropoda, Avialae, Alvarezsauridae), from the Late Cretaceous of Patagonia. *Journal of Vertebrate Paleontology* 17, 137-166.
- S33. Chiappe, L.M., Norell, M.A., and Clark, J.M. (2002). The Cretaceous, short-armed

- Alvarezsauridae: *Mononykus* and its kin. In Mesozoic birds: above the heads of dinosaurs, L.M. Chiappe and L.M. Witmer, eds. (Berkeley: University of California Press), pp. 87-120.
- S34. Ostrom, J.H. (1969). Osteology of *Deinonychus antirrhopus*, an unusual theropod from the Lower Cretaceous of Montana. Bulletin of the Peabody Museum of Natural History, Yale University 30, 1-165.
- S35. Soligo, C. (2005). Anatomy of the hand and arm in *Daubentonia madagascariensis*: a functional and phylogenetic outlook. Folia Primatologica 76, 262-300.

Phylogenetic Definitions Used in This Study

Coelurosauria von Huene, 1914 [S1]: the most inclusive clade sharing a more recent common ancestor with *Archaeopteryx lithographica* than with *Allosaurus fragilis*. Maniraptora Gauthier, 1986 [S2]: the most inclusive clade sharing a more recent common ancestor with *Archaeopteryx lithographica* than with *Ornithomimus edmontonicus*. Alvarezsauria Bonaparte 1991 *sensu* Agnolin et al., 2012 [S3, 4]: the most inclusive clade sharing a more recent common ancestor with *Alvarezsaurus calvoi* than with *Passer domesticus* or *Ornithomimus velox*. Alvarezsauridae Bonaparte, 1991 [S3]: the least inclusive clade containing *Alvarezsaurus calvoi*, *Mononykus olecranus* and their most recent common ancestor. Parvicursorinae Karkhu and Rautian 1996 [S5]: the least inclusive clade containing Parvicursor, *Mononykus* and their most recent common ancestor. Paraves Sereno 1997 [S6]: all maniraptorans sharing a more recent common ancestor with *Archaeopteryx lithographica* than with *Oviraptor philoceratops*.

Osteochronology

In both IVPP V22783 and IVPP V25026, the cortex is comprised entirely of fibrolamellar bone with predominantly longitudinal vascular canals. Neither thin section shows an EFS (external fundamental system; tightly packed growth lines indicative of an almost total cessation of growth), and both of them display a high density of rounded osteocyte lacunae. These suggest IVPP V22783 and IVPP V25026 were still growing rapidly and had not reached skeletal maturity before death. The degree of vascularization in the outer part of the cortex is quite low in IVPP V22783, but it is relatively high in IVPP V25026. In IVPP V22783, the inner cortex has been remodeled by several generations of secondary osteons, whereas only the early stages of secondary osteon development can be observed in IVPP V25026. There are 9 LAGs (lines of arrested growth) in IVPP V22783 and 8 LAGs in IVPP V25026. No early LAGs appear to have been obliterated by expansion of the medullary cavity in IVPP V22783 and IVPP V25026, based on the width of the largest interval between successive LAGs. Therefore we hypothesize that IVPP V22783 died at 9 years of age and IVPP V25026 at 8 years of age. In summary, the available histological information (such as the degree of cortical vascularization and remodeling of secondary osteons) indicates that IVPP V22783 and IVPP V25026 were at a relatively late ontogenetic stage (probably sub-adult) at the time of death. The histological evidence implies that IVPP V22783 was older than IVPP V25026 at the time of death, although the latter specimen is estimated to have been the larger of the two in terms of body mass.

Supplemental Phylogenetic Results

Character and character state descriptions. Character definitions below cite the publication from which our understanding of the character was derived. Where possible, we have traced the character to its original source, but in many cases this was not feasible. The citations are not intended to exhaustively list all uses of any given character in phylogenetic analyses.

The following characters are ordered in our analysis:

47 74 82 99 118 124 131 151 180 184 222 228 229 235 238 239 265 266 274 275 282 283
287 311 312 321 329 332 334 335 348 351 358 380 381 384 386 389 395 429 430 435
437 442 444 446 467 469 480 506 507 520 522 559 580 587

1. Contour feathers

0 absent

1 present

2. Vaned feathers on forelimb [S7] [S8]

0 symmetric

1 asymmetric

- 3. Shape of premaxillary body (portion in front of the external naris)**
 - 0 wider than high, or approx. as wide as high
 - 1 significantly higher than wide
- 4. Premaxillae**
 - 0 unfused
 - 1 fused
- 5. Premaxillary-nasal suture dorsal view**
 - 0 v-shaped
 - 1 w-shaped
- 6. Premaxillary-maxillary suture**
 - 0 scarf or butt joint
 - 1 interlocking joint
- 7. Premaxillary body in front of external nares**
 - 0 rostrocaudally shorter than body below nares and angle between anterior margin and alveolar margin more than 75 degrees
 - 1 rostrocaudally longer than body below the nares and angle less than 70 degrees, naris overlaps premaxillary tooth row
 - 2 much longer than body below naris, naris located posterior to premaxillary tooth row
- 8. Ventral process at the posterior end of premaxillary body (gives the posterior process a forked appearance in lateral view)**
 - 0 absent
 - 1 present
- 9. Maxillary process of premaxilla**
 - 0 contacts nasal to form posterior border of nares
 - 1 reduced so that maxilla participates broadly in external naris
 - 2 extends posteriorly to separate maxilla from nasal posterior to nares
- 10. Internarial bar**
 - 0 dorsoventrally rounded
 - 1 dorsoventrally flat
- 11. Crenulate margin on buccal edge of premaxilla**
 - 0 absent
 - 1 present
- 12. Caudal margin of naris**
 - 0 farther rostral than the rostral border of the antorbital fossa
 - 1 nearly reaching or overlapping the rostral border of the antorbital fossa
- 13. Premaxillary symphysis**
 - 0 acute, V-shaped
 - 1 rounded, U-shaped
- 14. Subnarial foramen**
 - 0 absent
 - 1 present
- 15. Groove on lateral surface of premaxilla, extending ventrally from the narial fossa**
 - 0 absent
 - 1 present
- 16. Maxillary fenestra**
 - 0 absent
 - 1 present
- 17. Maxillary fenestra recessed within a shallow, caudally or caudodorsally open fossa, which is itself located within the maxillary antorbital fossa**
 - 0 absent
 - 1 present
- 18. Longitudinal position of maxillary fenestra**
 - 0 situated at rostral border of antorbital fossa

- 1 situated posterior to rostral border of antorbital fossa
- 19. Latitudinal position of maxillary fenestra**
 - 0 situated approximately mid-height of the antorbital fossa
 - 1 displaced dorsally in antorbital fossa
- 20. Foramen on caudal edge interfenestral bar between the maxillary and antorbital fenestrae**
 - 0 absent
 - 1 present, pierces ventral portion of bar
- 21. Promaxillary fenestra (fenestra promaxillaris)**
 - 0 absent
 - 1 present
- 22. Palate formed by**
 - 0 premaxilla only
 - 1 premaxilla, maxilla and vomer
- 23. Palatal shelf of maxilla**
 - 0 flat
 - 1 with midline ventral "tooth-like" projection
- 24. Ventrolateral margin of the maxilla posterior to ascending process**
 - 0 flat or rounded as it grades onto tooth row
 - 1 developed as a sharp, ventrolaterally-projecting ridge
- 25. Anteroposterior length of palatal shelf of maxilla**
 - 0 short
 - 1 long, with extensive palatal shelves
- 26. Orientation of the maxillae towards each other as seen in dorsal view**
 - 0 acutely angled
 - 1 subparallel
- 27. Ascending process of the maxilla**
 - 0 confluent with anterior rim of maxillary body and gently sloping posterodorsally
 - 1 offset from anterior rim of maxillary body
- 28. Form of anterior projection of maxilla**
 - 0 offset from anterior rim of maxillary body, with anterior projection of maxillary body shorter than high
 - 1 offset from anterior rim of maxillary body, with anterior projection of maxillary body as long as high or longer
- 29. Ascending process of maxilla**
 - 0 prominent, exposed laterally and medially
 - 1 weakly developed, lacking lateral exposure and only slight medial exposure (Most theropods, including *Velociraptor mongoliensis*, have a prominent ascending ramus of the maxilla. In derived avialans this lamina becomes reduced or absent.)
- 30. Anterior margin of maxillary antorbital fossa**
 - 0 rounded or pointed
 - 1 square
- 31. Dorsal border of the internal antorbital fenestra lateral view**
 - 0 formed by lacrimal and maxilla
 - 1 formed by nasal and lacrimal
- 32. Dorsal border of the antorbital fossa lateral view**
 - 0 formed by lacrimal and maxilla
 - 1 formed by nasal and lacrimal
 - 2 formed by maxilla, premaxilla and lacrimal
- 33. Lateral exposure of lamina of the ventral ramus of nasal process of maxilla**
 - 0 present, large broad exposure
 - 1 present, reduced to small triangular exposure
- 34. Maxillary antorbital fossa in front of the internal antorbital fenestra**

- 0 40% or less of the length of the external antorbital fenestra
- 1 more than 40% of the length of the external antorbital fenestra
- 35. Extent of antorbital fossa on jugal ramus of maxilla**
 - 0 less than half the dorsoventral height of jugal ramus
 - 1 more than half dorsoventral height of jugal ramus
- 36. Maxilla, pneumatic region on medial side of maxilla posteroventral to maxillary fenestra**
 - 0 absent
 - 1 present
- 37. Horizontal ridge on the lateral surface of maxilla at the ventral border of the antorbital fossa**
 - 0 absent
 - 1 present
- 38. Medial constriction between articulated premaxillae and maxillae in dorsal or ventral view**
 - 0 absent
 - 1 present
- 39. Subnarial gap between maxilla and premaxilla at the alveolar margin**
 - 0 absent
 - 1 present
- 40. Maxillary parodontal plates**
 - 0 unfused
 - 1 fused
- 41. Medial surface of maxillary parodontal (interdental) plates**
 - 0 smooth or finely pitted
 - 1 dorsoventrally striated
- 42. Maxillary parodontal (interdental) plates, ventral extent**
 - 0 to the same ventral level as lateral maxillary wall
 - 1 dorsal to ventral level of maxillary wall
- 43. Maxillary parodontal plates, dorsal margin of anterior end**
 - 0 horizontal
 - 1 inclined anteroventrally
- 44. Ventral edge of maxillary body and ventral ramus**
 - 0 ventrally flat
 - 1 ventrally convex
- 45. Nasals**
 - 0 unfused
 - 1 fused
- 46. Dorsal surface of the nasals**
 - 0 smooth
 - 1 rugose
- 47. Nasal crest**
 - 0 absent
 - 1 present, single median crest
 - 2 present, bilateral crests along lateral nasal margins
- 48. Pneumatic foramen in ventrolateral margins of the nasals**
 - 0 absent
 - 1 present
- 49. Shape of nasals**
 - 0 expanding posteriorly
 - 1 of subequal width throughout their length
- 50. Pronounced lateral rims of the nasals, sometimes bearing lateral cranial crests**
 - 0 absent
 - 1 present
- 51. External nares**

- 0 facing laterally
- 1 facing anterolaterally
- 52. Length of nares**
 - 0 less than 20 percent skull length
 - 1 greater than 20 percent skull length
- 53. Jugal pneumatic recess in posteroventral corner of antorbital fossa**
 - 0 present
 - 1 absent
- 54. Medial jugal foramen**
 - 0 present on medial surface ventral to postorbital bar
 - 1 absent
- 55. Sublacrimial part of jugal**
 - 0 tapering
 - 1 bluntly squared anteriorly
 - 2 expanded
- 56. Anterior end of jugal**
 - 0 reaches internal antorbital fenestra
 - 1 excluded from the internal antorbital fenestra
- 57. Form of anterior end of jugal**
 - 0 without anterior process underneath antorbital fenestra
 - 1 expressed at the rim of the internal antorbital fenestra and with a distinct process that extends anteriorly underneath it
- 58. Jugal antorbital fossa**
 - 0 absent or developed as a slight depression
 - 1 large, crescentic depression on the anterior end of the jugal
- 59. Jugal**
 - 0 broad, plate-like
 - 1 very slender, rod-like
- 60. Jugal contribution to postorbital bar**
 - 0 contribute equally to postorbital bar
 - 1 ascending process of jugal reduced
- 61. Anteroposterior width of postorbital bar**
 - 0 subequal to preorbital bar
 - 1 expanded, greater than twice width of preorbital bar
- 62. Rugosity on ventrolateral surface of jugal below orbit**
 - 0 absent
 - 1 present
- 63. Jugal and quadratojugal**
 - 0 separate
 - 1 fused and not distinguishable from one another
- 64. Quadratojugal** [In basal theropods the quadratojugal has a small medially directed tab that wraps around the lateral surface of the quadrate and is visible in posterior view. In derived theropods, the process is anteroposteriorly long, dorsoventrally short and visible in lateral view, but not in posterior view.]
 - 0 hook-shaped, with a dorsoventrally tall, mediolaterally short process that wraps around the lateral margin of the quadrate and is visible in posterior view
 - 1 with a dorsoventrally short, anteroposteriorly long process only visible in lateral view
- 65. Quadratojugal and quadrate**
 - 0 sutural connection present
 - 1 sutural connection absent
- 66. Anteriormost level of jugal process of quadratojugal relative to infratemporal fenestra**
 - 0 ventral to
 - 1 anterior to

- 67. Supraorbital crests on lacrimal in adult individuals**
 0 absent
 1 present
- 68. Form of supraorbital crests**
 0 dorsal crest above orbit
 1 lateral expansion anterior and dorsal to orbit
- 69. Enlarged foramen or foramina opening laterally at the angle of the lacrimal**
 0 absent
 1 present
- 70. Lacrimal foramen number**
 0 single
 1 paired
- 71. Lacrimal foramina**
 0 exposed laterally
 1 developed within a pocket formed by a lateral lacrimal sheet of bone and a rostrally open pocket in the lacrimal angle
- 72. Height of the lacrimal**
 0 significantly less than height of the orbit, and usually fails to reach the ventral margin of the orbit
 1 as high as the orbit, and contacts jugal at the level of the ventral margin of orbit
- 73. Orientation of jugal ramus of lacrimal**
 0 strongly sloping anteroventrally
 1 subvertical
 2 sloping posteroventrally
- 74. Dorsoventral thickness of maxillary ramus of lacrimal**
 0 very slender, much less than anteroposterior thickness of jugal ramus
 1 moderate, less than or subequal to anteroposterior thickness of jugal ramus
 2 greater than anteroposterior thickness of jugal ramus
- 75. Suborbital spur on posterior edge of ventral ramus of lacrimal**
 0 absent
 1 present
- 76. Lacrimal posterodorsal process**
 0 absent
 1 present
- 77. Length of lacrimal posterodorsal process**
 0 subequal in length to maxillary ramus
 1 much shorter than maxillary ramus
- 78. Direction of lacrimal posterodorsal process**
 0 projects horizontally
 1 projects posterodorsally or completely dorsally
- 79. Passage of the nasolacrimal duct**
 0 leading through the body of the ventral process of the lacrimal
 1 ventral process of lacrimal not pierced, lateral side depressed below the level of the surrounding bones, and nasolacrimal duct passes lateral to the process
- 80. Jugal ramus of lacrimal**
 0 broadly triangular, articular end nearly twice as wide anteroposteriorly as lacrimal body at lacrimal angle
 1 strut-like, roughly same width anteroposteriorly throughout ventral ramus
- 81. Prefrontal**
 0 absent
 1 present
- 82. Size of prefrontal**
 0 small, forms anterolateral rim of orbit with descending process proceeding along medial surface of the descending process of the lacrimal
 1 small, forms small portion of skull roof and not expressed at orbital margin, no

descending process
2 hypertrophied, forms portion of orbital rim and skull roof, with descending process

83. Configuration of lacrimal and frontal

0 lacrimal separated from frontal by prefrontal
1 lacrimal contacts frontal

84. Frontals

0 narrow anteriorly as a wedge between nasals
1 end abruptly anteriorly, suture with nasal transversely oriented
2 nasals extend further medially than laterally, invading anteromedial contact between frontals

85. Frontal supratemporal fossa

0 limited extension of supratemporal fossa onto frontal
1 supratemporal fossa covers most of postorbital process of the frontal and extends anteriorly onto the dorsal surface of the frontal

86. Groove on orbital rim of frontal, possibly for reception of frontal process of postorbital

0 absent
1 present

87. Anterior emargination of supratemporal fossa on frontal

0 straight or slightly curved
1 strongly sinusoidal and reaching onto postorbital process

88. Frontal postorbital process (dorsal view):

0 smooth transition from orbital margin
1 sharply demarcated from orbital margin

89. Frontal edge

0 smooth in region of lacrimal suture
1 edge notched

90. Postorbital in lateral view

0 with straight anterior (frontal) process
1 frontal process curves anterodorsally and dorsal border of temporal bar is dorsally concave

91. Lateral surface of anterior process of postorbital

0 thin and unornamented
1 dorsoventrally thickened into a laterally projecting and rugose platform

92. Contact between lacrimal and postorbital

0 absent
1 present

93. Cross-section of the ventral process of the postorbital

0 triangular
1 U-shaped

94. Jugal process of the postorbital

0 ventrally directed and tapering
1 with suborbital anterior spur

95. Postorbital jugal process form of anterior suborbital spur

0 small
1 large curving flange

96. Supraorbital shelf formed mostly by an additional ossification (palpebral)

0 absent
1 present

97. Orbit

0 circular in lateral or dorsolateral view
1 dorsoventrally taller than anteroposteriorly wide, often keyhole shaped

98. Parietals

0 separate

1 fused

99. Parietal supratemporal fenestra

0 separated by a horizontal plate formed by the parietals

1 contact each other posteriorly, but separated anteriorly by an anteriorly widening triangular plate formed by the parietals

2 nearly confluent over parietals and only separated by a thin line of bone along the sagittal suture

100. Anteromedial corner of supratemporal fossa

0 open dorsally

1 roofed by shelf of frontoparietal

101. Sagittal crest

0 dorsal surface of parietals smooth with no sagittal crest

1 sagittal crest present

102. Form of sagittal crest

0 parietals dorsally convex with very low sagittal crest along midline

1 dorsally convex with well-developed sagittal crest

103. Posteriorly placed, knob-like dorsal projection of the parietals

0 absent

1 present

104. Connections of quadratojugal process of squamosal

0 contacts quadratojugal

1 does not contact quadratojugal

105. Infratemporal fenestra shape

0 rectangular, postorbital bar parallels quadratojugal and squamosal articular area

1 lower temporal fenestra constricted mesially by squamosal and quadratojugal approaching postorbital bar

106. Shape of quadratojugal process of the squamosal

0 tapering

1 broad, and usually somewhat expanded

107. Posterolateral shelf on squamosal overhanging quadrate head

0 absent

1 present

108. Quadrate head

0 covered by squamosal in lateral view

1 quadrate cotyle of squamosal open laterally exposing quadrate head

109. Descending process of squamosal

0 parallels quadrate shaft

1 nearly perpendicular to quadrate shaft

110. Supratemporal fenestra

0 bounded laterally and posteriorly by the squamosal

1 supratemporal fenestra extended as a fossa on to the dorsal surface of the squamosal

111. Quadrate

0 solid

1 hollow

112. Mandibular joint

0 approximately straight below quadrate head

1 significantly posterior to quadrate head

2 significantly anterior to quadrate head

113. Quadrate medial pneumatic recess (depression and foramen in the area of the mandibular condyle on medial surface)

0 absent

1 fossa adjacent to mandibular condyle, foramen at base of pterygoid ramus

114. Quadrate posterior pneumatic recess

0 absent

- 1 present as a lens-shaped fossa extending dorsally or dorsomedially from the quadrate foramen
- 115. Dorsal end of the quadrate**
 - 0 with a single head that fits into a slot on the ventral side of the squamosal
 - 1 double-headed, medial head contacts the braincase
- 116. Quadrate foramen**
 - 0 absent
 - 1 present
- 117. Quadrate foramen**
 - 0 developed as a distinct opening between the quadrate and quadratojugal
 - 1 almost entirely closed in the quadrate
- 118. Ectopterygoid**
 - 0 slender, without ventral fossa
 - 1 expanded, with a ventral depression medially
 - 2 expanded, with a deep groove leading into the ectopterygoid body medially
 - 3 deeply excavated and medial opening constricted into a foramen
- 119. Dorsal recess on ectopterygoid**
 - 0 absent
 - 1 present
- 120. Ectopterygoid**
 - 0 posterior to palatine
 - 1 lateral to palatine
- 121. Palatine and ectopterygoid**
 - 0 separated by pterygoid
 - 1 contact
- 122. Contact between pterygoid and palatin**
 - 0 continuous
 - 1 discontinuous in the mid-region, resulting in a subsidiary palatal fenestra
- 123. Flange of pterygoid**
 - 0 well developed
 - 1 reduced in size or absent
- 124. Shape of palatine in ventral view**
 - 0 plate-like trapezoidal or subrectangular
 - 1 tetraradiate
 - 2 jugal process strongly reduced or absent
- 125. Suborbital fenestra**
 - 0 similar in length to orbit
 - 1 reduced in size or absent
- 126. Infratemporal fenestra**
 - 0 smaller than or subequal in size to orbit
 - 1 strongly enlarged, more than 1.5 times the size of the orbit
- 127. Postorbital part of the skull roof**
 - 0 as high as orbital region
 - 1 deflected ventrally in adult individuals
- 128. Preorbital region of the skull in post-hatchling individuals**
 - 0 elongate, nasals considerably longer than frontals, maxilla at least twice the length of the premaxilla
 - 1 shortened, nasals subequal in length to frontals or shorter, maxillary length less than twice the length of the premaxillary body
- 129. Occipital region of the skull faces**
 - 0 posteriorly
 - 1 posteroventrally
- 130. Basipterygoid processes**
 - 0 well-developed, extending as a distinct process from the base of the basisphenoid

- 1 abbreviated or absent
- 131. Basipterygoid processes well developed and**
 - 0 anteroposteriorly short and finger-like (approximately as long as wide)
 - 1 longer than wide
 - 2 significantly elongated and tapering
- 132. Basipterygoid processes**
 - 0 ventral or anteroventrally projecting
 - 1 lateroventrally projecting
 - 2 caudally projecting
- 133. Basipterygoid processes**
 - 0 solid
 - 1 hollow
- 134. Basipterygoid recesses on dorsolateral surfaces of basipterygoid processes**
 - 0 absent
 - 1 present
- 135. Basisphenoid bulla**
 - 0 absent
 - 1 present
- 136. Paired foramina at anterior end of basisphenoid recess, separated by a thin bar of bone**

[New character. Added to homologize condition in *Shuvuuia* and *Xiyunykus*. In *Shuvuuia*, these foramina are hypertrophied and developed outside of the basisphenoid recess (which has been lost), but they agree closely in topological position with the foramina from the Tugulu specimen. Many theropods have paired foramina at the posterior end of the basisphenoid recess (e.g., dromaeosaurids), but having paired foramina at the anterior end is to our knowledge only known in alvarezsaurids.]

 - 0 absent, single or no opening may be present
 - 1 present
- 137. Basisphenoid recess**
 - 0 absent or poorly developed
 - 1 deep and well-developed
- 138. Passage of internal carotids between posterior end of skull and pituitary fossa**

[New character. In some alvarezsaurids, e.g., *Shuvuuia* and in some small-bodied troodontids, e.g., *Byronosaurus*, the internal carotids are clearly demarcated by hemicylindrical bony tubes projecting ventrally from the ventral surface of the basisphenoid]

 - 0 no bony tubes present
 - 1 enclosed by bony tubes extending along ventral surface of basisphenoid
- 139. Basisphenoid recess position**
 - 0 between basisphenoid and basioccipital
 - 1 entirely within basisphenoid
- 140. Posterior opening of basisphenoid recess**
 - 0 single
 - 1 divided into two small, circular foramina by a thin bar of bone
- 141. Basisphenoid between basal tubera and basipterygoid processes**
 - 0 approximately as wide as long, or wider
 - 1 significantly elongated, at least 1.5 times longer than wide
- 142. Basisphenoid in lateral view**
 - 0 oriented subhorizontally
 - 1 anterior portion located much more ventrally than posterior portion, recess visible in posterior view
- 143. Base of cultriform process**
 - 0 not highly pneumatised
 - 1 expanded and pneumatic (parasphenoid bulla)

144. Cultriform process, dorsal surface

[New character. In *Xiyunykus* and in some dromaeosaurs, e.g., *Tsaagan*, the dorsal surface of the cultriform process bears a deep groove along its length. We add this character in the hopes it will be informative when braincase features become more broadly known in transitional alvarezsauroids and other maniraptoran taxa.]

- 0 without deep longitudinal groove
- 1 with deep axial groove

145. Cultriform process, ventral surface

[New character. In *Shuvuuia* and in *Xiyunykus*, the ventral surface of the cultriform process bears a keel-like ridge along much of its length. This feature is certainly absent in *Haplocheirus*, but its distribution within the rest of Alvarezsauroidea is poorly known. At least one other maniraptoran, *Citipati*, possesses this feature homoplastically, but its distribution needs more research.]

- 0 without ventrally projecting, mediolaterally narrow ridge
- 1 with ridge

146. Exits of CN X-XII

- 0 flush with surface of exoccipital
- 1 located together in a bowl-like basisphenoid depression

147. Exits of CN X and XI

- 0 laterally through the jugular foramen
- 1 posteriorly through a foramen (metotic foramen) lateral to the exit of cranial nerve XII and the occipital condyle

148. Exoccipital lateral to occipital condyle (Added by JNC Oct 2011 to assess homology between this region in troodontids and parvicursorines)

- 0 forms roof over exits for CN X and XII
- 1 unexpanded and does not form roof

149. Supraoccipital sagittal crest

- 0 with pronounced sagittal crest
- 1 sagittal crest reduced or absent

150. Paroccipital process shape

- 0 elongate and slender
- 1 short, deep

151. Paroccipital process direction

- 0 straight, projects laterally or posterolaterally
- 1 project ventrolaterally
- 2 pendant

152. Paroccipital process dorsal edge

- 0 with straight dorsal edge
- 1 distal end twists rostrally, distal ends of the processes oriented transversely rather than vertically

153. Ventral rim of the base of the paroccipital processes

- 0 above or level with the dorsal border of the occipital condyle
- 1 situated at mid-height of occipital condyle or lower

154. Foramen magnum

- 0 subcircular, slightly wider than tall
- 1 oval, taller than wide

155. Foramen magnum size

- 0 smaller than or subequal in width to occipital condyle
- 1 larger in width than occipital condyle

156. Occipital condyle

- 0 without constricted neck
- 1 subspherical with constricted neck

157. Infracondylar fossa of occipital condyle

- 0 absent
- 1 present

- 158. Form of infracondylar fossa of occipital condyle**
0 narrow and groove-like
1 broad depression approximately two-thirds the width of the occipital condyle
- 159. Basal tubera**
0 present
1 absent
- 160. Basal tubera composition**
0 equally formed by basioccipital and basisphenoid and not subdivided
1 subdivided by a lateral longitudinal groove into a medial part entirely formed by the basioccipital, and a lateral part, entirely formed by the basisphenoid
- 161. Basal tubera spacing**
0 set far apart, level with or beyond lateral edge of occipital condyle and/or foramen magnum (may be connected by a web of bone or separated by a large notch)
1 tubera small, directly below condyle and foramen magnum, and separated by a narrow notch
- 162. Subcondylar recess**
0 absent
1 present in basioccipital/exoccipital lateral and ventral to occipital condyle
- 163. Subcondylar recess form**
0 isolated from nervous foramina CNX-CNXII
1 subcondylar recess and cranial nerves exit together in a deep depression encompassing multiple pneumatic fossae and enclosed by a well-developed rim
- 164. Exit of mid-cerebral vein**
0 included in trigeminal foramen
1 vein exits braincase through a separate foramen anterodorsal to the trigeminal foramen
- 165. Brain proportions**
0 forebrain small and narrow
1 forebrain significantly enlarged and triangular
- 166. Anterior tympanic recess in the braincase**
0 absent
1 present
- 167. Prootic pneumatic recess**
0 absent
1 present
- 168. Form of pneumatic prootic recess**
0 dorsally open fossa on prootic/opisthotic
1 deep, posterolaterally directed concavity
- 169. Crista interfenestralis**
0 confluent with lateral surface of prootic and opisthotic
1 distinctly depressed within middle ear opening
- 170. Accessory dorsal tympanic recess (dorsal to crista interfenestralis)**
0 absent
1 present
- 171. Form of dorsal tympanic recess**
0 small pocket present
1 extensive with indirect pneumatisation
- 172. Caudal (posterior) tympanic recess**
0 absent
1 present
- 173. Form of caudal tympanic recess**
0 present as opening on anterior surface of paroccipital process
1 extends into opisthotic posterodorsal to fenestra ovalis, confluent with this fenestra

- 174. Exoccipitals ventral to posterior pneumatic recess**
 0 no lip
 1 form anteriorly projecting, posterodorsally curling, dorsally concave, tab-like process
- 175. Otosphenoidal crest**
 0 vertical on basisphenoid and prootic, and does not border an enlarged pneumatic recess
 1 well-developed, crescent-shaped, thin crest forms anterior edge of enlarged pneumatic recess
- 176. Subotic recess (pneumatic fossa ventral to fenestra ovalis)**
 0 absent
 1 present
- 177. Depression (possibly pneumatic) on ventral surface of postorbital process of laterosphenoid**
 0 absent
 1 present
- 178. Interorbital region in adults**
 0 unossified
 1 ossified
- 179. Prominent endocranial expansion of vertical semicircular canal** (Often forms a "vestibular pyramid", a mound-like structure on the posteroventral edge of the semicircular canal)
 0 absent
 1 present
- 180. Mandibular foramen**
 0 absent or reduced
 1 large
 2 hypertrophied, greater than 50% dentary length
- 181. Shape of mandibular foramen**
 0 oval
 1 subdivided by a spinous rostral process of the surangular
- 182. Paradental plates of dentary**
 0 lack paradental plates
 1 with paradental plates on the medial surface of the tooth row
- 183. Internal mandibular fenestra**
 0 small and slit-like
 1 large and rounded
- 184. Shape of anterior end of dentary**
 0 blunt and unexpanded
 1 dorsoventrally expanded, rounded and slightly upturned
 2 with anteroventral process giving a "squared off" appearance in lateral view
- 185. Dorsal edge of anterior end of dentary in lateral view**
 [In spinosaurids, *Masiakasaurus*, and in *Haplocheirus*, there is a dorsally arcing eminence on the anterior tip of the dentary along the dorsal margin, but given the phylogenetic distance between these taxa this feature is likely a homoplasy. The distribution of this character within transitional alvarezsauroids, however, is virtually unknown because there is so little cranial material]
 0 dorsally flat
 1 with dorsally expanded, arcuate eminence
- 186. Symphyseal region of dentary**
 0 Broad and straight, paralleling lateral margin
 1 medially recurved
- 187. Degree of medial recurvature of dentary symphysis**
 0 medially recurved slightly
 1 strongly recurved medially

- 188. Dentary symphyseal fusion**
 0 absent
 1 present
- 189. Dentary anterior end in lateral view**
 0 in line with main part of buccal edge
 1 anterior end deflected ventrally
- 190. Width of dentary symphyseal region**
 0 no broader than transverse width of post-symphyseal region
 1 broader than post-symphyseal region
- 191. Orientation of dentary symphysis in lateral view**
 0 vertical to subvertical
 1 projects strongly cranially, oblique with respect to dentary ventral margin
- 192. Posterior end of dentary**
 0 without posterodorsal process dorsal to mandibular fenestra
 1 with dorsal process
- 193. Form of dentary posterodorsal process**
 0 developed only above anterior end of mandibular fenestra
 1 with elongate dorsal process extending over most of fenestra
- 194. Labial face of dentary**
 0 flat
 1 with lateral ridge and inset tooth row
- 195. Nutrient foramina on external surface of dentary**
 0 superficial
 1 descend strongly posteriorly within a deep groove
- 196. Form of nutrient foraminal groove**
 0 thin groove of constant height as it extends posteriorly
 1 posterior end of groove is dorsoventrally expanded
- 197. Dentary shape in lateral view**
 0 with subparallel dorsal and ventral edges
 1 subtriangular in lateral view
- 198. Form of triangular dentary** (character added by JNC to homologize condition in some oviraptorosaurs)
 0 low triangular
 1 high triangular
- 199. Ventral edge of dentary in lateral view**
 0 straight or nearly straight
 1 descends strongly posteriorly
- 200. Dentary paradental groove separating interdental plates from medial wall of dentary**
 0 absent
 1 present
- 201. Pronounced coronoid eminence on the surangular**
 0 absent
 1 present
- 202. Foramen in lateral surface of surangular rostral to mandibular articulation**
 0 absent
 1 present
- 203. Number of surangular foramina**
 0 one
 1 two
- 204. Laterally inclined flange along lateral surface of surangular**
 0 absent
 1 present
- 205. Position of lateral flange along dorsal side of lateral surface of surangular**
 [New character. Basal alvarezsauroids and many theropods, e.g., tyrannosauroids,

ornithomimosaurs, bear a laterally projecting flange along the lateral surface of the surangular. In most theropod taxa, the flange is set below the level of the dorsal margin of the surangular. However, in the basal alvarezsauroids *Haplocheirus*, *Xiyunykus*, and *Bannykus*, and in the spinosaurid *Baryonyx*, the flange is developed along the dorsal margin of the bone, often resulting in a flattened, platform-like surface on the dorsal margin of the surangular.]

0 ventral to dorsal margin

1 along lateral side of dorsal margin

206. Anterior portion of the surangular

0 less than half the height of the mandible above the mandibular fenestra

1 more than half the height of the mandible at the level of the mandibular fenestra

207. Retroarticular process of the mandible

0 narrow, rod-like

1 broadened, with groove posteriorly for the attachment of the m. depressor mandibulae

208. Attachment of the m. depressor mandibulae on retroarticular process of mandible

0 facing dorsally

1 facing posterodorsally

209. Retroarticular process

0 points posteriorly

1 curves gently posterodorsally

210. Articular

0 without elongate, slender medial, posteromedial, or mediodorsal process from retroarticular process

1 with process

211. Angular

0 exposed almost to end of mandible in lateral view, reaches or almost reaches articular

1 excluded from posterior end angular suture turns ventrally and meets ventral border of mandible rostral to glenoid

212. Coronoid ossification

0 absent

1 present

213. Form of coronoid ossification

0 large

1 thin splint

214. Splenial

0 not widely exposed on lateral surface of mandible

1 exposed as a broad triangle between dentary and angular on lateral surface of mandible

215. Foramen in the ventral part of the splenial (mylohyal foramen)

0 absent

1 present

216. Form of mylohyal foramen

0 completely enclosed in the splenial

1 opened anteroventrally

217. Posterior end of splenial

0 straight

1 forked

218. Articular glenoid fossa

0 as long as distal end of quadrate

1 twice or more as long as quadrate surface, allowing anteroposterior movement of mandible

219. Palatal teeth

- 0 present
- 1 absent
- 220. Premaxillary teeth**
 - 0 present
 - 1 absent
- 221. Number of premaxillary teeth**
 - 0 three
 - 1 four
 - 2 five
 - 3 more than five
- 222. First premaxillary tooth size**
 - 0 slightly smaller or the same size as 2 and 3
 - 1 much smaller than 2 and 3
 - 2 much larger than 2 and 3
- 223. Second premaxillary tooth**
 - 0 approximately equivalent in size to other premaxillary teeth
 - 1 markedly larger than third and fourth premaxillary teeth
- 224. Premaxillary tooth direction**
 - 0 decumbent or ventrally projecting
 - 1 procumbent
- 225. Serrations on premaxillary teeth**
 - 0 present
 - 1 absent
- 226. In cross section, premaxillary tooth crowns**
 - 0 sub-oval to sub-circular
 - 1 D-shaped with flat lingual surface
- 227. Maxillary teeth**
 - 0 present
 - 1 absent
- 228. Length of maxillary tooth row**
 - 0 extends posteriorly to approximately half the length of the orbit
 - 1 ends at the anterior rim of the orbit
 - 2 completely antorbital, tooth row ends anterior to the vertical strut of the lacrimal
 - 3 ends below the junction between the maxillary body and the ascending process
- 229. Number of maxillary teeth**
 - 0 10-14
 - 1 15-19
 - 2 20 or more
- 230. Maxillary tooth direction**
 - 0 ventrally or posteriorly inclined
 - 1 procumbent
- 231. Maxillary and dentary teeth, mesial (anterior) carina**
 - 0 present
 - 1 absent
- 232. Mesial (anterior) carina of maxillary and dentary teeth present and**
 - 0 extends to base of crown
 - 1 terminates ventrally at approximately mid-crown level or more apically
- 233. Shape of maxillary teeth**
 - 0 labiolingually flattened, apicobasally taller than mesiodistally wide
 - 1 lanceolate and subsymmetrical (as in therizinosaurs)
 - 2 simple, conical, incisive crowns (as in alvarezsaurids)
- 234. Degree of curvature of maxillary tooth crowns**
 - 0 crowns curve posteriorly as they extend distally
 - 1 very little curvature or crowns straight

235. Serrations on maxillary and dentary teeth

- 0 present
- 1 some without serrations anteriorly (except at base in *Saurornithoides mongoliensis*)
- 2 absent

236. Maxillary tooth implantation

- 0 separate alveoli
- 1 set in an open groove

237. Roots of maxillary and dentary teeth

- 0 mediolaterally compressed
- 1 circular in cross-section

238. Dentary tooth row

- 0 fully toothed
- 1 only teeth rostrally
- 2 edentulous
- 3 fully toothed with short edentulous anterior portion

239. Number of dentary teeth

- 0 large, fewer than 25 in dentary
- 1 moderate number of small teeth (25-30 in dentary)
- 2 relatively small and numerous (more than 30 in dentary)

240. Dentary teeth distributio

- 0 homodont
- 1 increasing in size anteriorly, becoming more conical in shape
- 2 Decreasing in size anteriorly, becoming more densely packed

241. Shape of dentary teeth

- 0 labiolingually flattened, apicobasally taller than mesiodistally wide
- 1 lanceolate and subsymmetrical (as in therizinosauroids)
- 2 simple, conical, incisive crowns (as in alvarezsaurids)

242. Third dentary alveolus

- 0 subequal in size to other alveoli
- 1 circular and enlarged relative to other alveoli

243. Dentary tooth implantation

- 0 separate alveoli
- 1 set in an open groove

244. Dentary tooth direction

- 0 dorsally or posteriorly inclined
- 1 procumbent (anteriorly inclined)

245. Serrations on maxillary and dentary teeth

- 0 simple, denticles convex
- 1 distal and often mesial edges of teeth with large, hooked denticles that point toward the tip of the crown

246. Serration size

- 0 large
- 1 small

247. Constriction between tooth crown and root

- 0 absent
- 1 present

248. Enamel of tooth crowns

- 0 smooth
- 1 horizontally wrinkled, especially flanking the serrations

249. Form of enamel wrinkles

- 0 bands extending across labial and lingual tooth surfaces
- 1 adjacent to carinae but do not extend across labial and lingual tooth surfaces

250. Vertical striations of enamel of tooth crowns

- 0 absent

- 1 present
- 251. Axial diapophyses**
 - 0 moderate
 - 1 reduced or absent
- 252. Axial parapophyses**
 - 0 prominent or moderate
 - 1 reduced or absent
- 253. Axial neural spine**
 - 0 flared transversely and sheet-like
 - 1 compressed mediolaterally, anteroposteriorly reduced, and rodlike
- 254. Epipophyses on axis**
 - 0 absent
 - 1 present
- 255. Form of axial epipophyses**
 - 0 present as small ridges
 - 1 strongly pronounced (overhanging the zygapophyses)
- 256. Pleurocoel in axis**
 - 0 absent
 - 1 present
- 257. Number of cervical vertebrae**
 - 0 10
 - 1 More than 10
- 258. Pleurocoels in cervical vertebrae**
 - 0 absent
 - 1 present
- 259. Number of pleurocoels in cervicals**
 - 0 one
 - 1 two
- 260. Arrangement of two foramina in cortical surface of cervical centra**
 - 0 one in anterior half of lateral surface, one in posterior half
 - 1 both foramina in anterior half
- 261. Pleurocoels developed as**
 - 0 deep depressions
 - 1 foramina
- 262. Interior pneumatic spaces in cervicals (**
 - 0 Structure camerate (few chambers)
 - 1 Structure camellate (many chambers separated by delicate lamellae)
- 263. Ventral surface of anterior cervicals**
 - 0 keeled
 - 1 smooth
 - 2 ventral depression
- 264. Posterolateral crests on lateral surfaces of cervical centra**
 - 0 absent
 - 1 present
- 265. Anterior cervical centra length**
 - 0 less than twice transverse centrum width
 - 1 between two and three times transverse width
 - 2 three to five times transverse width
- 266. Anterior articular facet of anterior cervical vertebrae**
 - 0 approximately as high as wide or higher
 - 1 significantly wider than high
 - 2 wider than high and higher laterally than medially (kidney-shaped), with neural canal emarginating dorsal aspect
- 267. Anterior cervical centra relative length**
 - 0 level with or shorter than posterior extent of neural arch

- 1 centra extending beyond posterior limit of neural arch
- 268. Articulation surfaces of cervical centra**
 - 0 amphi- to platycoelous
 - 1 opisthocoelous
 - 2 heterocoelous
- 269. Carotid process on posterior cervical centra**
 - 0 absent
 - 1 present
- 270. Epipophyses in anterior cervical vertebrae**
 - 0 absent or poorly developed
 - 1 well-developed
- 271. Form of well-developed cervical epipophyses**
 - 0 proximal to postzygapophyseal facets
 - 1 strongly overhanging postzygapophyseal facets
- 272. Prezygapophyseal-epipophyseal lamina on dorsal surface of neural arch**
 - 0 absent or poorly developed
 - 1 extending anteriorly from epipophysis as a mediolaterally thin ridge that separates dorsal surface of diapophysis from rest of dorsal neural arch
- 273. Postzygapophyses of cervical vertebrae 2-4**
 - 0 well-separated, or connected only at the base
 - 1 medially connected along their entire length by a intrazygapophyseal lamina that is dorsally concave for attachment of the interspinous ligaments
- 274. Cervical neural spines**
 - 0 anteroposteriorly long
 - 1 anteroposteriorly short and centered on neural arch, giving arch an "X" shape in dorsal view
 - 2 extremely short anteroposteriorly, less than 1/3 length of neural arch
- 275. Cervical neural spine height**
 - 0 dorsoventrally tall, subequal to or exceeding height of neural arch from centrum to base of neural spine
 - 1 moderate, less than neural arch height
 - 2 strongly reduced, less than half height of neural arch (not including spine itself)
- 276. Prezygapophyses in anterior cervicals**
 - 0 transverse distance between prezygapophyses less than width of neural canal
 - 1 prezygapophyses situated lateral to the neural canal
- 277. Prezygapophyses in anterior postaxial cervicals**
 - 0 straight
 - 1 anteroposteriorly convex, flexed ventrally anteriorly
- 278. Cervical neural arches, posterior surface above neural canal**

[New character. In all alvarezsauroids where the condition is observable, the posterior surface of the cervical neural arches immediately lateral and dorsal to the neural canal bears several deep fossae, which are readily seen in posterior view. This feature is variably present in many other theropods, e.g., ceratosaurs.]

 - 0 without multiple deep fossae
 - 1 with multiple deep fossae surrounding neural canal
- 279. Postzygapophyses of posterior cervical vertebrae**

[New character. This refers to the direction of the main axis of the postzygapophyses, not the midline web of bone that may or may not connect them.]

 - 0 diverge only weakly laterally
 - 1 diverge strongly laterally
- 280. Pneumaticity of dorsal neural arches**
 - 0 absent to moderate
 - 1 extreme
- 281. Hypapophyses in anterior dorsals**
 - 0 absent or poorly developed

- 1 pronounced
- 282. Pleurocoels in dorsal vertebrae**
 - 0 absent
 - 1 present in anterior dorsals ('pectorals')
 - 2 present in all dorsals
- 283. Dorsal centra articular surfaces**
 - 0 amphiplatyan
 - 1 some opisthocoelous
 - 2 most opisthocoelous
- 284. Ventral keel in anterior dorsals**
 - 0 absent or very poorly developed
 - 1 pronounced
- 285. Shape of dorsal centra in anterior view**
 - 0 subcircular or oval
 - 1 significantly wider than high
 - 2 triangular
- 286. Dorsal vertebrae, size of neural canal**

[New character. In most theropods, the neural canal in the dorsal vertebrae is considerably smaller than the posterior articular facet of the corresponding centrum. Uniquely in parvicursorine alvarezsauroids, the neural canal is much larger in diameter than the posterior articular facet. This has long been recognized in alvarezsaurs]

 - 0 small, much smaller than posterior articular facet
 - 1 large, subequal to posterior articular facet
- 287. Posterior dorsal vertebrae**
 - 0 strongly shortened, centra much shorter than high
 - 1 relatively short, centra approximately as high as long, or only slightly longer
 - 2 significantly elongated, much longer than high
- 288. Posterior dorsal vertebrae, basal webbing of neural spines**
 - 0 absent
 - 1 present
- 289. Posterior dorsal vertebrae, orientation of neural spines**
 - 0 vertically or posteriorly
 - 1 anteriorly
- 290. Anterior dorsal vertebrae height of prezygadiapophyseal lamina**
 - 0 less than or subequal to height of centrum
 - 1 hypaxially inflated, height significantly greater than centrum height
- 291. Dorsal vertebrae neural arches, anterior neural pedicle**
 - 0 without tubercle at base
 - 1 pronounced tubercle at base
- 292. Dorsal vertebrae neural arches, posterior neural pedicle**

[New character. In *Haplocheirus*, the base of the anterior neural pedicle, immediately dorsal to the centrum contact, bears a small tubercle that projects anteriorly. A similar tubercle is present on the posterior neural pedicle in *Xiyunykus* and *Patagonykus*, although these taxa lack the anterior tubercle. In the readily observable dorsal vertebral neural arches of *Haplocheirus*, this posterior tubercle isn't present, but it is possible that the more poorly preserved neural arches did bear this feature.]

 - 0 without tubercle at base
 - 1 pronounced tubercle at base
- 293. Anterior dorsal vertebrae, anterior and posterior infrazygapophyseal fossae**
 - 0 single
 - 1 with one or more accessory centrodiapophyseal laminae dividing fossa into multiple chambers
- 294. Transverse processes of anterior dorsal vertebrae**
 - 0 subhorizontal to vertically inclined
 - 1 pendant

- 295. Parapophyseal facets of anterior dorsal vertebrae**
 0 moderate in size (less than half height of centrum)
 1 hypertrophied (greater than two thirds centrum height)
- 296. Hyposphene-hypantrum articulation in dorsal vertebrae**
 0 absent
 1 present
- 297. Step-like ridge lateral to hyposphene running posterodorsally from the dorsal border of the neural canal to the posterior edge of the postzygapophyses of dorsal vertebrae (visible in lateral view)**
 0 absent
 1 present
- 298. Postzygapophyses of the dorsal vertebrae in posterior view** (Benson et al., 2009 #214)
 0 without lateral flanges
 1 with lateral, small, flange-like lateral extensions of postzygapophyseal facets
- 299. Postzygapophyses of dorsal vertebrae**
 0 abutting one another above neural canal, opposite hyposphenes meet to form lamina
 1 zygapophyses placed lateral to neural canal and separated by groove for interspinous ligaments, hyposphenes separated
- 300. Neural spines on posterior dorsal vertebrae in lateral view**
 0 rectangular or square
 1 anteroposteriorly expanded distally, fan-shaped
- 301. Neural spines of dorsal vertebrae in dorsal view**
 0 not expanded distally
 1 expanded laterally in dorsal view to form "spine table"
- 302. Dorsal vertebrae neural arches, spinopostzygapophyseal lamina**
 [New character. In *Bonapartenykus*, the spinopostzygapophyseal laminae terminate abruptly on the dorsal surface of the postzygapophyses, leaving a steep demarcation of the contact. In *Haplocheirus* and in parvicursorines, this feature is absent, but its distribution is unclear in transitional alvarezsaurids because of poor preservation.]
 0 grades smoothly into postzygapophyseal dorsal surface or poorly developed
 1 well developed and terminates abruptly on dorsal surface of postzygapophysis
- 303. Middle dorsal vertebrae, anterior centrodiapophyseal lamina (connects the parapophysis and the diapophysis)**
 [New character. Within alvarezsauroids, this feature is present in *Xiyunykus* and *Patagonykus*, but it is variably present in many other theropods, including some oviraptorosaurs, dromaeosaurs, and non-coelurosaurian tetanurans.]
 0 absent or poorly developed
 1 well developed
- 304. Scars for interspinous ligaments**
 0 terminate at apex of neural spine in dorsal vertebrae
 1 terminate below apex of neural spine
- 305. Neural spines of posterior dorsals**
 0 broadly rectangular and approximately as dorsoventrally high as anteroposteriorly long
 1 high rectangular, significantly dorsoventrally higher than anteroposteriorly long
- 306. Hook-like extension on anterior end of dorsal neural spines in lateral view**
 0 absent
 1 present (with associated depression immediately caudal to the projection for spinous ligament attachment)
- 307. Parapophyses of posterior dorsal vertebrae**
 0 flush with neural arch
 1 distinctly projected on pedicels
- 308. Parapophyses in posteriormost dorsals**

- 0 on same level as transverse process
- 1 distinctly below transverse process
- 309. Transverse processes of anterior dorsal vertebrae**
 - 0 proximodistally long and anteroposteriorly thin
 - 1 proximodistally short, anteroposteriorly wide
- 310. Notarium of dorsal vertebrae**
 - 0 absent
 - 1 present
- 311. Number of sacral vertebrae**
 - 0 two
 - 1 three
 - 2 four
 - 3 five
 - 4 six
 - 5 seven
 - 6 eight
 - 7 nine or more
- 312. Pleurocoels in centra of sacral vertebrae**
 - 0 absent
 - 1 present on anterior sacrals only
 - 2 present on all sacrals
- 313. Anteriormost sacral centrum, ventral surface**

[In *Parvicursor*, and likely in most parvicursorine alvarezsauroids, the ventral surface of the anteriormost sacral centrum has a V-shaped cross section with a deep ventral keel. This feature is not present in the non-parvicursorine alvarezsaurid *Alvarezsaurus* but its distribution amongst other alvarezsaurs and theropods is poorly known]

 - 0 rounded, convex
 - 1 mediolaterally constricted and forms a keel
- 314. Ventral surface of posterior sacral centra**
 - 0 gently rounded, convex
 - 1 flattened ventrally, sometimes with shallow sulcus
 - 2 centrum strongly constricted transversely, ventral surface keeled
- 315. Transverse dimensions of mid-sacral centra relative to other sacral centra**
 - 0 subequal
 - 1 mediolaterally narrower
 - 2 mediolaterally wider (State added by JNC 2011-09-26 to include the pattern seen in birds e.g., *Apsaravis*)
- 316. Sacral vertebrae**
 - 0 with unfused zygapophyses
 - 1 with fused zygapophyses forming a sinuous ridge in dorsal view
- 317. Last sacral centrum**
 - 0 with flat posterior articulation surface
 - 1 convex articulation surface
- 318. Fenestrae between neural spines of sacral vertebrae**
 - 0 present
 - 1 absent
- 319. Sacral ribs**
 - 0 slender and well-separated
 - 1 forming a more or less continuous sheet in ventral or dorsal view
 - 2 very massive and strongly expanded
- 320. Sacral neural arch pneumaticity**
 - 0 absent to moderate
 - 1 extreme
- 321. Number of caudal vertebrae**
 - 0 more than 40

- 1 25-40
- 2 fewer than 25
- 322. Pygostyle**
 - 0 absent
 - 1 present, centra of distal caudal vertebrae fused
- 323. Pleurocoels in centra of anterior caudal vertebrae**
 - 0 absent
 - 1 present
- 324. Caudal centra**
 - 0 amphiplatyan
 - 1 procoelus
- 325. Shape of anterior caudal centra in cross section**
 - 0 oval
 - 1 subrectangular and box-like
 - 2 laterally compressed with a ventral keel
- 326. Ventral surface of anterior caudals**
 - 0 rounded
 - 1 with a distinct keel sometimes bearing a narrow, shallow groove on its midline
 - 2 grooved
- 327. Relative length of distal caudal centra**
 - 0 significantly elongated in relation to centrum height
 - 1 not elongated in relation to centrum height
- 328. Caudal vertebrae**
 - 0 with distinct transition point, from shorter centra with long transverse processes proximally to longer centra with small or no transverse processes distally
 - 1 homogeneous in shape, with no transition point
- 329. Position of transition point**
 - 0 distal to the tenth caudal vertebra
 - 1 between the 7th and 10th caudal vertebrae
 - 2 proximal to the 7th caudal vertebra
- 330. Location of transverse processes of proximal caudals**
 - 0 centrally positioned on centrum
 - 1 anteriorly displaced
- 331. Centrodiapophyseal laminae of anterior caudal vertebrae**
 - 0 weak
 - 1 prominent, as well developed as those of dorsal vertebrae
- 332. Neural spines on distal caudals**
 - 0 form a low ridge
 - 1 spine absent
 - 2 midline sulcus in center of the neural arch
- 333. Neural spines of caudal vertebrae**
 - 0 simple, undivided
 - 1 separated into anterior and posterior alae throughout much of caudal sequence
- 334. Neural spines of mid-caudals**
 - 0 rod-like and posteriorly inclined
 - 1 rod-like and vertical
 - 2 subrectangular and sheet-like
- 335. Prezygapophyses of distal caudal vertebrae**
 - 0 between 1/3 and whole centrum length
 - 1 with extremely long extensions of the prezygapophyses (up to 10 vertebral segments in some taxa)
 - 2 strongly reduced as in *Archaeopteryx lithographica*
- 336. Anterior margin of neural spines of anterior mid-caudal vertebrae**
 - 0 straight
 - 1 with distinct kink, dorsal part of anterior margin more strongly inclined

- posteriorly than ventral part
- 337. Long, hair-like cervical ribs**
 - 0 absent
 - 1 present
- 338. Shaft of cervical ribs**
 - 0 slender and longer than vertebra to which they articulate
 - 1 broad and shorter than vertebra
- 339. Posterior cervical ribs and centra**
 - 0 separate
 - 1 fused
- 340. Ossified uncinat processes**
 - 0 absent
 - 1 present
- 341. Ossified sternal ribs**
 - 0 absent
 - 1 present
- 342. Lateral gastral segment**
 - 0 shorter than medial one in each arch
 - 1 distal segment longer than proximal segment
- 343. Cranial process at base of chevrons**
 - 0 absent
 - 1 present
- 344. Proximal surface of chevrons**
 - 0 distinct transverse ridge dividing surface into anterior and posterior facets
 - 1 no ridge, low mounds may be present laterally
- 345. Proximal end of chevrons of proximal caudals**
 - 0 short anteroposteriorly, shaft cylindrical
 - 1 proximal end elongate anteroposteriorly, flattened and plate-like
- 346. Mid-caudal chevrons**
 - 0 rod-like or only slightly expanded ventrally
 - 1 L-shaped
- 347. Distal chevrons**
 - 0 rod-like or L-shaped
 - 1 skid-like
- 348. Distal caudal chevrons**
 - 0 simple
 - 1 anteriorly bifurcate
 - 2 bifurcate at both ends
- 349. Ossified sternal plates**
 - 0 separate in adults
 - 1 fused
- 350. Sternum**
 - 0 without distinct lateral xiphoid process posterior to costal margin
 - 1 with lateral xiphoid process
- 351. Ventral keel on sternum**
 - 0 absent
 - 1 present
- 352. Midline groove on sternal keel**
 - 0 absent
 - 1 present
- 353. Anterior edge of sternum**
 - 0 grooved for reception of coracoids
 - 1 without grooves
- 354. Articular facet of coracoid on sternum (conditions may be determined by the**

articular facet on coracoid in taxa without ossified sternum

- 0 anterolateral or more lateral than anterior
- 1 almost anterior

355. Furcula

- 0 absent
- 1 present

356. Furcula shape

- 0 v-shaped
- 1 u-shaped, with bowed epicleidea

357. Hypocleidium on furcula

- 0 absent
- 1 present

358. Coracoid in lateral view

- 0 subcircular, with low ventral blade and no or small posterior process
- 1 shallow ventral blade with elongate posterior process
- 2 subquadrangular with extensive ventral blade
- 3 strut-like, very tall ventral blade with little or no posterior process

359. Posterior edge of coracoid

- 0 not or shallowly indented below glenoid
- 1 posterior edge of coracoid deeply notched just ventral to glenoid, glenoid lip everted

360. External surface of coracoid ventral to glenoid fossa and along dorsal margin of posterventral blade

- 0 unexpanded
- 1 expanded, forms triangular subglenoid fossa bounded laterally by coracoid tuber

361. Coracoid tubercle

- 0 absent
- 1 weakly developed, only a low structure
- 2 strongly developed

362. Coracoid tubercle form

- 0 anteroposteriorly short, mound-like
- 1 anteroposteriorly elongated, ridge-like

363. Strong lateral ridge on coracoid extending posteriorly from coracoid tuber along posteroventral process

- 0 absent
- 1 present

364. Coracoid, ventral half of lateral surface

- 0 bone smooth or only lightly textured
- 1 cortical bone surface rugose and heavily textured

365. Coracoid, anterior view

- 0 dorsal and ventral portions coplanar or subcoplanar
- 1 ventral portion directed ventromedially at obtuse angle to dorsal portion

366. Coracoid foramen

- 0 present
- 1 absent

367. Scapula shape

- 0 short and broad (ratio length/minimal height of shaft <9)
- 1 slender and elongate (ratio >10)

368. Scapulocoracoid junction anterior surface

- 0 indented or notched between the scapular acromial process and the coracoid suture
- 1 smoothly curved and uninterrupted across the contact between the scapula and coracoid

369. Acromion margin of scapula

- 0 continuous with blade
- 1 anterior edge enlarged and projects anteriorly at approximately a right angle

370. Notch on posterior margin of scapular blade immediately dorsal to glenoid lip

- 0 absent
- 1 present, associated with a small posterior protuberance

371. Posterior surface of scapular blade distal to glenoid buttress

- 0 without deep groove
- 1 with deep groove

372. Flange on supraglenoid buttress on scapula

- 0 absent
- 1 present

373. Tubercle on posterior surface of scapula dorsal to glenoid

[New character. Added to homologize condition in alvarezsaurids. This feature is easily distinguished from the supraglenoid buttress of Nichols and Russel 1985, which projects laterally and forms a portion of the anterior border of the glenoid facet of the scapula.]

- 0 absent
- 1 present

374. Distal end of scapula

- 0 expanded
- 1 not expanded

375. Glenoid fossa

- 0 faces posteriorly or posterolaterally
- 1 faces laterally

376. Scapula and coracoid

- 0 separate
- 1 fused into scapulocoracoid

377. Scapula and coracoid orientation

- 0 continuous arc in posterior and anterior views
- 1 coracoid inflected medially, scapulocoracoid L shaped in anterior or posterior view

378. Scapula length

- 0 longer than humerus
- 1 shorter than humerus

379. Deep fossa on anterior side of lateral surface of proximal end of scapula immediately dorsal to scapulocoracoid junction

- 0 absent
- 1 present

380. Deltopectoral crest length

- 0 less than one quarter humeral length
- 1 approximately one third humeral length
- 2 greater than one half humeral length

381. Deltopectoral crest

- 0 large and distinct, proximal end of humerus quadrangular in anterior view
- 1 less pronounced, forming an arc rather than being quadrangular
- 2 very weakly developed, proximal end of humerus with rounded edges
- 3 extremely long (as in *Shuvuuia* and *Mononykus*)

382. Deltopectoral crest orientation

- 0 longitudinal
- 1 oblique distolaterally and distal end of crest oriented laterally rather than anteriorly from the humeral shaft

383. Lateral surface of distal end of deltopectoral crest

- 0 smooth
- 1 with distinct muscle scar near lateral edge along distal end of crest for insertion

of biceps muscle

384. Ratio femur/humerus

- 0 more than 2.5
- 1 between 1.2 and 2.2
- 2 less than 1

385. Outline of proximal articular facet of humerus

- 0 broadly oval (more than twice as broad transversely than anteroposteriorly)
- 1 distinctly rounded, often globular (less than twice as broad anteroposteriorly than transversely)

386. Internal tuberosity of humerus

- 0 small and confluent with humeral head
- 1 offset from humeral head by distinct notch, often projects proximally above humeral head
- 2 hypertrophied but not distinct from humeral head (as in *Suchomimus*)

387. Shape of internal tuberosity on humerus in anterior view

- 0 triangular, often rounded
- 1 rectangular

388. Humerus in lateral view

- 0 sigmoidal
- 1 straight

389. Transverse width of distal humerus

- 0 greater than 2.7 times shaft width
- 1 between 2 and 2.5 times humeral shaft width
- 2 less than twice shaft width

390. Ectepicondyle of humerus (lateral epicondyle)

- 0 small, often rectangular and does not form articular surface
- 1 large, rounded and forms articular surface

391. Ectepicondyle of humerus

[New character. In alvarezsaurids including *Patagonykus* and more crownward taxa, there is a distinct notch between the distal end of the humerus and the ectepicondyle.]

- 0 confluent with humeral distal end
- 1 set off from humeral distal end by a distinct notch

392. Entepicondyle of humerus (medial epicondyle)

- 0 absent or small and tabular
- 1 large, projects medially from ulnar condyle as a distinct process and is distally separated from ulnar condyle by a groove

393. Distal humeral condyles

- 0 primarily developed on distal end of humerus, but may also have some articular surface extending to anterior edge
- 1 limited to anterior surface, condylar surfaces not present on distal end

394. Ulnar shaft

- 0 straight
- 1 bowed

395. Olecranon process of ulna

- 0 absent or weakly developed
- 1 well-developed
- 2 hypertrophied

396. Shape of olecranon process

- 0 transversely broad
- 1 mediolaterally thin, blade-like

397. Crest extending along posterior surface of ulnar shaft from olecranon process

- 0 absent
- 1 present

398. Proximal surface of ulna

- 0 single continuous articular facet

- 1 divided into two distinct fossae
- 399. Proximal end of the ulna in proximal view**
 - 0 without extensive coronoid process and radial process on radial side of proximal end (without extensive coronoid process on radial side of proximal end)
 - 1 coronoid and radial processes large (coronoid process large, extends at right angle to olecranon)
- 400. Distal articular surface of ulna**
 - 0 flat
 - 1 convex, semilunate surface
- 401. Distal condyle articular surface of ulna**
 - 0 unexpanded or spatulate, articular surface limited to distal end
 - 1 bulbous, trochlear articular surface extends onto dorsal surface of ulna
- 402. Radius length**
 - 0 more than half the length of humerus
 - 1 less than half the length of humerus
- 403. Radial shaft**
 - 0 straight
 - 1 bowed laterally
- 404. Radius and ulna**
 - 0 well-separated
 - 1 with distinct adherence or syndesmosis distally
- 405. Ossified carpals**
 - 0 absent
 - 1 present (Personal observation, but may appear in some ceratosaur matrices)
- 406. Lateral proximal carpal (ulnare?)**
 - 0 quadrangular
 - 1 triangular in proximal view
- 407. Trochlea on the proximal surface of distal carpal 1**
 - 0 absent
 - 1 present
- 408. Two distal carpals**
 - 0 in contact with metacarpals, one covering the base of Mc I (and perhaps contacting Mc II), the other covering the base of Mc II
 - 1 two distal carpals not present, single distal carpal capping Mc I and II
- 409. Distal carpals**
 - 0 not fused to metacarpals
 - 1 fused to metacarpals, forming carpometacarpus
- 410. Rectangular buttress on ventrolateral surface of proximal end of Mc I**
 - 0 absent
 - 1 present
- 411. Length of Mc I**
 - 0 approximately half the length of Mc II
 - 1 subequal in length to Mc II
- 412. Shape of Mc I**
 - 0 significantly longer than broad
 - 1 very stout, approximately as long as broad
- 413. Contact between Mc I and Mc II**
 - 0 metacarpals contact each other at their bases only
 - 1 Mc I closely appressed to Mc II, at least the proximal half of McI flattened
- 414. Medial tab on proximal end of Mc I**
 - 0 absent or poorly developed
 - 1 well-developed
- 415. Proximomedial tab projects**

[New character. Added to differentiate between *Haplocheirus*, where this process is present but not hypertrophied, and other alvarezsaurs, where the process is

hypertrophied.]

- 0 mostly medially, does not extend proximally beyond proximal articular surface
- 1 far proximally, well beyond proximal articular surface

416. Distal end of Mc I

- 0 condyles more or less symmetrical
- 1 condyles strongly asymmetrical, the medial condyle being positioned more proximally than the lateral

417. Distal articular end of metacarpal I

- 0 ginglymoid
- 1 rounded and smooth

418. Distal condyles of Mc I

[New character. In most alvarezsaurids, including *Haplocheirus*, *Tugulusaurus*, and *Bannykus*, but notably not in *Ceratomykus*, the collateral ligament pits on the lateral and medial surfaces of the distal condyles of metacarpal I are absent or reduced to shallow concave areas]

- 0 with collateral ligament fossae
- 1 collateral ligament fossae absent

419. Medial side of Mc II

- 0 expanded proximally
- 1 not expanded

420. Shaft of Mc II

[New character. In *Haplocheirus*, the shaft of Mc II is straight, but in the alvarezsaurids *Bannykus* and *Linhenykus*, the shaft of Mc II is conspicuously bowed. The hand of other non-parvicursorine alvarezsaurids is incompletely known, but it appears that this may be a transient feature in the reduction of the alvarezsaur manus.]

- 0 straight
- 1 curved, medial surface is concave, lateral surface is bowed
- 2 curved, medial surface is convex, lateral surface is concave

421. Distal articular end of McII

- 0 ginglymoid
- 1 without ginglymus

422. Shaft of Mc III

- 0 subequal in width to Mc II
- 1 considerably more slender than Mc II (less than 70% of the width of Mc II)

423. Proximal articular end of Mc III

- 0 expanded and similar in width to Mc I and II
- 1 not expanded, very slender when compared to Mc I and II

424. Proximal articular surface of Mc III

[New character. Added to differentiate the flat proximal condition in *Haplocheirus* and most other theropods from the cuplike condition in parvicursorine alvarezsaurids.]

- 0 flat or slightly convex
- 1 deeply concave and cuplike

425. Length of Mc III

- 0 much longer than Mc I
- 1 subequal in length to Mc I
- 2 much shorter than Mc I

426. Proximal outline of Mc III

- 0 subrectangular
- 1 triangular, apex dorsal

427. Shaft of Mc III

- 0 straight
- 1 bowed laterally

428. Extensor pits on the dorsal surface of the distal end of metacarpals

- 0 absent or poorly developed
- 1 deep, well-developed

- 429. Number of manual digits with one or more phalanges**
0 five
1 four
2 three
3 two (as in *Tyrannosaurus rex*)
- 430. Number of metacarpals**
0 five
1 four
2 three
- 431. Paired flexor processes on proximal ventral surfaces of proximalmost phalanges**
0 absent
1 present
- 432. Lateral and medial surfaces of phalanx I-1**
0 face predominantly medially and laterally, either flat or convex
1 face dorsolaterally and dorsomedially and are shallowly concave
- 433. Flexor surface of manual phalanx I-1**
0 convex or flat
1 concave, 'axial furrow' along proximodistal axis
- 434. Shaft diameter of phalanx I-1**
0 less than shaft diameter of radius
1 greater than shaft diameter of radius
- 435. Proximodistal length of phalanx I-1/length of Mc I**
0 1 or less
1 between 1 and 1.5
2 more than 1.5
- 436. Penultimate phalanx of the second finger**
0 shorter than first phalanx
1 longer than first phalanx
- 437. Penultimate phalanx of the third finger**
0 as long as, or shorter than, more proximal phalanges
1 longer than each of the more proximal phalanges
2 longer than both proximal phalanges taken together
- 438. Length of third manual digit**
0 longer than second finger
1 shorter than or equal in length to second finger
- 439. Proximal articular surface of manual ungual I-2**
0 dorsoventrally much taller than mediolaterally wide
1 mediolaterally as broad as tall
- 440. Unguals on all manual digits**
0 generally similar in size
1 digit I bearing large ungual and unguals of other digits distinctly smaller
- 441. Transverse ridge immediately dorsal to the articulating surface of unguals**
0 absent
1 present
- 442. Flexor tubercle placement**
0 proximal
1 distal
2 absent
- 443. Curvature of ventral surface manual ungual I**
0 strongly curved
1 weakly curved
2 straight
- 444. Curvature of ventral surface of manual unguals II and III**
0 strongly curved
1 weakly curved

- 2 straight
- 445. Flexor tubercle size**
 - 0 large ($> 1/3$ articular facet height)
 - 1 small ($< 1/3$ articular facet height)
- 446. Lateral grooves of manual ungual I-2 in ventral view**
 - 0 unenclosed
 - 1 proximal end of grooves partially enclosed by lateral notches
 - 2 proximal end of grooves passes through foramina on ventral surface of ungual
- 447. Fusion of pelvic elements in adults**
 - 0 absent
 - 1 present
- 448. Ilium**
 - 0 brachyliac
 - 1 dolichoiliac
- 449. Ilium pneumaticity**
 - 0 little or none
 - 1 large external pneumatic foramina and internal spaces
- 450. Dorsal margin of ilium**
 - 0 subhorizontal or gently inclined relative to axis of pubic and ischial contact
 - 1 rises steeply as it extends anteriorly, at least 30 degree angle from the axis of the pubic and ischial contact
- 451. Ventral edge of anterior ala of ilium**
 - 0 straight or gently curved
 - 1 ventral edge hooked anteriorly
- 452. Form of hook of preacetabular ala of ilium**
 - 0 weak
 - 1 strong
- 453. Preacetabular part of ilium**
 - 0 significantly shorter than postacetabular part
 - 1 subequal in length to postacetabular part
 - 2 significantly longer than postacetabular process
- 454. Anterior rim of ilium**
 - 0 shallowly convex or straight
 - 1 strongly convex or pointed anteriorly
- 455. Dorsally-positioned, anteriorly-concave notch on anterior rim of ilium**
 - 0 absent
 - 1 present
- 456. Preacetabular part of ilium (height)**
 - 0 approximately as high as postacetabular part (excluding the ventral expansion)
 - 1 significantly higher than postacetabular part
 - 2 significantly lower than the postacetabular part
- 457. Cuppedicus fossa**
 - 0 absent
 - 1 present
- 458. Form of cuppedicus fossa**
 - 0 deep, ventrally concave
 - 1 fossa shallow or flat, with no lateral overhang
- 459. Cuppedicus fossa position**
 - 0 ridge bounding fossa terminates rostral to acetabulum or curves ventrally onto anterior end of pubic peduncle
 - 1 rim extends far posteriorly and is confluent or almost confluent with acetabular rim
- 460. Preacetabular portion of ilium**
 - 0 parasagittal
 - 1 moderately laterally flaring

461. Brevis fossa shape

- 0 shelf-like, narrow with subparallel margins
- 1 deeply concave, expanded posteriorly with lateral overhang

462. Brevis fossa lateral view

- 0 Poorly developed adjacent to ischial peduncle, without lateral overhang and medial edge of the brevis fossa is visible
- 1 well developed fossa along full length of postacetabular blade, lateral overhang extends along full length of fossa, medial edge of brevis fossa covered in lateral view

463. Medial brevis shelf

- 0 strongly developed, projects medially
- 1 low ridge on medial surface of postacetabular ala

464. Shape of postacetabular ala of ilium in lateral view

- 0 squared
- 1 acuminate

465. Postacetabular ala of ilium in lateral view

[New character. Added to homologize the condition of the ilium in *Haplocheirus* and other alvarezsaurids (state 2). In some dromaeosaurs and some oviraptorosaurs, the ventral edge is concave but does not extend far ventrally.]

- 0 ventral edge flat
- 1 ventral edge concave
- 2 ventral edge concave and distal end extends ventrally below level of the ventral margin of the ischial peduncle

466. Articulation of iliac blades with sacrum

- 0 vertical, well-separated above sacrum
- 1 strongly inclined mediodorsally, almost contacting each other or sacral neural spines at midline

467. Vertical ridge on iliac blade above acetabulum

- 0 absent
- 1 low ridge with associated foramina
- 2 well-developed

468. Shape of pubic peduncle of ilium

- 0 transversely broad and roughly triangular in outline
- 1 anteroposteriorly elongated and narrow

469. Iliac pubic peduncle length relative to iliac ischial peduncle

- 0 significantly longer than ischial peduncle, ischial peduncle tapering ventrally and without clearly defined articular facet
- 1 subequal in length to ischial peduncle
- 2 anteroposteriorly shorter than the ischial peduncle

470. Articulation facet of pubic peduncle of ilium

- 0 facing more ventrally than anteriorly, and without a pronounced kink
- 1 with pronounced kink and anterior part facing almost entirely anteriorly

471. Anterior margin of pubic peduncle

- 0 straight or convex
- 1 concave

472. Supraacetabular crest

- 0 absent
- 1 present

473. Form of supraacetabular crest

- 0 forms hood over femoral head
- 1 reduced, not forming hood

474. Antitrochanter posterior to acetabulum

- 0 absent or poorly developed
- 1 prominent

475. Postacetabular blades of ilia in dorsal view

- 0 parallel
- 1 diverge posteriorly
- 476. Tuber along dorsal edge of ilium, dorsal or slightly posterior to acetabulum**
 - 0 absent
 - 1 present
- 477. Dorsal margin of postacetabular ala in lateral view**
 - 0 convex or straight
 - 1 concave, brevis shelf extends caudal to lateral ilium making it appear concave in lateral view
- 478. Caudal end of postacetabular ala in dorsal view**
 - 0 rounded or squared in dorsal view
 - 1 lobate, with brevis shelf extending caudally beyond caudal terminus of the postacetabular ala
- 479. Ilium and ischium articulation**
 - 0 flat or slightly concavo-convex
 - 1 with process projecting into socket in ischium
- 480. Pubic orientation**
 - 0 propubic
 - 1 vertical
 - 2 moderately posteriorly oriented
 - 3 opisthopubic
- 481. Prepubic tubercle on proximal end of pubis anterior to acetabular portion**
 [New character. In parvicursorine alvarezsauroids as well as in *Bonapartenykus*, the anterior margin of the dorsal portion of the pubis is anteriorly expanded into a tubercle]
 - 0 absent
 - 1 present
- 482. Strongly expanded pubic boot**
 - 0 absent
 - 1 present
- 483. Pubic boot projects**
 - 0 anteriorly and posteriorly
 - 1 with little or no anterior process
 - 2 only expanded anteriorly
- 484. Ratio length of pubic boot to length of pubic shaft**
 - 0 less than 0.3
 - 1 more than 0.5
- 485. Pubic boot outline, distal view**
 - 0 triangular
 - 1 narrow, with subparallel margins
- 486. Pubic apron**
 - 0 present
 - 1 absent
- 487. Form of pubic apron**
 - 0 extends medially from middle of cylindrical pubic shaft
 - 1 shelf extends medially from anterior edge of anteroposteriorly flattened shaft
- 488. Pubic apron**
 - 0 about half of pubic shaft length
 - 1 less than 1/3 of shaft length
- 489. Pubic apron**
 - 0 completely closed
 - 1 with medial opening distally above the pubic boot
- 490. Pubic obturator foramen**
 - 0 present
 - 1 absent
- 491. Form of pubic obturator foramen**

- 0 completely enclosed
- 1 open ventrally (obturator notch)
- 492. Pubic fenestra below obturator foramen**
 - 0 absent
 - 1 present
- 493. Pubic shafts in lateral view**
 - 0 straight
 - 1 anteriorly convex
 - 2 anteriorly concave
- 494. Lateral face of pubic shafts**
 - 0 smooth
 - 1 with prominent lateral tubercle about halfway down the shaft
- 495. Length of Ischium**
 - 0 more than two-thirds pubis length
 - 1 two thirds or less of pubic length
- 496. Obturator process of ischium**
 - 0 absent
 - 1 present
- 497. Position of obturator process**
 - 0 proximal in position
 - 1 located near middle of ischiadic shaft
 - 2 located at distal end of ischium
- 498. Ischial shaft**
 - 0 rodlike
 - 1 anteroposteriorly wide and plate like
- 499. Lateral blade of ischium**
 - 0 flat or laterally convex
 - 1 laterally concave
 - 2 with longitudinal ridge subdividing lateral surface into anterior (including obturator process) and posterior parts
- 500. Ischium, lateral view**
 - 0 straight
 - 1 distally curved anteriorly
 - 2 distally curved posteriorly
- 501. Ischium, anterior view**
 - 0 straight
 - 1 laterally convex
 - 2 twisted at midshaft and with flexure of obturator process toward midline so that distal end is horizontal
 - 3 laterally concave
- 502. Contact of obturator process of ischium**
 - 0 does not contact pubis
 - 1 contacts pubis
- 503. Ventral notch at distal edge of ischial obturator process**
 - 0 absent, grades smoothly into ischial shafts
 - 1 present
- 504. Obturator process on ischium**
 - 0 confluent with pubic peduncle
 - 1 offset from pubic peduncle by a distinct notch
- 505. Morphology of offset triangular obturator process of ischium**
 - 0 wide base along ischiac shaft, rostral process short
 - 1 narrow base, rostral process elongate
- 506. Distal end of ischium**
 - 0 strongly expanded, forming ischial "boot"
 - 1 slightly expanded

- 2 tapering
- 507. Distal ends of ischia**
 - 0 form symphysis
 - 1 approach one another but do not form symphysis
 - 2 widely separated
- 508. Distally placed process on caudal margin of ischium**
 - 0 absent
 - 1 present
- 509. Tubercle on anterior edge of ischium**
 - 0 absent
 - 1 present
- 510. Posterior process (ischial tuberosity) on posteroproximal part of ischium**
 - 0 absent
 - 1 well-developed
- 511. Form of posteroproximal ischial process (ischial tuberosity)**
 - 0 small, tab-like
 - 1 large, proximodorsally hooked and separated from the iliac peduncle by a notch
- 512. Semicircular scar on posterior part of the proximal end of the ischium**
 - 0 absent
 - 1 present
- 513. Femoral length**
 - 0 longer than tibia
 - 1 shorter than tibia
- 514. Femoral head**
 - 0 without fovea capitalis
 - 1 circular fovea present in center of medial surface of head
- 515. Oblique ligament groove on the posterior surface of femoral head**
 - 0 absent or very shallow
 - 1 deep, bound medially by a well-developed posterior lip
- 516. Femoral head and greater trochanter**
 - 0 confluent with greater trochanter
 - 1 separated from greater trochanter by a distinct cleft
- 517. Femoral head direction anteroposterior**
 - 0 directed anteromedially
 - 1 directed strictly medially
- 518. Femoral head direction dorsoventral**
 - 0 ventromedial
 - 1 horizontal
 - 2 dorsomedial
- 519. Greater trochanter**
 - 0 anteroposteriorly narrow and narrowing from medial to lateral
 - 1 anteroposteriorly expanded, forming a trochanteric crest
- 520. Lesser trochanter**
 - 0 separated from greater trochanter by a deep cleft
 - 1 trochanters separated by small groove
 - 2 completely fused (or absent) to form crista trochanteris
- 521. Lesser trochanter shape**
 - 0 alariform (Additional taxa coded from state 2 of Rauhut, 2003 #198 "broadened (wing-like)")
 - 1 cylindrical in cross section
 - 2 very short and ridge-like
- 522. Proximal extent of lesser trochanter**
 - 0 at distal end of femoral head
 - 1 more proximally placed, but distal to greater trochanter
 - 2 as proximal or more proximal than greater trochanter

- 523. Accessory trochanteric crest on distal end of lesser trochanter**
0 absent
1 present
- 524. Posterolateral trochanter**
0 absent or represented only by rugose area
1 posterior trochanter distinctly raised from shaft, mound-like
- 525. Fourth trochanter on femur**
0 present
1 absent
- 526. Broad groove on extensor surface of distal femur**
0 absent or poorly developed
1 well developed
- 527. Femoral medial epicondyle (medial distal crest, expanded medial lamella)**
0 stout ridge or absent
1 flange like, medially extensive
- 528. Popliteal fossa on distal end of femur**
0 open distally
1 closed off distally by contact between distal condyles
- 529. Infrapopliteal ridge present posteriorly between medial condyle and crista tibiofibularis**
0 absent
1 present
- 530. Distal end of femur**
0 anteroposteriorly broad and distally flattened
1 less broad and well rounded
- 531. Lateral femoral distal condyle**
0 distally rounded
1 distally conical
- 532. Distal projection of lateral femoral distal condyle**
0 approximately the same level as the medial condyle
1 distinctly further than medial condyle and distal surface of medial condyle is flattened
- 533. Anteroposterior length of proximal end of tibia in proximal view**
0 exceeds mediolateral width
1 less than mediolateral width
- 534. Cnemial crest proximal projection**
0 approximately at the same level as posterior condyles
1 projects strongly proximal to posterior condyles
- 535. Anteroposterior length of cnemial crest**
0 prominent but not expanded
1 anteroposteriorly expanded
- 536. Accessory ridge on lateral surface cnemial crest**
0 absent
1 present
- 537. Medial cnemial crest and lateral cnemial crest (also called the cranial cnemial crest in birds)**
0 absent, only one cnemial crest
1 present, two cnemial crests
- 538. Fibular condyle on proximal end of tibia**
0 confluent with cnemial crest anteriorly in proximal view
1 strongly offset from cnemial crest
- 539. Medial proximal condyle on tibia**
0 round in proximal view
1 arcuate and posteriorly angular in proximal view
- 540. Posterior cleft between medial part of the proximal end of the tibia and fibular**

condyle

- 0 absent
- 1 present

541. Fibular crest (ridge on lateral side of tibia for connection with fibula)

- 0 absent
- 1 present

542. Form of fibular crest

- 0 extending from proximal articular surface distally
- 1 clearly separated from proximal articular surface

543. Shape of fibular crest

- 0 quadrangular
- 1 low and rounded

544. Fibular crest distal extension

- 0 proximally positioned
- 1 extends to midshaft of tibia

545. Fibular crest length

- 0 short, less than one fifth tibial length
- 1 long, between one quarter and one third tibial length

546. Bracing for ascending process of astragalus on anterior side of distal tibia

- 0 distinct 'step' running obliquely from mediodistal to lateroproximal
- 1 anterior side of tibia flat
- 2 Step-like ridge running proximodistally rather than obliquely

547. Fibula

- 0 reaches proximal tarsals
- 1 short, tapering distally, and not in contact with proximal tarsals

548. Lateral surface of proximal fibula

- 0 shallow longitudinal trough situated posteriorly
- 1 trough absent or weak groove present, surface convex

549. Proximal fibular margin

- 0 subhorizontal
- 1 cranial portion extends proximally beyond level of posterior portion

550. Fibular proximal dimensions in proximal view

- 0 anterior portion subequal to posterior portion in mediolateral width
- 1 anterior portion mediolaterally wider than posterior portion

551. Insertion of m. iliofibularis on fibular shaft

- 0 not especially marked
- 1 present as a well-developed anterolateral tubercle

552. Position of insertion of m. iliofibularis on fibular shaft

- 0 proximal
- 1 midshaft

553. Ridge on medial side of proximal end of fibula, that runs anterodistally from the posteroproximal end

- 0 absent
- 1 present

554. Medial surface of proximal end of fibula

- 0 concave along long axis
- 1 flat

555. Deep oval fossa on medial surface of fibula near proximal end

- 0 absent
- 1 present

556. Astragalus and Calcaneum

- 0 condyles indistinct or poorly separated
- 1 distinct condyles separated by prominent vertical tendinal groove on anterior surface

557. Astragalus and calcaneum

- 0 separate from tibia
- 1 fused to each other and to the tibia in late ontogeny
- 558. Fibular facet on astragalus**
 - 0 large and facing partially proximally
 - 1 reduced and facing laterally or absent
- 559. Height of ascending process of the astragalus**
 - 0 lower than astragalar body
 - 1 higher than astragalar body
 - 2 more than twice the height of astragalar body
- 560. Shape of ascending process of the astragalus**
 - 0 broad, covering most of anterior surface of distal end of tibia
 - 1 narrow, covering only lateral half of anterior surface of tibia
- 561. Notch on medial edge of ascending process of the astragalu**
 - 0 absent
 - 1 present
- 562. Fossa on anterior surface of mesial base of ascending process of astragalus, sometimes bearing accessory fenestrations**
 - 0 absent
 - 1 present
- 563. Ascending process of astragalus and astragalar body**
 - 0 confluent or only slightly offset from astragalar body
 - 1 offset from astragalar body by a pronounced groove
- 564. Astragalar condyles**
 - 0 almost entirely below tibia and face distally
 - 1 significantly expanded proximally on anterior side of tibia and face anterodistally
- 565. Horizontal groove across astragalar condyles anteriorly**
 - 0 absent
 - 1 present
- 566. Calcaneum**
 - 0 without facet for tibia
 - 1 well-developed facet for tibia present
- 567. Distal tarsals**
 - 0 separate, not fused to metatarsals
 - 1 form metatarsal cap with intercondylar prominence that fuses to metatarsal early in postnatal ontogeny
- 568. Metatarsals coössification**
 - 0 not co-ossified
 - 1 coossified
- 569. Shafts of metatarsals II-IV**
 - 0 not closely appressed beyond proximal half of metatarsus
 - 1 closely appressed throughout most of metatarsus, adjacent surfaces flattened for contact
- 570. Maximum length of metatarsals**
 - 0 greater than 50% tibia length
 - 1 less than 50% tibia length
- 571. Metatarsal I**
 - 0 present
 - 1 absent
- 572. Metatarsal I**
 - 0 attenuates proximally, without proximal articulating surface
 - 1 proximal end of Mt I similar to that of Mt II-IV
- 573. Metatarsal**
 - 0 contacts the ankle joint
 - 1 does not contact the ankle joint

574. Position of distally-placed Mt I

- 0 reduced, elongated and splint-like, articulates in the middle of the medial surface of Mt II
- 1 broadly triangular and attached to the distal quarter of Mt II

575. Metatarsal II proximal end of flexor surface

- 0 flat or small tab present
- 1 large quadrangular flange present

576. Distal end of metatarsal II

- 0 smooth, not ginglymoid
- 1 with developed ginglymus

577. Tuber along extensor surface of MtII

- 0 absent
- 1 present

578. Posteromedial margin MtII diaphysis

- 0 well-developed flange absent or area rugose
- 1 with flange projecting caudally or medially

579. Distal end of metatarsal III

- 0 smooth, not ginglymoid
- 1 with developed ginglymus

580. Metatarsal III

- 0 subequal in width to Mt II and IV proximally
- 1 pinched between II and IV and not visible in anterior view proximally
- 2 does not reach the proximal end of the metatarsus
- 3 mediolaterally much wider than either II or IV

581. Metatarsal III shape of proximal end

- 0 rectangular, medial and lateral surfaces pinched
- 1 hourglass-shaped, medial and or lateral surface(s) concave

582. Medial side of anterior surface of distal end of MtIII

- 0 unexpanded
- 1 expanded

583. Metatarsal III shape of shaft in cross section

- 0 rectangular
- 1 wedge-shaped, plantar surface pinched

584. Shaft of MT IV

- 0 round or thicker dorsoventrally than wide in cross section
- 1 shaft of Mt IV mediolaterally widened and flat in cross section

585. Length of MtIV

- 0 subequal to Mt II
- 1 markedly longer than Mt II

586. Posterolateral margin of MtIV diaphysis

- 0 well-developed flange absent or area rugose (in *Allosaurus* and tyrannosaurids, a flattened, ridge-like and long rugosity is present in this area)
- 1 with flange projecting caudally or laterally

587. Metatarsal V

- 0 with rounded distal articular facet
- 1 strongly reduced and lacking distal articular facet
- 2 short, without articular surface, transversely flattened and bowed anteriorly distally

588. Pedal digit IV

- 0 significantly shorter than III and subequal in length to II, foot is symmetrical
- 1 significantly longer than II and only slightly shorter than III, foot is asymmetrical

589. Extensor ligament pits on dorsal surface of phalanges of pedal digit IV

- 0 shallow, extensor ridges not sharp
- 1 deep and extensive proximally, corresponding extensor ridges sharply defined

in dorsal view

590. Pedal phalanges of digit IV

0 anteroposteriorly short, with proximal and distal articular surfaces very close together, particularly in distal elements

1 anteroposteriorly long, proximal and distal articular surfaces well-separated

591. Shape of ventral surface of pedal unguals

0 ventrally concave in lateral view

1 straight in lateral view

592. Ungual and penultimate phalanx of pedal digit II

0 similar to those of III

1 highly modified for extreme hyperextension, ungual more strongly curved and about 50% larger than that of III

593. Ventral surface of pedal unguals

0 without a flexor fossa, ventral surface of proximal end convex

1 with a pronounced flexor fossa on ventral surface of proximal end

594. Form of flexor fossa on pedal unguals

0 without development of flexor tubercle

1 small flexor tubercle present within flexor fossa

Data matrix. The matrix is also available on Morphobank [S9] at the following link:

<http://morphobank.org/permalink/?P2127>.

'Herrerasaurus_ischigualastensis'?000000?00?100---??0010-0000000000?000?000
00001?201000000000-0--01100--00100000??-?00?0-00?00?000?1???01???11?0000?0?000
0?0?0?0?0?0?000?0?01?1?0?0?0-000?0?0?0?0?0?0?0?0?0?000-0?0011?0?0?0?010?000?
0?0?0?0?0?01010?000?010000000?0?0?000?000-0000100?0?0?0?001000?0000000000000
00000000100?0?01?1?0?000?00?0?00000000?000?0000?0?0?0?0?0?0?0?0?0?0?0-??0
0?1000010?001110?10000100?0100?0?00001?0?01000-0?0120000000110000?11100000?
??0000?0-0?0?0?0?00-000001001?0?0?0?01010?0?00000?0101?0?0?00-1?1?0-??010000?200
000000000000?0000---0?0?100?0?0?001000000?000?0-0?0?0000?000?01000-

'Dilophosaurus_wetherilli' ??001020?00?0?0---1?0?0?0-010?0010011(0 1)0(0
1)1?0?0?1001?2010001000010?0--1111?0010?0?0?000010-01?0?0?0?111?0?000?011??
0?0?0?0000?0?0?0?1?0?000?0?1?1?0?0?0?10000?0101?0?0?0?0?0?0?0?0?0?0?0-10?0
01010?01?0?0?0?0?01010?000?1000000000?0?1?0?0?00-0110110?1101?0011?0011?0?0?0?
00110000200?0?10?10000?0?0?1100?030?00?0?0?000020?000?01000?0?0?10?0?0?0?0?0?
0?0?2000000100?0?0?0?0?100?100001000?0100?0?010?01?00?000-1?0020100000110000?
1?11000?0?0?11000-??0?0?0?1?00?0001101?0?0?100?00-00?0?100?00?100?0?0?10-??0-??1
1000001000000000?0000?000110?000?0?0?100?0?0?001000000?0?0?10?0?0?0000?0?20010
00-

'Coelophysis_bauri' ??000011?0?0?000---??0?0?00-0101001?1?10?0?0?
00001001?0?0000000000-0--11100--00100?0?0?-000?0-01?00?0?0?0?0?0?0?0?0?0?0?
000?0?0?001?0?
0?0?0?0?0?01010?010?020000000?0?0?000?000-1?0100?11000?02?0010?0?100?00(0
1)00002001?0000?
0?0?0?0?0?01100?000?0?01?0?10000100?0100?0?0?0?0?0?0?0?0?0?0?0?0?0?0?0?0?
00?0?0?0?0?01000-0000?0?0?100000001101?0?000?000-00?0?0001101100?0?0?10-1?0?0-??1100
?0?0?0?0000000?00101?0?110?
00-1000-

'Tawa_hallae' ??0001201000?000---01001?11000?00000?1?0?
0?000?0011?200?001000010-0--12100--?1100?0?0?000?0-00?0?0-??11010000?0?0?0?0?
0?
?0?
?0?
?10000100?00100110000?
000000-0?0?0--?0?00?0?00000100?000?0?110?0?0?0?0?0?0?0?0?0?0?0?0?0?0?0?
0?0100?

'Carnotaurus_sastrei' ??10000000001000---0?00?010000100010001?0?1?

1001110??200000000?000-10101000--?10-1100000001?1101100101000010000?000-??0??
??1000??2??0?????0?00??00?1001??0?0??????????????1?101100?00?01000-100?010
0-0??0?11101000101000?01000000?0?0000000??0-000010101101?10?00??11102?10111
00?000100?0010?1000010011?110040??11?0?0????000??0?0????0000??0?0????00--00
00-000?01000011010?0221?0110?2000000-000111000----??????1?0??01?????????????
??????11000-0000?0????00?00?00?0?000000100??01000000100?000?0-00000-??000?10
000?0111011?0011?00?110?0??

'Ceratosaurus_nasicornis' ??10100010001100---00?00?0100000001000010001
111010101101-1000000001110?11100--0010010000000010-011101010010100010?00-0?00
?0?1000?02??0?1??000??0?0?1?1??10?00?0?0????????????1??0000-??0?0?0-10?001
00-0?0?????100?100?0000?11000?0000?0?0?0?00-000011?11011000000011??0?00111
01?000100?00??10000000110110040?01?0?1?000?01000?0?01000010??10000??????????0
0020000?0100?0?1000????????????????10001100101??0?0100??10000010001011100?1?
????2????1100??0000??0?1?00000010010000000000-000101000100100000010-00000-0?1
100000000001101100011101110?0?0000?1000??001000011????????????00?0?0?????0?
0?

'Limusaurus_inextricabilis' ??1000101001110101?00?000?11?0?1?01?000?---000
00?000?01-?000000000-10012100--00120??0??00000-00?1??0000?0?020?00-????01?0
00??020-?00?01?1110-?0-1000-??0?10
?0?0?0??11-----1-----000?0?1101?1?2?0000-??01?0?0?0?????????????????
?00?0?1??0?0????????1000?000??020000000-0??1101000??0-100020000001100001000
01?10011011?000?00000?000000----?0000-010001000101(1 2
3)100-00011--02??000000-000110001000?1001001001000000100??0?0000?00-??000?0?0
0?00?1??00?010?0?0?0?0?0?0?00011??????????0?0?10?0?0?1??????001?0?0?00?0?0?00?0?2
?00000-

'Majungasaurus_crenatissimus' ??10100010001000--??10000010000100011100
?1011010112010000000010-101?1010--010-1100000011?11011111011000100010?00-0000
001?1000012??001?00000001??1????0??0?0?0??0-????????0?10110??0?00?0??010?0?
100-010000100100010100000011000000000000000100-0000111010-1?10000?011?02000
111010000100100101?0000001010110030??1?001100002000000110000000?100100?????
????000-00000??0000?0?00022100100120000????????0?0?0?0?0?0?0?0?0?0?0?0?0?0?0?
????????????010010000010001000?0001001000000100????????0?0?0?0?0?0?0?0?0?0?0?
?????000000?000100011101101010000111100010000100010?0?0?0?0000000?0?0?0000
0011

'Cryolophosaurus_elliotti' ????????????????????????????1?1?1?0000?0?0?
????0?2????0?00001011??1100--001000????00000-01?00?10?10?00?0??10?0?0?0?0?0?
0????????????0?0?0?10101????000?0?0?0?0?0-??0?0?0?0?0?0?0?0?0?0?0?0-0-110?0
????????????0(1 2)?0?0000?
1)?0?
0?00?
????????????0?
????01001?010?011?0?0000????????0?
???

'Monolophosaurus_jiangi' ??001000100101?10000?00?01110001000?0000??
001111000100201100000001111??11100--0010000000-000110011000-0011000001?010??
?????0000?0??0?1??00?0??0?10100?100000-????????0?0011110-?0000-00-100?
0100-1??0?0100211?1010000002000?00000000000?010100?1101?10-1?100?01011?00010
?100101001000000011?000000?10010030?00?0?0?0?0?0?0?0?0?0?0?0?0?0?0?0?0?0?
??
????0100100000100100?0?01000010000000000-??0101000100100?00110-100?0-?????
??

'Piatnitzkysaurus_floresi' ????0?
????????????????????????????????0?
??0?1??0?0?0?0?0?1?1?0?10?0010?010-????0?0?0?0?0?0?0?0?0?0?0?0?0?0?0?0?
????????0?0?1?01?00?0?0?0?0?0?010011110?10-1010?1?0011????10?001?10010?0?0?

'Baryonyx_walkerii' ??0101201001110?????10??011?0?000?0000
00101????0??2?????0??0101??10100--0010011???10?000??1????11??????020?010?????
?????0000000??1?10010??0?010100011000-0?10-00-10?0?0????11110-?0100-00-10010?
?1111000??0101?103000000?20000010102101000100-110111?10-1010?001011?00010??
01121001100??000110000??0100100?????????0?0002????????????00?0?01?0?01010?0??
000-??00?00?0?10000?2010?02010001012100110101????????????????????0000????
0100?????1?0??????????1000??00000100????00?0-????0???0?0100000?100?0000-0?01011
0?????1000100??????????????0?0100000?00????????????????????????????????

'Eustreptospondylus_oxiensis' ?0?020100?1100---00000?1100?0001001000?0??
?????1?????????000?1-11011000--0011011?00000010-010?0????010?00000?00-?????????
??0?????0?1?00010?0?01010001?0111?100-??10-00-10000?0?0?1?110-?0????0101001?????
??????0?0??010000002000?0000000101000100-0110111010-11100101011?00?10?00100
002000??000110000??01000?030?00?0?0?(0
1)00002??00?00????????????????????????????????1?00?0?100?0?200010001?0000??????
??10??0?0?0??01000?0000001100000000
10000001010000100010?0?01?000-0101001000000010001000100000111000000011000000
00100011?00?0???00000100000?001000-

'Afrovenator_abakensis' ?????0?0?????1?101001??0??11010100110?00000?
1??????0?201100??0?001010011100--00?????????00010-01?0?0??010000001?010?0?????
0?0?0??
????????????????????02000100000?0?????0100-0110110?10-1?0001?1?11??010?0?(0
1)?10?10?0?????1?00?0?????0?0?????????0?0?0?0?0?0?100?0?????11?00?0????????????
????????????????????0?0?01?0?????00?0?????1?0011??1?00?0?????121000?2??01000
0000100100?0?0??00?00010000100?0000000-0?0?01??000100010011010000-?0?0?11000
10001000100?0?0?0????001??00?0000100?111??1?0?110?0??01????2??0???

'Allosaurus_fragilis' ??0010(0
1)01001010?0000?0000?1000010?110?0100100001?1?011?1-000000000101???0
1)100--?111010000-01000-010?0?0?01?0100010101120?00010?00001001001?00?000010?0
0101001100100-1?10-?0-0-?000000010000-?0000-00-10000110-11?0001001010102000000
210010000000000000010100000111010-100000010110000100101101000010000001000000
1010010030?000000000000020000001001000?0?1?0100?0??0100000210000101000000000
01000000001000000000000000101000011101000010001012100002111000000000100101
0001000100000100001000000000101000?1010000100000011010000-000101100011001100
10001000101110000?00010000000110001110?1?00110000001010?02001000-

'Neovenator_salerii' ?00?01010000101000010000?11000100110001010
00101110????????????????????????????????????0?0?????????????????????1??
??1?100-?000?000-?00?0?????????
????????102100000?100100000000010?01010000111101111100001011?00010?00200000
010?0001101101??1100100?0?10?0?????000100000100010?10??100100?0????????00021001
01?10?0?1010?0??01
10100?0?10001000??000001000??110010100101010000100000011000000-0001012000110
0110010101010111110010001101001????100?0??01?0????000?01?10002001000-

'Sinraptor_dongi' ?0001000000000?10000000?010-000110110000?0
000001000000200000000100101??11210--?110011000-010010011000-00010000010?01130
0000100001000010?1?00000??10?00101000100100-??10-?0-0-?0?00?1011000-?0000-0101
00?01110010000?0?010101010000002100?00000000000?010100110111010-10100001011?0
01100101101001010001001100000101?010030?0000????0002?00?0?1?1001???1??1??1?
0000??0?0??????1010?00100?0?0?????0?0????????????????????????0?0??1100101210
0?????1000000100100101001??000?0?1000010000000001100?110100001000000110100
00-00010?1000110011001000010101011?000000?00?0000001000011000?00110000001010
?0100?000-

1j07707???00?111710700???01012?1001?011?07?700100?101????7070????7070??100????001
?000-00??0?1010??2?01000-

'Giganotosaurus_carolinii' ???0?00???????0????10????10????1?001000100??01
?1?0????2??????????1010?1110--??1?0?????01101111?01??1???????1?0??10(1

2)?????????1????????????0?????101????????????1?????0-????1?????201-?0?0???10???
0???10?11????????????1???000200?0?10?0?0?0?0???110001???1111110??(0

1)?1?11??0?10??0?2?0???0??????10010????1?01?????0??0?000?01??????000???0???100
0????? ??????0?????????10??010?0???
?????????????????0???10000?110?1??0?0?000?11?????10?1010??010100?0???????11?1????
???01012?100??01??0?????0??10111???0?0??1?000????1????????????????????????????????
??

'Aorun_zhaoi' ??00??00?10?110101001100??0-00010011100???
?00000?0000?2000100000000-0--1110110?1100?0???100?0-00?????010??0?0000?11????

[illegible]

'Ornitholestes_hermanni' ??00?0000?01?00101011100??10000?01101000000
000?0?001110001100000010-10011100--00101?0100?10000-000201000?001000000011(2

3j0????100000??0?0????0?0100111101?100-???-????????????0010?10-?0000-00-1
00?00-0-11100011010001012011102101-001000000?010100-???????10-1?101200011??11
1100?11?1001??0001001??100001010110?0???10?0?10?0020000?10?0?????????1?1?????
?????????????????????0?10?11000010001?0?0?0?0?0????0?????????????0?????????
?????????????1?0101?0?100000?0?0010011000000?10???010?01000010?000001?10000-0??
??????????10?0?10????????????????00?0????????????0011?????0?100?0?0?0010?0-

'Zuolong_sallee' ??00??00?00?010101001?0?0?-000000111000000
0?????00???????0?010?0-0--1?10111011????00?00000-0?1100-00?100000001011300?0

????0??
 ??????????10100001020?0000100??????010100??????10-0?101100011??0?100???00?001
 ???????????????????????40?001?000?000000?0?00??????????????????????????????????1?1
 0???1???0?10001???0100??????00?000????????????????????????????????????0???00100?
 ?????????00?0???0??100?00000011?0010112?00??????????????????1?011000100001001
 000001010111?0???011?0000????????????010????100010101000????0???

'Albertosaurus_sarcophagus' ??1????0000011??0???10?1???0??01000001011
10?11??002011001100011111011201??000-12000010111100112010101?001010100103000

00100000000000?1?00010?01??1000?00110000100?10-?00???0000?001??00-?0?00-00-100
00101011?011100???010?00?10?00???0?0000000?0001010???011?0???????0000011?00???
???0?0?00?????????1??000?0?00?0041?0?00???10?0?00?0?0?0?00?0???0?0000001??0
00020000??00?0?0000?11?001???????00?0?00?0?01000000010-?0????????????3200?0?-
?0000?????????10101?100000000?20???1000000?0010?0?0001??00010000000102000101?1
101100110000100100000001?1110011001?1000100?2000110?001?0011000001111000?0?1
000-

'Daspletosaurus_torosus' ??100020100111110100??00?10-00000101?000???1
1101??????000110001111011101100011?01001?000?0-01120101010?1?101001030??

701?20000?2?222222222222200?2222222222222100?10-?0-10?20000?2?1?0000-0000?200-100001
0101?22222222211210100001020000000000000000010100?22222222222220?2220?2220?22222222

00?1000????110?0000?0-0-?1?0???1???1???????0-?0?0?0???0?0???0?0???0?0???0
 ???0?001?000-00?00-00-0-0?0?????????
 ??????10?0?00?0?1-00100000000?0100-0?0???0?0?????????11??10???0?0?0?100???
 ??????10???01??10????????????0???00?0?120?1000??1?0000?????10000020000?1110?00
 000000100?????????00???00?00?0100?001???00?010?0?1?22???12111?000000?01?00-
 10001010???0?0?0?0?2???000?1011????????000100000001010000-?1?????0???????????

707?????????0??0??00?2000110?001?0011?0??00?0??020?000-

'Sinosauropteryx_prima'

000000000001?001??0?0????0-0000????0?0???0000??????????100????00-0--?1100????1
1?????????0?0-00?????00?000012?0?10?????????0?????????????????????0?????????0????
?????????????0?001?000-00?0?0?0?0-0?0?????????????????10100?1002101-0?1000000?000
100-0?????010-1?1?0?10?10?11?????0?20??100?00?0000?1000?01????03?????????000?0?
000??1120?10000-1?110?????????00020000?1110000100001200?00?00?000?01?0?00000
?1100?011110?1??11?010?22???121110100010001000-1000??0??0?0?001020?000?101
1?????1??000100000011?100?0-?1??01?0001??0?0?1????0?01??10?00?0??0?0?00?200
01101001?001100?00?0?0020?000-

'Nqwebasaurus_thwazi'

?????????2?????1000??1011?0-00?00?1??-0?

?????????????????????0-10?1?2011101100201001??0????010?0-0?????0?00?10?????????
?????????????????????010?00?101??0000-???
?????????????????????03?11-21211?????--00-0??????10-1??01200?0-?11111??100100?????
???0?0?????0?????????????1002100001?10000
000?0100?100?0100?10?0?00000010?000000101001001000101221001111001010110????
?????????????????????????????????????1??0?0????00?0?????????????????????1??0?1????000001000
001011111?0010?0010?0?0002001110?001?0011000000001000?0101010

'Anserimimus_planinychus'

??

??
????????????????????????????????0??
??1?????????????-??
??0??????????11200000????0100000?012??
?????2?????????????????10000?1010-01?1001001?002210??111110012210?????10100?100?11
?0???????1010000?0010?0??00?000?1000100010?000-????????????????????????????????
????????????????????????????????001?1---?00?010110??0?1???

'Archaeornithomimus_asiaticus'

??

??
??
??0????????????????????
???00---20220011000121100000000200000001000
0000000010031?1010?0?1000020000000?00?0?0??0?0?????????????101210000111001?1000
?00200100012000010000000000?001010-11?100110110022??011??00011210010?0-00
00100010000100000100010?00101100011-010010101000100000100101001000110110001
0000010111100010?0???100002000110100101---100010011000?0??1?1?

'Beishanlong_grandis'

??

??
??
??1????????????????????
???1??????????112100001?00010000?0002??
?000100000000?0000?0000????????????????????????????????000002?0????????????????
????????????????????????????????1????????????10?0?00021?0110?10001010???1100010
?0?1010100?1000110???1?001????00?10?0001011

'Gallimimus_bullatus'

?0?0??00210000000101?101110-0?000??000-???

0000000?11001?110?000?0-0--1??111011200010000?0?0-?000?0-001?010112??00-??01?0
10?10?0?110?1?0000100010?0001001?000011??110?0-100010?0?10-0?10?1010-00-0-0?01
?10?1?1000-0??011-----1---??-?-?-2---??-???10??010-??202210010??12?????0?0????
????00?1?000?0?0?0040?1??0??100?0?00?0?0?01?0????0?0?????????011200000??
10?1??0000?02?0?0???2?0000?0000?1?0?001010-?10?????????0?2????0?2?00011010?
1?010100?100011?0?0???1010000?0010?01001-?000100010001010000-110????00?100
1?0????00?00????00?00?0?0100?0001??00101---100?01?1?010?0001010

'Garudimimus_brevipes'

?0000002?000001001?0101110-00000111000----

0?0000000?001-0110000010-0--111011101120?0100-000?0-00?000-00?00?00?001?113?01?
01001000?11?0?0??00010001?000010?01100?11?????????0??00??-0001001?10-00-000?0
0?1001?1000-0?1?11-----1-----2-----000?1-?????????????0-??2??00000100100
0001001??000000001?040?10100?0?0000??00?0?0?0?0????????????????????????????

'Harpymimus_okladnikovi' ??00000021000?010?0??1011?0-000?0?11100-
000000000? ??????0? ??????0--1110111?112010?00-000?0-00?000-00100100? ?????? ??????
????0? ?????? ?????? ?????? ?????? ?????? ?????? ?????? ??????0010001001011000-000001010
0? ?0000000-0011-----1-----?--11?0?0?--?--????1010-??0? ?0000-??02?0? ?0001?02??0
00?00? ???00??110?11040?1?10? ??1000020000?0000001? ???0?0110? ?????? ??11? ??????1?1
0?1?100?0?12?0?000120000010000000011?10000010-100100110011022100021110001111
00100101001????11?0?0?0?00100?000000? ???010? ???00? ?????? ?????? ??????0101?00? ???0?
 ?????? ?????? ??????10? ?????? ?0001000110?00101---100000?0?000?0001011

[illegible]

'Struthiomimus_altus' ???00021000??1?10?110?110-0000011?000----?0
000100?11???1110?00010-0--11?01111?120001000100?0-?000?0-0010010112?1011?01?0
???1?0?0???0?1000?????0?0000?0?0?0?010?1110?0-100010?000-0001001011000-00?0?01
010?1?1010-0???011--?-?1-----2-----?10-?010-?????2100???002?????000?????0
?????1?0000?0?0?00040?1?00???100?0?00?0?0?1?01?0?0???0?10?0?????111210000?010
010?000000200100012000001000000001?0?0001010-01010111011002210001?2?00011210
0100101???10001100?10????1010000000100100001-0000100010001010000-110?01?00011
001?0010?0?0000???1100010?0?10?0100?200011?00101---100?01011010?0001010

'Albertonykus_borealis'

??

??
??
??
??
??
??
??
????????????????001?0011000002-?11112010?0??

'Linhenykus_monodactylus' ???
??
??
??
00??0?11?0?(0
1)?20?10??10?121?00??0020??????1???1011?0????????????????????????????????
??????????????1?1010111101011111-21003211?2??11011?120????????????????????
??0??1?1??0010??11?0?0??011??11????
?112?0?1?1?01?00110?0002-?1000????0??

'Mononykus_olecranus' ???
??
????????????????????1100????????????1001011?0??1????????????????????????????
????????????????1-212?1??0??-10-0??????0-?-1010?11??1211?101021012001000000
-?10100??1010??2??1????0121?0?1????????????????101100??1000-00001?11001100
000230000101111-0021000111011?10101111010111002211112-?111011?120?0?0-?
??????????????1?00111?00?310---??1??00?0-0000??-????0-?10011112-2001001011100
0011011110011?11??1011?1101101001?0011000102-11000?010100-

'Parvicursor_remotus' ???
??
??
??
0
1)2??12?0?00??0?0??00?010??1???1????0121??10????????????????????????
??
?0??????0-????2?01?0?0-?1???3?0---1--1-0000-0000---1(1
2)00??1?011112-20010010111000010111100011000?01?101211011010010??000102-1
1001?001100-

'Patagonykus_puertai' ???
??
????????????????????????0????????????????1????????????????????????????????
??0?00?001?0?01??1000
0?01??1??30?2011000?012100?002????????????????????0??1000-1110??????001??
?0?011?1111002010011??????00?10?101??????1??1112????011?11010??????110
??????00100111????02?11011--01001????????????0-0????111200010001110000111
1111?10111?000010(1 2)001100110????1????000????010?0-

'Shuvuuia_deserti' ?0000000110000010101?101102100000?11000-??
00000000011000-11001-1?100--12201110112020000-10000-001000-0100000000??10-??01
?1200000021110101--01001011111?00100-0010-??11001011110001100?001000001000-0-0
000-0-010011110?001????0?03201-212110202?10--10-0??10-??10-10100211110?112101
1?102?01??000??0?10000?001?1050?20?1?0010012100110100200101????1110101100?
??1000-0000110?001000000230000101?11-002????110?11?101011110-011010112--022111
12---1101121201000-10020--0111021012001111000?310--1--11-00000-0000---22000-010
011112-200100101??0?1??101?001????101112110110100100011000102-11000?01110
0-

'Tugulusaurus_faciles' ???
??
??
??
????????????????????0?00????0?0??

??

??

??0??????????

~~~~~

??100000100110000?-0?101110-00001101000????0

????????????????????0?????????010??001?0??

?101000?1000120010011000010???101111????010110020001?1?100001001?11001?00

????????????????????????????????????????????????????????



????????????????????????????????????????????????????????????????????????????????????  
????????????????????????????????????????????????????????212????????2????20?00?001??11????  
????10??04??10?0?02010??10?0?0?000100????00?????10100?2????00??0?010000  
110?1?1111001??100?100000????????-??0?0?????22????????000000001011120011??  
1??1?0??100??1100?10101000111--2?0121?0?11102?10??0??112111100??00?000?0010  
110??111??1101?0??0?2000?1?0001010-0000001?0110?0?0??0-

'Segnosaurus\_galboensis' ?????????????????????????????????????????????  
????????????????????????????????????????????????????????????????????????????????  
????????????????????????????1????????????????0010?????1?1??1??101??0-0-?1?000??0?  
??0??????0??001?0?10111?00101????????????????????2????????????????????  
??????????????1?0????????????????????????????????2?????????10?????1??11?  
0?0?1100110????????????????????22??????00?????1011110011102010  
000101000-01000?201010????01000011110?1?102?101??0??????????0?0??1?0?0????  
?11??11????0??10000??001010-?00000?01102001???

'Nothronychus\_mckinleyi' ?????????????????????????????????????????  
????????????????????????????????????????????????????????????????????????????  
??????????????0?1?00?0?0??1??????1??1??10?10?0????????????????????????  
????????????0??00110?101?1??1010-0??????110?2??010011?11?????112010?001??11  
100100??010?00??????????100????0????????????????????10?????????1?0?0?110?  
0?1101?011110?1101000100?0??????????0??????0????????????0000????1??????  
????0????????????12????????????12110?111021100-00????????0??????0?0??  
??11??111?1?10????????????0-0?0????????????

'Avimimus\_portentosus' ??????????1?1????????????????????????  
????????????11??1????????????????0000????0-01?????0?00?000??11????????  
1?1?0??1?10?00?01??120?0?0?0?00-?110-??????0?00???11????????11??10-0-?0?00  
??????111-??-??????????2??2??-?-?????110?111010012000110?1121110010010010000  
0111100000?0000011060?1010?0?2?0000????????????????????2002000001100  
10000100011001001010000100100000001?111????0-????1??????0?2????????????010  
0??1??100001110101000111?00?00100100011-00011110230010?0000-011011210110100  
000101000001001100011?11100010112000110111100?11000102-110102010100-

'Caudipteryx\_zhoui' ?????????0?0?0?11????????00??01????000?01?0?????1?0101?1  
0-?10000010?0-00?0?0??00?0?0?????????1????????????????????????0??  
????????????0?201?001101111100-110?1??0-??0?0?0??0?10??1101?--??-12??2????01-  
-0-0-????0?0-??1?000????????0?(0  
1)0????00????????????????04??1?0???2100??11????0?00?0??1?011?0?00??11000?  
?????1?00?001?0?0?????1??10?00?0000?0?0001?110?0000-0?1?111?010?22??021-100  
?000000100101001??0?1?10?0?000????00????????01??2011110?00102?0?0-?100?111  
111?0?????10?00????????011??10????01200011?1001??0???01?1?0??1?0?000-

'Chirostenotes\_pergracilis' ??1??????1?00?????1101????????????-??????  
????????????????????????????????????????????????????????????????????????????  
00??01?1??0??120?011??0?00-1?110?????1????10-0?0111111100-100-10-0-?0?00??0  
????????????1?--??-??2??-????????????110?211?0?0??12????1??????0??10?1?  
1?????????52?10????0?1?0????????0????????????20?200000????0??10??  
????????????????????????????00?0??0?0??22000??????10000??1000-100010000?  
?1??010000-000000??12??00????201111023001121000-01????0?0?????0?0?11?0?0????  
??00????????00????1??0?1?0?000?01?010?0?0?00??

'Citipati\_osmolskae' ??1000000010100101?0?110100-00020111000---0  
000100101?0010100001000-1101100101?10-1111000100?0-001200-000?000000?010?011  
011111101?0?001?01010?101011200000-0?001??11111110?0000021-0201101111100-11  
0-10-0-1010001100-0111-----1-----2-----??10-?110-????210010??1?????1?0?10?  
????????1?1100?0?0?1?52????0??10?????1??0?2201?1????0??0010011111200?????  
00?0?1100?10?1?????1?000?0??000?0?1?10?00????0??????0?22??0??0010000??  
??0-100????001?1??????0-01000?1010?0110??20?11102300102?000-01?????2110010?  
0?10????0?0????????????0000?0000????001?0?0?00?0?0?0?0?0?000-

'Buitreraptor\_gonzalezorum' ?????????0000?1?10???0?1??0??????????1?????  
 ?0??????????00????0?????????????????1?10010?0-001?0????0??0?10?001?????????????  
 ?????????????????????????0?????????????????????????1?0?0-?0????01010?????????????  
 ??????????????0?01-0020??00?00??00-0??110?010-??201210110??12????010??????????0  
 ??1????0?????1?1??0?1??0??????1?01??10?2?01?????1??2???????102?1???????100???  
 101101001????????????0?1?????1?110????????????????22????????????????0100??????



1)00??0?2?????1100???1??????2-???1????1????????????????0????????????????1???0??0011

'Jinfengopteryx\_elegans' ????????1?01????1?10?0?????????001?????????????  
0????????????????????????????????1?????????00?????????0?0?????????????2?0?????????????????  
?????????????????????100?????????????????????????????0????0-?0?0-0?????????????1?????1?  
????0?000?0?????????1?????0?????????1?????????????????????????????????????????  
?????????0?????????10?????02?????????0?011?????2?????????2?1?????????1?????1010????  
?????????????????????????110?0?????????????????22?????????0?0?????????????????????1??  
?????????????????3?????????????0?????????????????????????????????????????????????????0???  
?????????????????????????????????????????????????????

'Byronosaurus\_jaffeei'                   ??00000011000010001?100110-000001110001???

?00001000?0000??0???110--11101110?0-?0????????????????????????????????????

?0000?11?0?1???0?00011?100111???010-??11001010111?????0?000-00000-0110-0?010?

????????????????101?001002201-002000120000--10-0??10-?????????2?0??????210???1????

???????????1??1??????0?????????????????????0???2????????????????????????????????

????????????????????????????????????????????????????????????????????????????

????????????????????????????????????????1????????????????????????????????1??????????0?0?01

??11??????????0????????????????????????????????????????1??

'Saurornithoides\_mongoliensis'    ??1000??1100000??10?01?0????0??0?1???01000??  
 ?0?????????1?????????????110?????????0??????0-00??0?????????????????????1?01????0  
 0?11?????????1??????????????0-0??0-??????0-?11?0?000?0?100000??011??0?0??????????  
 ??1?????0?000?02101-0010001000001010-0??????????????????????1?????0?00?0?????0??  
 000?00?0?0??000?0?0?010?000??001????00?0????????????????????????????????????????  
 ?????????????????????????????????????????????????????????????????0????????????????????  
 ?????????????????????????????01?1??0??111023001020000-0??111111011????????????????  
 ?????????????????????????????01?????????1????0??1??21??

[illegible]

[illegible]

??0??0010100?100?011-2120?2-----?0-0?????0?????????2?????211????0?????0?????  
?????????????05??01??0?210-0??1-0000?????0?????????????1112010-000?1100?00110  
11?11012?001?0011100?1000000111100010-10?10111?0?1022?0?020010010000001000-1  
1010-??1?1?1?010000-0?100?30110101101-01010-10001011010011010?11112-2?11?0010  
0?0????????????1????????11?1001??11100010??0?10??10?0?0??000-

'Jeholornis\_prima' ??????????0????????????????????1?????????  
0???0????????????????1?0????????????????????????????1????0?????????????  
????????????????????????????????100?????????0?????000-?0????????????????????  
????????????1-----?-?1?0????--0-0????????????????????????2?????????????????  
?????????3????1????20?02?02?0?1?????0????????????11?2?????????0??0?1011?1(0  
1)?0????????10?001?0?1?111?0?????????????0?1?22?0?????000000????00-110?10??  
0??1????????????????????????????????1??1????????????????????????????  
????????????????????1????????????????????????

'Yixianornis\_grabau' ???100?2?0?0????????1????????????????  
0?????????-????????????????????????????0-?0????????????????1????????????  
????0?????????????????????????????????????????0?0?0-10???00-???0?????1?0?0????  
??10100?101?--1--12??100?0?--10-011???110-?????0?0?????????02?????00????????  
?0?????0?0?0?000????21????1-?000?2???11???-???1100001003000-00011100?0?110110  
110???000100??1000100000010111?0?????????????0???22?????????01000??110?0-000?0-?  
????1???????0-1?1???3012--????-?1?01210000???20?01?010????2-201?????0?0?????  
?????11????????1?1??????11?0010?????0???????0??0??

**Phylogenetic analysis results and discussion.** In general, our results were consistent with most recently published studies of theropod phylogeny (Fig. S9). Non-coelurosaurian theropod relationships were an exception to this, being in several cases at odds with recent studies (e.g., *Ceratosaurus* basal to *Limusaurus* within the Ceratosauria contra to [S10]; *Monolophosaurus* within the Megalosauroida rather than sister to Orionides contra to [S11]). This discord was relatively minimal, however, and is likely to be the result of reduced taxon sampling relative to those studies. Coelurosaurian relationships were similar to the results of most recent phylogenetic research on this part of the theropod tree [See e.g., 12, 13]. *Zuolong salleei* is sister to the rest of Coelurosauria and Tyrannosauroida is sister to Ornithomimosauria plus Maniraptora. Compsognathidae is a basal member of Maniraptora, and is sister to the remaining members of that clade, and *Ornitholestes* is a relatively basal member of Compsognathidae. Alvarezsauria is sister to non-compsognathid Maniraptora. Scansoriopterygidae are nested within Oviraptorosauria, as recently hypothesized by [S12] and [S14]. The sister taxon to Paraves is Oviraptorosauria in some trees but is a clade formed by Therizinosauroida + Oviraptorosauria in other trees, reflecting the general lack of consensus in the literature about maniraptoran relationships in this region of the tree [S12, 13, 15-18]. Paraves is monophyletic, but the relationships among Troodontidae, Dromaeosauridae, and Avialae are poorly resolved.

*Alvarezsaurian relationships.* Surprisingly, the Chinese coelurosaur taxa *Aorun* [S13] and *Tugulusaurus* [S19] were recovered as basal members of the Alvarezsauria. *Aorun* is sister to the remaining alvarezsaurians, and as originally hypothesized by [S15], *Haplocheirus* is a basal non-alvarezsaurid alvarezsaurian, contra [S20]. *Tugulusaurus* is sister to *Xiyunykus* and this clade is recovered in an intermediate position among non-alvarezsaurid alvarezsaurians. *Bannykus* is recovered in a slightly more derived position, sister to *Bonapartenykus* plus the remaining alvarezsaurians. We recovered *Alvarezsaurus* in a derived position relative to *Patagonykus*, rather than as sister to *Patagonykus* [S4] or in a basal position relative to *Patagonykus* [S15, 21-23]. *Achillesaurus* thus emerges as sister to the Alvarezsauridae, and *Patagonykus* is sister in turn to Alvarezsauridae + *Achillesaurus*. The enigmatic taxon *Kol*, described as a relatively derived, large-bodied alvarezsaurid by Turner et al. [S24] but recently regarded as Coelurosauria incertae sedis by Agnolin et al. [S4], is here recovered as a relatively basal alvarezsaurid.

*Evolution of the Alvarezsauria.* Our analysis includes almost all known alvarezsaurian material, with the following notable exceptions: material referred to *Elopteryx nopscai* identified as an alvarezsaurid by [S25]; specimen YPM 1049, identified as an alvarezsaurid by [S26]; and *Alnashetri cerropoliciensis*, recovered as an alvarezsaurid by [S27]. These taxa were not included in our analyses because the authors have not been able to inspect them personally.

The Late Jurassic theropod *Aorun zhaoi* from the Shishugou Formation, and the Early Cretaceous theropod *Tugulusaurus faciles* from the Lianmugui Formation (both from Xinjiang, China but from localities more than 200km apart), are recovered here as alvarezsauroids. In the case of *Aorun*, this result is unsurprising – although this taxon was initially described as a basal coelurosaurian taxon by Choiniere et al., these authors acknowledged that it shares at least some features with alvarezsaurians [S13]. The unique holotype of *Aorun zhaoi* is a juvenile, suggesting the possibility it is an early ontogenetic stage of the Shishugou species *Haplocheirus sollers*. However, *Aorun zhaoi* is from an older part of the formation and differs from *Haplocheirus sollers* in 8 features (22), including features such as opisthocoelous cervical vertebrae that are not expected to change ontogenetically. With *Aorun* positioned as the sister taxon to all other alvarezsauroids, there is relatively good Bremer support (=3 with *Kol* excluded) for the monophyly of Alvarezsauroidae, and this clade is supported by four unambiguous synapomorphies: a dorsoventrally flattened narial bar (character 10); collateral ligament fossae on McII absent (character 418); digit 1 bearing a large ungual and all other unguals distinctly smaller (character 440); and a proximodistally oriented step-like ridge on the anterior surface of the tibia that braces the ascending process of the astragalus (character 546). Given that *Aorun* is only represented by a juvenile exemplar, it is likely that other alvarezsauroid features might have manifested in adult individuals of this taxon.

The recovery of *Tugulusaurus* as an alvarezsaurian, however, was an unexpected result, especially given that previous analyses [e.g., 18] have been equivocal as to its phylogenetic position and that it is represented by only scant skeletal material [S19]. However, its position as a non-alvarezsaurid alvarezsaurian is supported by several features, including: a strong medial tab on metacarpal II (character 414); dorsolaterally and dorsomedially facing lateral and medial surfaces of phalanx II-1 that are shallowly concave (character 432); axial furrow along the flexor surface of phalanx II-1 (character 433); and partially enclosed ‘flexor notches’ on the medial and lateral surfaces of the proximal end of the ventral surface of manual ungual II-2 (character 446). Its sister-taxon relationship with *Xiyunykus* is only supported by one synapomorphy – a mediolaterally narrow ascending process of the astragalus (character 560). However, the possibility that *Xiyunykus pengi* might be a junior synonym of *Tugulusaurus faciles* Dong, 1973, is contradicted by a number of differences between the two taxa, although none of them concern characters scored in the matrix: anterior mid-caudals with neural arch placed on nearly whole central length in the former vs on anterior two thirds of centrum in the latter; anterior mid-caudal centra deeper dorsoventrally than wide transversely in the former taxon vs the opposite condition in the latter; middle caudals without distinctive groove on their central ventral surface in the former vs with distinctive groove in the latter; caudal central articular ends with sub-rectangular outlines in the former vs sub-circular in the latter; posterior surface near the femoral distal end flat in the former vs distinctive groove bounded by two ridges emanating from tibial and fibular condyles, respectively, on posterior surface near the femoral end in the latter; posterior intercondylar groove proportionally wide in the former vs narrow in the latter; fibular condyle wider than tibial condyle in the former vs the opposite condition in the latter; ectocondylar tuber on the fibular condyle distally defined by a straight groove in the former vs by an oblique groove in the latter; vertical groove present on tibial posterior condyle in the former vs absent in the latter; and tibial lateral malleolus with relatively straight lateral margin in the former vs with pronounced, semicircular lateral expansion in the latter.



*Bremer support values.* Bremer supports were relatively low at most nodes, especially major stem nodes within Maniraptora and within Alvarezsauria. However, the results of the reduced Bremer support analyses (excluding the fragmentary taxon *Kol ghuva*), improved Bremer supports at many nodes, particularly within Alvarezsauroidae.

*Synapomorphies for selected nodes.* Synapomorphies below are unambiguously optimized character transformations present in all trees at the specified nodes.

Alvarezsauroidae

Internarial bar (10): dorsoventrally rounded → dorsoventrally flat

Distal condyles of Mc II (418): with collateral ligament fossae → collateral ligament fossae absent

Unguals on all manual digits (440): generally similar in size → digit II bearing large ungual and unguals of other digits distinctly smaller

Bracing for ascending process of astragalus on anterior side of distal tibia (546): anterior side of tibia flat → Step-like ridge running proximodistally rather than obliquely

*Tugulusaurus* + *Xiyunykus*

Shape of ascending process of the astragalus (560): broad, covering most of anterior surface of distal end of tibia --> narrow, covering only lateral half of anterior surface of tibia

*Patagonykus* + (*Achillesaurus* (*Alvarezsauridae*))

Cuppedicus fossa (457): present → absent

Astragalus and calcaneum (556): condyles indistinct or poorly separated → distinct condyles separated by prominent vertical tendinal groove on anterior surface

Alvarezsauridae

Brevis fossa shape (461): shelf-like, narrow with subparallel margins → deeply concave, expanded posteriorly with lateral overhang

Fibular facet on astragalus (558): large and facing partially proximally → reduced and facing laterally or absent

Unnamed node: *Kol ghuva*, *Albertonykus*, *Xixianykus* + *Albinykus*, Parvicursorinae

Metatarsal III (580): subequal in width to Mt II and IV proximally → does not reach the proximal end of the metatarsus

*Xixianykus* + *Albinykus*

Distal tarsals (567): separate, not fused to metatarsals → form metatarsal cap with intercondylar prominence that fuses to metatarsal early in postnatal ontogeny

Metatarsals coössification (568): not co-ossified → coossified

Parvicursorinae

Height of ascending process of the astragalus (559): higher than astragalar body → more than twice the height of astragalar body

Fossa on anterior surface of mesial base of ascending process of astragalus, sometimes bearing accessory fenestrations (562): present → absent

Posteromedial margin MtII diaphysis (578): well-developed flange absent or area rugose → with flange projecting caudally or medially

Length of MtIV (585): markedly longer than Mt II → subequal to Mt II

Coelurosauria

Ascending process of the maxilla (27): offset from anterior rim of maxillary body → confluent with anterior rim of maxillary body and gently sloping posterodorsally

Dorsal border of the antorbital fossa lateral view (32): formed by nasal and lacrimal → formed by lacrimal and maxilla

Supraorbital crests on lacrimal in adult individuals (67): present → absent

Lacrimal posterodorsal process (76): absent → present

In cross section, premaxillary tooth crowns (226): sub-oval to sub-circular → D-shaped with flat lingual surface

Pleurocoels in dorsal vertebrae (282): present in anterior dorsals ('pectorals') → absent

Brevis fossa shape (461): deeply concave, expanded posteriorly with lateral overhang → shelf-like, narrow with subparallel margins  
Pubic boot projects (483): anteriorly and posteriorly → with little or no anterior process  
Broad groove on extensor surface of distal femur (526): well developed → absent or poorly developed

#### Maniraptora

Caudal margin of naris (12): farther rostral than the rostral border of the antorbital fossa → nearly reaching or overlapping the rostral border of the antorbital fossa  
Form of anterior end of jugal (57): expressed at the rim of the internal antorbital fenestra and with a distinct process that extends anteriorly underneath it → without anterior process underneath antorbital fenestra  
Infracondylar fossa of occipital condyle (157): present → absent  
Laterally inclined flange along dorsal side of lateral surface of surangular (204): present → absent  
Form of coronoid ossification (213): large → thin splint  
Neural spines on distal caudals (332): form a low ridge → spine absent  
Pubic orientation (480): propubic → vertical

#### Scansoriopterygidae + non-*Incisivosaurus* oviraptorosauria

Pronounced coronoid eminence on the surangular (201): absent --> present  
Premaxillary tooth direction (224): decumbent or ventrally projecting --> procumbent  
Dentary tooth direction (244): dorsally or posteriorly inclined --> procumbent (anteriorly inclined)

#### Paraves

Shape of nasals (49): expanding posteriorly → of subequal width throughout their length  
Proximal end of chevrons of proximal caudals (345): short anteroposteriorly, shaft cylindrical → proximal end elongate anteroposteriorly, flattened and plate-like  
Distal caudal chevrons (348): simple → anteriorly bifurcate, or bifurcate at both ends  
Glenoid fossa (375): faces posteriorly or posterolaterally → faces laterally  
Ulnar shaft (394): straight → bowed  
Tuber along dorsal edge of ilium, dorsal or slightly posterior to acetabulum (476): absent → present  
Posterolateral trochanter (524): absent or represented only by rugose area → posterior trochanter distinctly raised from shaft, mound-like  
Shape of fibular crest (543): quadrangular → low and rounded  
Ungual and penultimate phalanx of pedal digit II (592): similar to those of III → highly modified for extreme hyperextension, ungual more strongly curved and about 50% larger than that of III

### **Alvarezsaurian biogeography**

Recently, Xu et al. [S28] investigated the biogeographic history of Alvarezsauria and found that the evidence in support of either a pre-Aptian vicariance hypothesis [Se.g., 16, 29] or a dispersal hypothesis [S21, 23] was equivocal. At that time, however, no Early Cretaceous alvarezsaurians were known. The data presented here clearly show that intermediate alvarezsaurians were present in Asia during the Early Cretaceous before alvarezsaurian taxa of similar phylogenetic position are known to have inhabited South America. It thus seems more likely that Alvarezsauria enjoyed a lengthy evolutionary history in Asia prior to dispersing to other continents. This biogeographical hypothesis is further supported by our statistical analysis of alvarezsaurian biogeography (see below).

The result of the SDVA for the nodes within Alvarezsauria is described below in detail (Fig. S4). At the early evolutionary stage of Alvarezsauria, this group is inferred to have dispersed to

North America from Asia (although no North American fossil record at this stage has been found). The later intercontinental dispersal from North America to South America and vicariance would have led to the formation of South American alvarezsaurians at node 23. Interestingly, the opposite intercontinental dispersal route (e.g. South America–North America–Asia) is proposed to have occurred at the early evolutionary stage of Alvarezsauridae, along with a series of vicariance events. Similarly, fossil record at the base of Alvarezsauridae is relatively rare in North America, where *Albertonykus* material was recovered. Overall, based on the result of the SDVA, we speculate that insufficient samplings or taphonomic biases for North American alvarezsaurians may be correlative with the high incompleteness of fossil record in this continent, especially at the early evolutionary stages of Alvarezsauria (around the earliest Cretaceous) and even Alvarezsauridae (around the early half of the Late Cretaceous).

**Node 27:** The ancestral taxon at node 27 (now representing the most recent common ancestor of Alvarezsauria) is inferred to be present in Asia. No intercontinental dispersal and vicariance events had occurred when this taxon split.

**Node 26:** The ancestral taxon at node 26 is inferred to be located in Asia. No events of intercontinental dispersal and vicariance had occurred when this taxon split.

**Node 25:** The ancestral area at node 25 is inferred to be restricted to Asia. Node 25 would have split into the Asian node 15 and node 24 widespread in Asia and North America, along with an intercontinental dispersal event from Asia to North America.

**Node 15:** The ancestral taxon at this node is inferred to be present in Asia. No events of intercontinental dispersal and vicariance had occurred when this taxon split.

**Node 24:** The ancestral taxon at node 24 is inferred to be widespread in Asia and North America. This taxon would have experienced an intercontinental dispersal event from North America to South America, and later would have split into the Asian *Bannykus* and ancestral taxon at node 23 widespread in North America and South America because of intercontinental vicariance.

**Node 23:** The ancestral taxon at node 23 is inferred to be widespread in North America and South America. No intercontinental dispersal and vicariance events had occurred when this taxon split into the South American *Bonapartenykus* and ancestral taxon at node 22. In the most likely case that denotes the South American origin of the ancestral taxon at node 22, an extinction event in North America for the ancestral taxon at node 23 should be expected to occur.

**Node 22:** The ancestral area at node 22 is inferred to be restricted to either South America or North and South America. RASP regards South America as the most likely ancestral area of this node. No intercontinental dispersal and vicariance events had occurred when the ancestral taxon at node 22 split.

**Node 21:** Likewise, the ancestral area at node 21 is inferred to be restricted to either South America or North and South America. RASP regards South America as the most likely ancestral area of the node; in this condition, the ancestral taxon at node 21 would have split into the South American *Achillesaurus* and ancestral taxon at node 20 widespread in North and South America, along with an intercontinental dispersal event from South America to North America.

**Node 20:** The ancestral taxon at node 20 (currently representing the most recent common ancestor of Alvarezsauridae) is inferred to be widespread in North and South America. This taxon would have experienced an intercontinental dispersal event from North America to Asia, and later would have split into the South American *Alvarezsaurus* and ancestral taxon at node 19 widespread in Asia and North America because of vicariance.

**Node 19:** The ancestral taxon at node 19 is inferred to be widespread in Asia and North America. This taxon would have split into the North American *Albertonykus* and Asian ancestral taxon at node 18 as the result of intercontinental vicariance.

**Node 18:** The ancestral taxon at node 18 is inferred to be present in Asia. No events of intercontinental dispersal and vicariance had occurred when this taxon split.

**Node 17:** The ancestral taxon at node 17 is inferred to be present in Asia. No events of intercontinental dispersal and vicariance had occurred when this taxon split into *Kol* and Parvicursorinae both from Asia.

**Node 16:** The ancestral taxon at node 16 is inferred to be present in Asia. No events of intercontinental dispersal and vicariance had occurred when this taxon split.

### **Forelimb allometry and reduction**

**Results.** Complete forelimb length (N = 28 taxa) has a strongly significant relationship with body mass (Table S2), and the coefficient of the phylogenetic signal parameter ( $\lambda$ ) is approximately 1.0 (median  $\lambda$  across analyses using 100 phylogenies = 0.98). This indicates that the intercept of the relationship between arm length and body mass evolves in a Brownian motion-like manner along branches of theropod phylogeny. The median coefficient of body mass is 0.30, indicating weak negative allometry. Partial forelimb length yields similar results (Table S2), with a slightly greater coefficient of 0.35, consistent with isometry or weak positive allometry (coefficients from analyses across 100 phylogenies range from 0.33–0.37; isometry = 0.33).

**Forelimb reduction in theropods.** Visualization of our data clearly indicates that lineage-specific forelimb-reduction events occurred in several theropod lineages, at both large and small body sizes. The distribution of residuals from our regression analyses is asymmetric (Figure S3), consistent with the hypothesis that forelimb reduction (relative to the plesiomorphic scaling relationship with body mass) can be more extreme than forelimb enlargement in theropods. Specifically, forelimb reduction in some ceratosaurs, tyrannosauroids and alvarezsaurians has a greater magnitude than forelimb enlargement in long-forelimbed taxa for which complete forelimb measurements are available (predominantly ornithomimosaurs and some early tyrannosauroids). Analysis of partial forelimb lengths shows the same pattern (Fig. S6).

Although the face-value distribution of residuals is highly non-normal, this does not necessarily invalidate the assumptions of pGLS. We confirmed that pGLS was an appropriate mode of analysis for our data distribution by making use of the equivalence between pGLS with ordinary least squares (OLS) regression of phylogenetic independent contrasts (when  $\lambda = 1$ ) [S30, 31]. Normality of the residuals of an OLS regression of the independent contrasts of forelimb length on body mass could not be rejected using Anderson-Darling ( $p = 0.874$ ), Cramer-von Mises (08523), Lilliefors ( $p = 0.942$ ) or chi-squared ( $p = 0.801$ ) tests.

### **Functional morphology of *Bannykus manus*.**

The manual digits of *Bannykus* appear less specialized than those of Late Cretaceous alvarezsaurians. The pollex is broadly similar to that of *Haplocheirus* [S15], the proximal phalanx bearing a ventral groove but lacking the pronounced ventrolateral ridge seen in parvicursorines and particularly in *Patagonykus* [S32]. This robust digit appears well suited to hooking and raking, given that the ungual could evidently be flexed to the point where its long axis formed an acute angle with that of the proximal phalanx. Digit III, which forms an elongate grasping structure in *Haplocheirus* [S15] and is greatly reduced in parvicursorines [S33], is well-developed but specialized in a highly distinctive manner. The proximal end of the first phalanx bears a proximovertrally expanded ‘heel’ similar to that of pedal phalanx II-2 in derived dromaeosaurids [S34], suggesting attachment of powerful flexor musculature but only a limited range of flexion. The second phalanx had a large range of extension and particularly flexion with respect to the first, and bears an unusual articular surface for the

ungual. This surface is restricted to the wide, medially deflected medial condyle, which projects farther distally than the much smaller lateral condyle. The dorsal part of the medial condyle bears a midline groove, giving the condyle a degree of ginglymoidy, but the groove angles ventromedially and leaves the ventral part of the condyle unitary and broadly convex. The proximal surface of the ungual is not divided by a median ridge, and the ungual appears to have been capable not only of considerable flexion and extension but also of small but far from negligible amounts of abduction, adduction, pronation and supination. Tendons passing through the groove between the condyles of the phalanx to insert on the proximal end of the ungual would have been well-positioned to drive such off-axis rotational movements.

Because interphalangeal (IP) joints in tetrapods almost always approximate simple hinges, the second IP joint of digit III in *Bannykus* is extremely unusual and must have served a specialized function unless the condition of this specimen is pathological. It is unlikely that the additional degrees of freedom at the joint would have been particularly useful in grasping, raking or hooking, as they could bring about only relatively small changes in the orientation of the ungual. However, such flexibility would have been potentially advantageous if the ungual had been inserted into crevices or other confined spaces, either to directly extract prey such as insects and small vertebrates or to pull apart a fragile structure such as an insect nest or decaying log. The ability of the claw to rotate about multiple axes would have allowed it to be brought to bear at a variety of angles while, for example, maintaining a grip with the other digits on the object containing the crevice. The modern aye-aye (*Daubentonia madagascariensis*) uses its long and slender third finger as a probing device, particularly to pry wood-boring insect larvae out of small cavities, and the terminal phalanx of this digit is capable of “sideways movement” driven by laterally and medially inserting extensor tendons [S35]. The third digit of *Bannykus* is much less slender and elongate than that of *Daubentonia*, and would have been useful only in probing larger crevices and cavities, but the utility of the additional degrees of freedom at the second IP joint may have been analogous.